

**SUN proteins in higher eukaryotes, “structural bridges”
connecting the nuclear interior with the cytoskeleton**

INAUGURAL-DISSERTATION

zur

Erlangung des Doktorgrades
der Mathematisch-Naturwissenschaftlichen Fakultät
der Universität zu Köln



vorgelegt von

Wenshu Lu

aus

Changchun, Jilin, P. R. China

Köln, 2007

Referees/Berichterstatter: Prof. Dr. Angelika A. Noegel
Prof. Dr. Jens Brüning

Date of oral examination: 12.06.07

Tag der mündlichen Prüfung

The present research work was carried out under the supervision of Prof. Dr. Angelika A. Noegel and Dr. Akis Karakesisoglou, in the Institute of Biochemistry I, Medical Faculty, University of Cologne, Cologne, Germany from April 2004 to December 2006.

Diese Arbeit wurde von April 2004 bis Dezember 2006 am Institut für Biochemie I der Medizinischen Fakultät der Universität zu Köln unter der Leitung von Prof. Dr. Angelika A. Noegel und Dr. Akis Karakesisoglou durchgeführt.

TABLE OF CONTENTS

1. Introduction

1.1 Nuclear envelope	1
1.1.1 Inner and outer nuclear membranes	1
1.1.2 The nuclear lamina	2
1.1.3 Nuclear envelope proteins	4
1.2 Nuclear envelope related human diseases	6
1.3 The nuclear envelope and nuclear positioning	7
1.4 KASH domain proteins	8
1.5 SUN domain proteins	11
1.6 Aim of the work	12

2. Results

2.1 Characterization, distribution and functional analysis of Sun1	13
2.1.1 Sun1 is the closest orthologue of <i>C. elegans</i> UNC-84 in mouse	13
2.1.2 Phylogenetic tree of SUN domain containing proteins	15
2.1.3 Sun1 is broadly expressed in mice	16
2.1.4 Subcellular localization of endogenous human Sun1	17
2.1.5 Domain analysis of Sun1	18
2.1.6 Sun1 has three transmembrane domains	20
2.1.7 Sun1 dynamics at the nuclear envelope	21
2.1.7.1 iFRAPs of GFP-Sun1 full-length	23
2.1.7.2 iFRAPs of GFP-Sun1-2TM-N and GFP-Sun1-TM-C	24
2.1.7.3 iFRAPs of GFP-Sun1-TM-SD1, 2 and GFP-Sun1-TM- Δ CC-SUN	26
2.1.8 Sun1 interacts with chromatin	28
2.1.9 Sun1 oligomerizes via its coiled-coil domains	29
2.1.10 Sun1 forms SDS-resistant dimers under non-reducing conditions	35
2.1.11 The C-terminal domain of Sun1 forms SDS-resistant dimers under non-reducing conditions through disulfide bond formation	36
2.1.12 Sun1 interacts with Sun2	39
2.1.13 Sun1 is required for proper Nesprin-2 NE localization	41
2.1.14 Sun1 affects the nuclear envelope localization of emerin and LAP2 β	43

2.1.15 The luminal domain of Nesprin-1 interacts with the SD2 domain of Sun1	44
2.1.16 Construction of a Sun1 C-terminal dominant negative construct	45
2.1.17 Characterization of HaCaT cells stably transfected with SPGFP-Sun1-C	46
2.1.18 Nesprin-2 isoforms are mislocalized in SPGFP-Sun1-C stably transfected HaCaT cells	48
2.1.19 Nuclear shape changes in SPGFP-Sun1-C cells	50
2.1.20 Proliferative ability of SPGFP-Sun1-C stably transfected cells	53
2.1.21 Senescence analysis of SPGFP-Sun1-C stably transfected cells	56
2.1.22 The expression level of E-cadherin is increased in SPGFP-Sun1-C stably transfected cells	57
2.2 Generation of a Nesprin-1 knock-in mouse model	59
2.2.1 Knock-in strategy and ES clone screening	59
2.2.2 Generation of Nesprin-1 knock-in chimeric mice	61
3. Discussion	
3.1 Sun1 and Sun2 proteins display similar topologies at the nuclear envelope	63
3.2 Sun1 is a widely expressed INM protein	64
3.3 Sun1 displays a low lateral mobility at the NE	65
3.4 Sun1 oligomerizes via the coiled-coil domains	66
3.5 Sun1 binds to chromatin	68
3.6 Sun1 interacts with Nesprins to form a bridge across the NE	69
3.7 Overexpression of Sun1-C disrupts the SUN-Nesprin linkage across the NE	71
3.8 Proposed roles of Sun1 in higher eukaryotes	73
4. Summary/ Zusammenfassung	76
5. Materials and methods	
5.1 Cloning strategies	79
5.2 Primer sequences for cloning	80
5.3 RNA isolation and RT-PCR analysis	82
5.4 Tissue culture and transfection	83
5.5 Establishment of stably transfected HaCaT cell lines	83
5.6 Inverse fluorescence recovery after photobleaching experiments (iFRAP)	83
5.7 Antibodies and immunofluorescence microscopy	84

5.8 siRNA knockdown of Sun1	85
5.9 Chromatin immunoprecipitation assays (ChIP)	86
5.10 Purification of GST fusion proteins and <i>in vitro</i> binding assays	87
5.11 Native polyacrylamide gel-electrophoresis (Native-PAGE)	87
5.12 Chemical cross-linking experiments	87
5.13 Yeast two-hybrid assay	88
5.14 Site-directed Mutagenesis	88
5.15 His-tag pull-down assays	88
5.16 BrdU incorporation	89
5.17 Generation of Growth Curves	89
5.18 PI/FACS (cell cycle) analysis	89
5.19 Senescence-Associated β -Galactosidase Assays	90
5.20 Nuclear shape analysis	90
5.21 Statistical analysis	91
6. References	92
7. Appendix	
7.1 Abbreviations	104
7.2 Amino acid code	105
Acknowledgement	106
Erklärung	107
Curriculum Vitae/ Lebenslauf	108

1. Introduction

1.1 Nuclear envelope

The nucleus is the hallmark of eukaryotic cells, and is separated from the cytoplasm by a selective structural barrier - the nuclear envelope (NE). The nuclear envelope (Fig 1.1) is composed of a pair of membranes, the inner and outer nuclear membranes (INM and ONM, respectively) joined together by the nuclear pore complexes (NPCs) (Gerace & Burke, 1988). NPCs span the NE and are large macromolecular assemblies that form aqueous gated channels across the NE and regulate the transport of macromolecules between the nucleus and cytoplasm (Gorlich & Kutay, 1999; Macara, 2001). In addition to this function, the NE is essential in defining higher order nuclear structure by providing anchoring sites for chromatin at the nuclear periphery. A recent convergence of clinical and basic research has highlighted a link between NE functions and various human diseases, including cardiac and skeletal myopathies (Burke & Stewart, 2002), which underline the vital importance of NE functions.

1.1.1 Outer and inner nuclear membranes

The ONM is continuous with the peripheral endoplasmic reticulum (ER) and is functionally related to the ER (Franke *et al.*, 1981). In fact, these two structures share a similar set of proteins as well as ribosomes (Gerace & Burke, 1988). The ONM also provides attachment sites for structural elements of the cytoplasm (Burke & Ellenberg, 2002). The INM, in contrast, is composed by a distinct set of membrane proteins, which perform close associations with the underlying nuclear lamina and chromatin (Stuurman *et al.*, 1998). The INM is not known to participate in protein synthesis, and has no association with ribosomes. The lumen between the two membranes that makes up the nuclear envelope is continuous with the ER lumen, and is usually about 20 - 100 nm in width (Broers *et al.*, 2006).

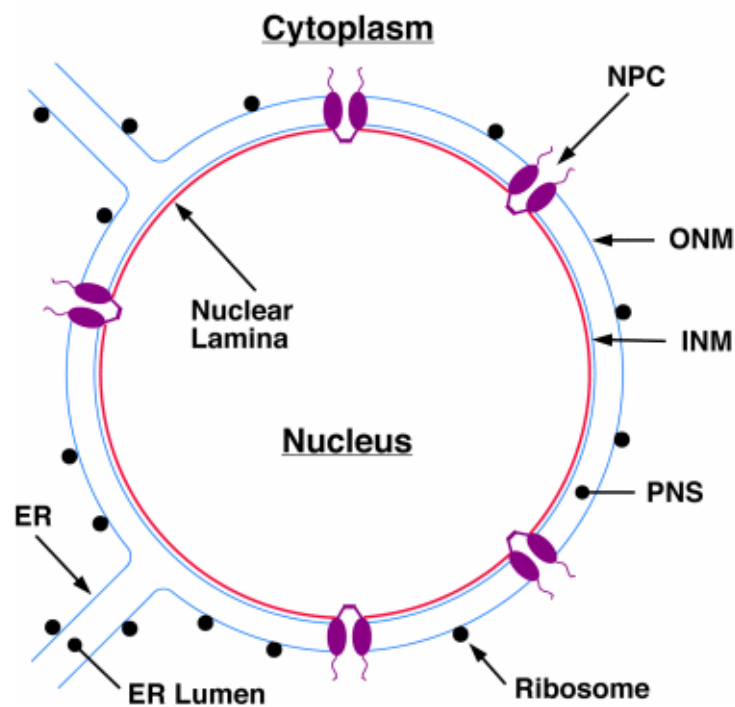


Figure 1.1. Overview of nuclear envelope organization. The outer nuclear membrane (ONM) is coated with ribosomes and is contiguous with the rough endoplasmic reticulum (ER). The inner nuclear membrane (INM) is connected to the ONM at the periphery of each nuclear pore complex (NPC). The nuclear lamina lines the nuclear face of the INM and is closely associated with peripheral heterochromatin (Burke *et al.*, 2001).

1.1.2 The nuclear lamina

The inner nuclear membrane (INM) is stabilized by an underlying filamentous meshwork called nuclear lamina. In mammalian cells, the nuclear lamina appears as a thin (20–50 nm) protein meshwork that lines the nuclear face of the INM (Dwyer & Blobel, 1976). The nuclear lamina associates with both INM integral proteins and chromatin, performing thus fundamental roles in the functional organization of the nucleus. Principal constituents of the lamina are the intermediate filament lamin proteins (Franke, 1987). Nuclear lamins are type V intermediate filament (IF) proteins containing a central α -helical rod, which is flanked by N- and C-terminal non-helical domains. Most lamins, except for lamin C, are farnesylated at their carboxy termini via a CaaX motif (Hutchison *et al.*, 2001) (Fig. 1.2). Based on their primary sequences and biochemical features, lamins are subdivided into A-type and B-type (Gerace *et al.*, 1978).

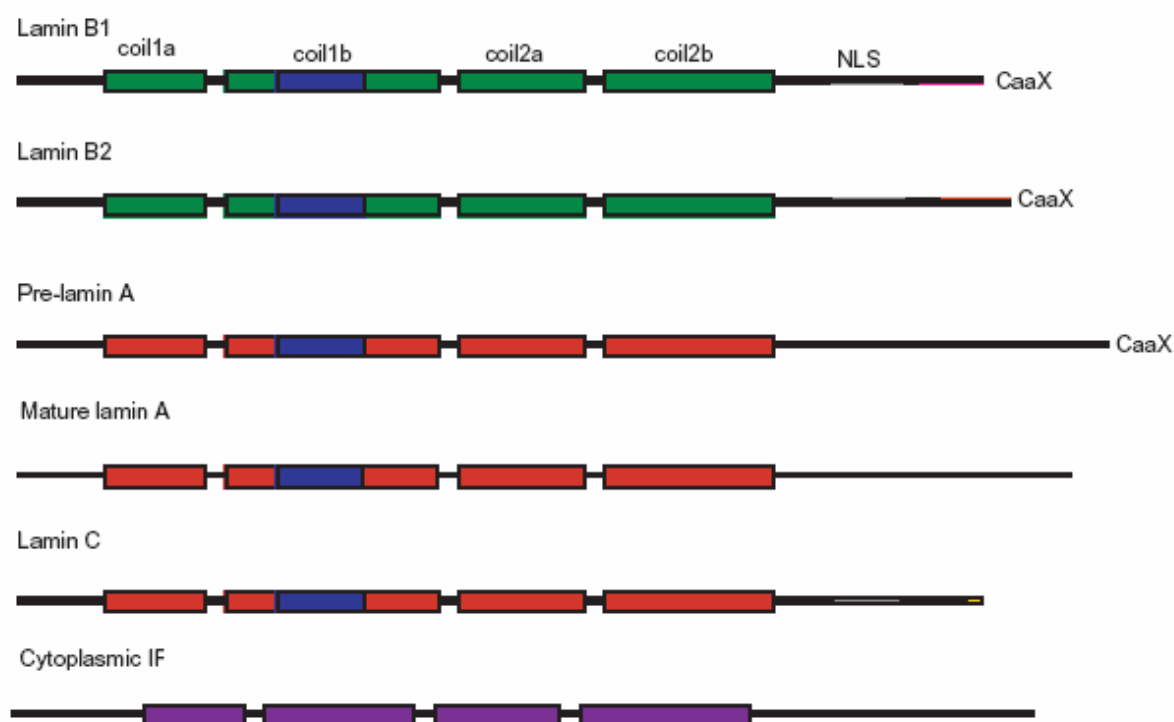


Figure 1.2. Schematic representations of somatic cell lamins. Colored rectangles represent α -helical coiled-coil domains; B-type lamins are shaded in green, and A-type lamins are shaded in red. The blue shaded area within coil 1b shows the position of the heptad repeat extension, which is unique to the lamins. NLS=nuclear localization signal sequence; CaaX is the site for carboxy methylation, prenylation and proteolytic cleavage. Colored regions in the C-terminal tail domains show the major sites of amino acid residue variation among the lamin subtypes. The stylized cytoplasmic IF illustrates differences in organization for comparison. The central rod domain is shorter (owing to the absence of the heptad repeat extension in coil 1b). The head domain is generally longer and varies between IF types. The tail domain lacks an NLS and CaaX (Hutchison *et al.*, 2001).

Both major (A and C) and minor (A Δ 10 and C2) A-type lamin species are encoded by a single developmentally regulated gene (*LMNA*), which arise through alternative splicing (Fisher *et al.*, 1986). By contrast, the main B-type lamins (B1 and B2) are encoded by two separate genes (*LMNB1* and *LMNB2*, respectively) (Hoeger *et al.*, 1988; Hoeger *et al.*, 1990). A single minor B-type lamin (B3) is a splice variant of lamin B2 (Furukawa & Hotta, 1993). A-type lamins are expressed in more differentiated cells (Rober *et al.*, 1990) and are nonessential for cell viability (Sullivan *et al.*, 1999). B-type lamins are expressed in all cell types and are essential for cell viability and normal development (Harborth *et al.*, 2001; Lenz-Bohme *et al.*, 1997; Vergnes *et al.*, 2004). *LMNB1* mutant mice are lethal after birth, but it is possible to culture and even immortalize *LMNB1* mutant embryonic fibroblasts, suggesting a partial functional substitution by lamin B1 and lamin B2 proteins (Vergnes *et al.*, 2004).

Individual lamin polypeptides — both A- and B-type — readily self-associate to form parallel coiled-coil homodimers, which can, in turn, assemble into higher-order filamentous structures. Growing lines of evidence point to the involvement of the nuclear lamina in various fundamental nuclear activities. These include maintaining and integrating cell shape (Lenz-Bohme *et al.*, 1997), anchoring chromatin (Gant *et al.*, 1999), association with nuclear bodies (Jagatheesan *et al.*, 1999), DNA replication (Jenkins *et al.*, 1995) and transcription (Spann *et al.*, 2002; Hutchison, 2002).

1.1.3 Nuclear envelope proteins

The first nuclear envelope proteins to be characterized were the nuclear lamins. In addition to lamins, several integral membrane proteins specifically localized to the INM were identified. However, the complete protein composition of the NE in vertebrates is not yet available. A recent proteomics analysis suggests that as many as eighty transmembrane proteins are localized to the INM in interphase cells (Schirmer *et al.*, 2003). As shown in Figure 1.3, most of these INM proteins have large nucleoplasmic domains performing interactions with nuclear lamins and/or chromatin.

LBR (lamin B receptor) is one of the best-characterized INM integral proteins. The nucleoplasmic N-terminal domain of LBR interacts *in vitro* not only with B-type lamins, but also with chromatin via HP1 (Ye & Worman, 1996). LBR is involved in the reassembly of the nuclear envelope after cell division (Drummond *et al.*, 1999; Okada *et al.*, 2005).

Lamin-associated proteins (LAPs), LAP1A, LAP1B, LAP1C, and LAP2, were initially identified in rat liver NE fractions (Foisner & Gerace, 1993). LAP1A, LAP1B and LAP1C, are closely related and are probably alternatively spliced products of the same gene. LAP2 proteins are also expressed as a variety of isoforms (α , β , γ , δ and ϵ), all being alternatively spliced products of a single gene. LAP2 α does not contain a transmembrane segment and is present diffusely throughout the nucleus, while other isoforms contain transmembrane domains and are thus INM integral proteins. LAP2 β associates specifically with lamin B1 and chromatin. The affinity of LAP2 β for lamin B1 and chromatin is reduced in the presence of CDC2 activity (Foisner & Gerace, 1993). Microinjection of peptides corresponding to the lamin binding domain of LAP2 β into mitotic and early G1 phase cells was able to inhibit lamina assembly, NE growth and entry into S phase (Yang *et al.*, 1997). Similarly, GST fusion proteins containing the N-terminal region of LAP2 β also inhibited some aspects of NE assembly and in particular, lamina assembly in cell-free extracts of *Xenopus* eggs (Gant *et al.*,

1999). Thus, these lines of evidence suggest that LAP2 β mediate membrane-chromatin attachment, lamina assembly, and probably also promotion of replication by influencing chromatin structure.

In 1994, positional cloning resulted in the identification of a gene responsible for X-linked Emery-Dreifuss muscular dystrophy. Sequencing demonstrated that it encoded for a protein named emerin, that contained a stretch of about 40 amino acids with sequence similarity to a portion of LAP2 (Bione *et al.*, 1994). Emerin was soon identified as an INM protein (Manilal *et al.*, 1996), which interacts with A-type and possibly B-type lamins (Fairley *et al.*, 1999; Clements *et al.*, 2000).

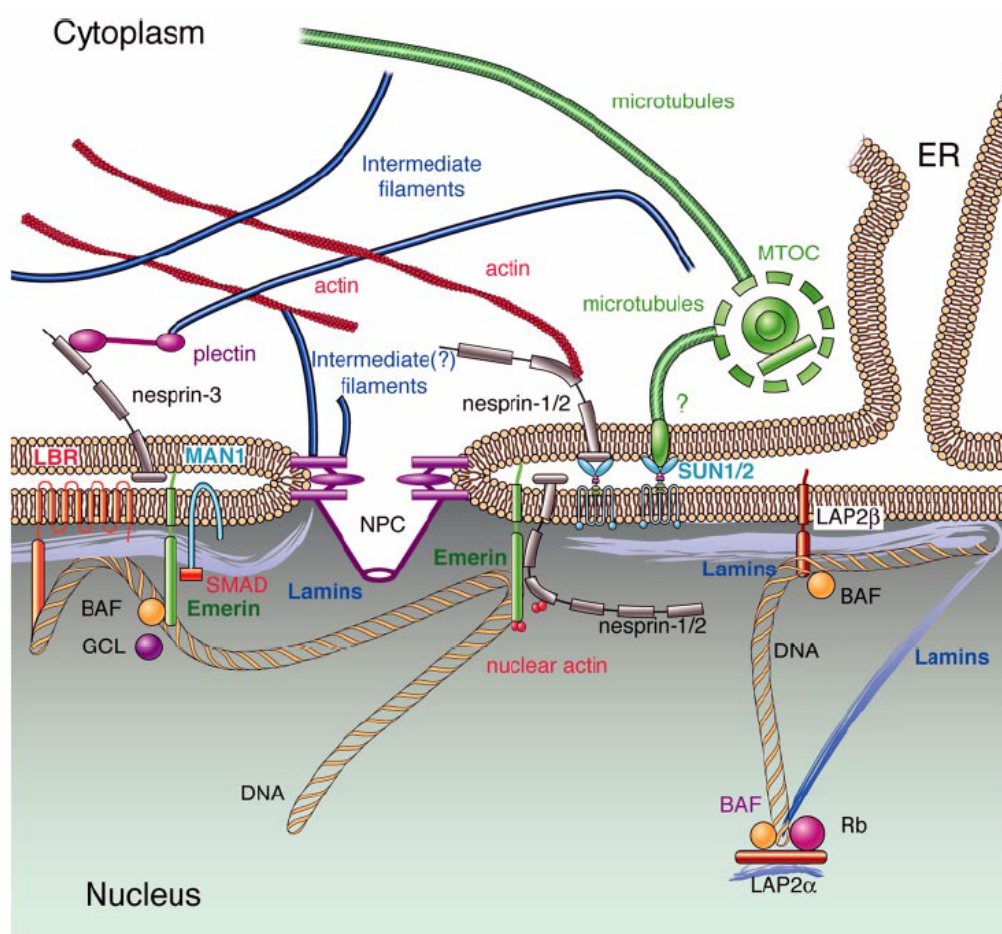


Figure 1.3. Model of nuclear envelope proteins and their interactions with nearby proteins. Most nuclear membrane proteins (LBR, LAP2, emerin, MAN1, nesprin-1 and -2) bind directly to lamins. LEM domain proteins (LAP2, emerin, MAN1) interact with the chromatin associated protein BAF. Nesprins interact with SUN proteins therefore connecting the nucleus with the cytoplasm. Question marks indicate suggested but not proven interactions (taken from Broers *et al.*, 2006).

Emerin, together with LAP2 (LAP2 β , LAP2 γ , LAP2 δ and LAP2 ϵ) and MAN1, belong to a growing family of proteins that is defined by the presence of a so-called “LEM domain”. The LEM domain is composed of a motif of about 43 amino acids that is exposed to the nucleoplasm and interacts with BAF (barrier to autointegration factor), an abundant chromatin-associated protein (Laguri *et al.*, 2001; Shumaker *et al.*, 2001). Therefore, BAF might form a link between chromatin and the INM. Although the function of BAF is still poorly understood, it is an essential protein, as reduction of BAF levels is lethal in *C. elegans* embryos (Zheng *et al.*, 2000).

Except for these NE proteins mentioned, there are two novel families of NE proteins, characterized by distinct domains (SUN or KASH). Proteins containing the KASH (Klarsicht, ANC-1 and Syne1 homology) domain interact with SUN domain (Sad1 and UNC-84 homology domain) containing proteins in the perinuclear space (Padmakumar *et al.*, 2005; Haque *et al.*, 2006) (Fig 1.3), and are involved in nuclear positioning and possibly in other unknown cellular processes (Starr & Han, 2002; Patterson *et al.*, 2004; Zhang *et al.*, 2007).

1.2 Nuclear envelope related human diseases

For many years, the nuclear envelope was thought to function mainly as an architectural stabilizer of the nucleus, participating in assembly and disassembly processes during mitosis. However, recent findings demonstrate that nuclear envelope proteins are involved in fundamental nuclear functions, such as gene transcription and DNA replication. To date, mutations in the genes encoding the nuclear envelope proteins were found to cause a wide range of human diseases, known collectively as nuclear envelopopathies (Somech *et al.*, 2005).

The first of these disorders to be recognized was Emery-Dreifuss Muscular Dystrophy (EDMD) (Emery & Dreifuss, 1966). This disorder is characterized by childhood onset with progressive muscle wasting and weakening. Late-onset defects of EDMD include abnormal cardiac rhythms, conduction block and cardiomyopathy that can lead to sudden cardiac arrest. Mutations that cause X-linked EDMD were originally mapped to the *EMERIN* gene. A clinically identical autosomal-dominant form of EDMD has been mapped to the *LMNA* gene coding for lamin A/C (Bonne *et al.*, 1999). Mutations in *LMNA* gene also associate with limb girdle muscular dystrophy (LGMD) with atrioventricular conduction disturbances (Muchir *et al.*, 2000), dilated cardiomyopathy (DCM) with conduction system disease (Fatkin *et al.*, 1999), autosomal recessive axonal neuropathy (Charcot-Marie-Tooth disorder type 2) (De Sandre-Giovannoli *et al.*, 2002), Dunnigan-type familial partial lipodystrophy (Speckman *et*

al., 2000) and Hutchinson-Gilford progeria syndrome (Eriksson *et al.*, 2003). Until now, more than 211 different mutations have been identified in the *LMNA* gene, and these mutations cause more than 15 different types of diseases (Broers *et al.*, 2006). However, the mechanisms by which *LMNA* gene mutations cause these diverse tissue-specific phenotypes have not been elucidated.

Lmna^{-/-} mice exhibit growth retardation from 2–3 weeks of age with clinical and histological features of muscular dystrophy and uniform death by 8 weeks of age (Cutler *et al.*, 2002). Lamin A/C deficiency primarily causes destabilization of nuclear lamina structure and enhances nuclear deformability, with intranuclear and extranuclear sequelae that promote the development of a severe form of DCM and limit compensatory hypertrophy (Nikolova *et al.*, 2004). *Lmna*^{-/-} cells have increased nuclear deformations, defective mechanotransduction, and impaired viability under mechanical strain (Lammerding *et al.*, 2004). Lamin A/C gene deficiency in mice is also associated with mislocalization of emerin and other NE proteins. Thus, one plausible pathomechanism for EDMD, limb-girdle muscular dystrophy type 1B, hypertrophic cardiomyopathy and familial partial lipodystrophy is the presence of specific abnormalities of the nuclear envelope. The recognition of these various disorders now raises the novel possibility that the nuclear envelope may have functions that go beyond housekeeping and which impact upon cell-type specific nuclear processes.

1.3 The nuclear envelope and nuclear positioning

Nuclear positioning is essential for many cellular processes, including cell division, migration, differentiation, fertilization and polarization (Starr & Fischer, 2005; Wilhelmsen *et al.*, 2006). In eukaryotes, the positioning of the nucleus within each cell is regulated. This positioning requires the activity of actin, microtubules and microtubule-dependent motors (Starr *et al.*, 2001; Starr & Han, 2002). Remarkably, various studies reveal that nuclear positioning also depends on the nuclear lamina, involving KASH and SUN domain proteins.

The SUN domain containing protein, UNC-84 is an INM integral protein of *C. elegans*, shown to be involved in nuclear migration and nuclear anchoring during *C. elegans* development (Lee *et al.*, 2002). *UNC-84* (null) mutants result in both uncoordinated and egg/laying defective animals and affect the nuclear envelope localization of ANC-1 (for anchorage defective), a huge protein of 8546 residues (Starr & Han, 2002). ANC-1 also failed to localize to the NE in alleles that have missense mutations in or near the conserved SUN domain of UNC-84. Similar phenotypes exhibited by both ANC-1 and UNC-84 mutants in *C.*

elegans suggested a genetic interaction between these proteins. The model in Figure 1.4 indicates that as an integral component of the inner nuclear membrane, the C-terminus of UNC-84 extends into the nuclear lumen where it interacts with the KASH domain of ANC-1. The calponin domains of ANC-1 (red) attach to actin microfilaments (green) to effectively anchor nuclei in the cytoplasm. UNC-84 binds directly to another KASH domain protein of the ONM, UNC-83 *in vitro* (Starr *et al.*, 2001). Mutations in either UNC-84 or UNC-83 affect the polarization of gut primordial cells and disrupt nuclear migration in P-cells (Malone *et al.*, 1999). With the C-terminus facing the nuclear lumen, UNC-84 could retain other proteins at the outer nuclear membrane as well. These data suggest that ANC-1, UNC-83, UNC-84, the nuclear lamina, and other unknown proteins create a structural bridge across both nuclear membranes in *C. elegans*.

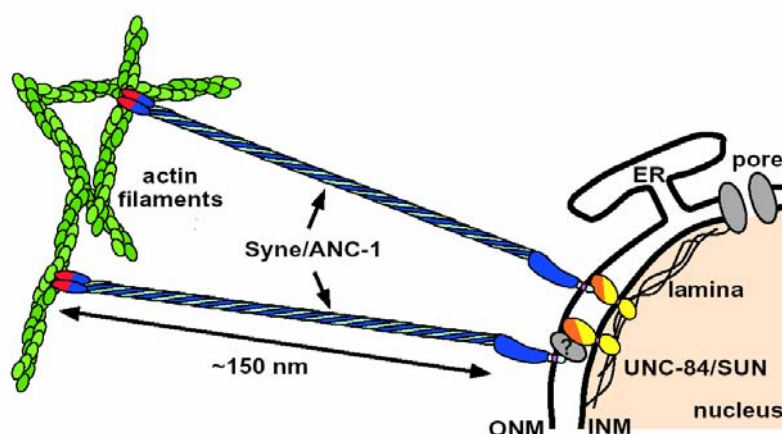


Figure 1.4. A model for nuclear anchorage in *C. elegans*. The KASH domain (light blue) is targeted to the outer nuclear membrane (ONM) through an interaction with the C-terminus of UNC-84 (yellow), which may occur through an unknown intermediate protein or complex (gray circle with question mark). The UNC-84/SUN N-terminus associates with lamins which are required for its proper NE positioning (Starr & Han, 2003).

1.4 KASH domain proteins

The importance of KASH domains was first speculated through studies on several proteins including Klarsicht, ANC-1 and Syne1. Klarsicht is important for the development of the compound eye in *Drosophila* (Fischer-Vize & Mosley, 1994) and also involved in the transport of lipid droplets in *Drosophila* embryos (Welte *et al.*, 1998). In *C. elegans*, ANC-1 tethers nuclei to the actin cytoskeleton (Starr & Han, 2002). The mammalian Syne1 protein

was originally identified in yeast two hybrid screens to identify binding partners of the MuSK, a tyrosine kinase of the postsynaptic membrane in muscle (Apel *et al.*, 2000). Syne1 was also named Nesprin-1 for nuclear spectrin repeat containing protein 1. These proteins contained a highly conserved short C-terminal region (Mosley-Bishop *et al.*, 1999; Apel *et al.*, 2000; Starr & Han, 2002), which has been termed the KASH domain standing for Klarsicht, ANC-1 and Syne1 Homology. The KASH domain is a highly conserved C-terminal short segment, which consists of a predicted transmembrane domain followed by about 35 amino acids situated in the nuclear lumen. KASH domain containing proteins have been discovered in a variety of species. Till now, the identified members of this family include Kms1 in *S. pombe*, ANC-1, UNC-83, ZYG-12 in *C. elegans*, Klarsicht and MSP-300 in *D. melanogaster*, Nesprin-1, -2 and -3 in mammals.

Many KASH domain proteins are giant molecules with a molecular weight of more than 800 kDa, such as *C. elegans* ANC-1 (Starr & Han, 2002), *D. melanogaster* MSP-300 (Rosenberg-Hasson, 1996; Zhang *et al.*, 2002) and the mammalian proteins Nesprin-1 (also termed as Enaptin, Syne1) and Nesprin-2 (also termed as Nuance, Syne2) (Padmakumar *et al.*, 2004; Zhen *et al.*, 2002). They share the same overall domain architecture and have been regarded as the membrane-anchored “dystrophins” of the nucleus due to their homology to dystrophin (Zhang *et al.*, 2001). They are composed of an N-terminal α -actinin type actin binding domain (ABD), a massive spectrin repeat containing rod and a highly conserved C-terminal KASH domain (Mosley-Bishop *et al.*, 1999). The C-terminal KASH domain is sufficient for nuclear envelope targeting of these proteins. ANC-1 functions to physically tether the actin cytoskeleton to the ONM. Mutations in ANC-1 disrupt the positioning of nuclei and mitochondria in *C. elegans* (Starr & Han, 2002). MSP-300 of *Drosophila* is required for embryonic muscle morphogenesis and in the formation of embryonic muscle attachments (Rosenberg-Hasson *et al.*, 1996), whereas, maternal MSP-300 appears to play an important role in actin-dependent nuclear anchorage during cytoplasmic transport (Yu *et al.*, 2006). The mammalian Nesprin-1 and Nesprin-2 genes display enormous complexity, generating a wide variety of transcripts that differ in length, domain composition, expression pattern and probably in their functional properties. To date, five smaller N-terminally truncated isoforms (Nesprin-1 α_1 , Nesprin-1 α_2 , Nesprin-1 β_1 , Nesprin-1 β_2 and Nesprin-1 γ) and two C-terminally truncated isoforms (CPG2 and ENAPTIN-165) of Nesprin-1 were identified (Apel *et al.*, 2000; Mislow *et al.*, 2002; Zhang *et al.*, 2001; Nedivi *et al.*, 1996). Similarly, Nesprin-2 α - γ are small C-terminal truncated isoforms of Nesprin-2 Giant (Zhang *et al.*, 2002)

(Fig 1.5). *Nesprin-1* and *Nesprin-2* encoded isoforms are broadly expressed. In contrast to *Nesprin-2*, which localizes predominantly to the nuclear envelope, *Nesprin-1* has a rather heterogeneous subcellular distribution. Antibodies against the ABD of *Nesprin-1* localize the protein at the F-actin rich structures throughout the cell as well as at the NE (Padmakumar *et al.*, 2004). Consistent with their subcellular localizations, genetic studies involving their orthologues in lower eukaryotes suggest roles for these proteins in the attachment of intracellular membrane compartments to the actin cytoskeleton (Starr & Fischer, 2005; Warren *et al.*, 2005).



Figure 1.5. Domain structures of major isoforms generated from the *Nesprin-1* and *Nesprin-2* genes. Isoforms are generated by alternative initiation and termination of transcription. The asterisks denote muscle specific isoforms *Nesprin-1 α_2* and *Nesprin-2 α_1* (Warren *et al.*, 2005).

1.5 SUN domain proteins

In 1999, Malone and his colleagues characterized UNC-84 as a nuclear envelope protein that is required for nuclear migration and anchoring during *C. elegans* development. UNC-84 consists of 1111 amino acids. It has a predicted transmembrane domain located approximately in the middle of the protein and a C-terminal region that has significant homology to a region in the *S. pombe* spindle pole body protein Sad1. This homologous region they called SUN domain (Sad1 and UNC-84 homology domain) (Malone *et al.*, 1999). SUN domain proteins are evolutionarily conserved. To date, UNC-84 and matefin have been found in *C. elegans*, Sad1 in *S. pombe*, Dd-Sun1 in *D. discoideum*, predicted proteins Q9V996 and Q9VKG2 in *Drosophila*, and Sun1, Sun2 Sun3 and SPAG4 proteins in human. Besides the SUN domain, members of this family share other structural features to various extents. Most SUN domain proteins have at least one predicted transmembrane domain. Several of them span the membrane multiple times. This is a potentially useful property for proteins that are proposed to anchor mechanical-load-bearing structures and to transmit mechanical force (Tzur *et al.*, 2006). Lastly most SUN domain proteins have at least one coiled-coil domain, which in human and mouse Sun1 is proposed to mediate homo-dimerization (Crisp *et al.*, 2006; Padmakumar *et al.*, 2005).

In *S. pombe*, Sad1 localizes to the spindle pole body (the yeast microtubule organizing centre) and when ectopically overexpressed, Sad1 also localizes to the NE (Chikashige *et al.*, 2006). Sad1 is required for setting up the mitotic spindle (Hagan & Yanmagida, 1995). In *C. elegans*, UNC-84 is required for the localization of ANC-1 at the NE (Starr & Han 2002), whereas, matefin is involved in the attachment of centrosomes to the nucleus and also in nuclear migratory events (Malone *et al.*, 2003). Matefin binds Ce-lamin (B-type lamin) directly *in vitro* but its NE localization does not depend on Ce-lamin *in vivo* (Fridkin *et al.*, 2004). Matefin links the NE to the centrosome or microtubule organizing centre through ZYG-12, a NE localized KASH domain protein (Malone *et al.*, 2003). In *D. discoideum*, consistent with the domain architecture of SUN proteins in *C. elegans* and human, Dd-Sun1 comprises an N-terminal nucleoplasmic domain, a single transmembrane domain, followed by two coiled-coil domains and the conserved SUN domain. Human Sun1, like UNC-84 in *C. elegans*, is also an INM protein. Epitope-tagged Sun1 localizes to the NE in transfected cells (Dreger *et al.*, 2001; Padmakumar *et al.*, 2005). The N-terminal domain of mouse and human Sun1 is sufficient to target the protein to the NE and directly binds to A-type lamins (Haque *et al.*, 2006). However, unlike most INM proteins, Sun1 localization seems to be lamin A/C

independent *in vivo* (Padmakumar *et al.*, 2005; Haque *et al.*, 2006; Hasan *et al.*, 2006). Hodzic *et al.* (2004) characterized Sun2 and reported that Sun2 localizes to the INM with the SUN domain located in the perinuclear space between the ONM and INM in human HeLa cells. The N-terminus of Sun2 interacts with A-type lamins as well (Crisp *et al.*, 2006). These findings implicate that Sun1 and Sun2 have similar topologies, with their N-terminal domains in the nucleoplasm and their SUN domains in the lumen of the nuclear envelope.

Current evidence indicates that INM positioned SUN domain proteins interact with ONM positioned KASH domain proteins, and in this manner creates protein “bridges” that span both nuclear membranes (Lee *et al.*, 2002; Starr & Fischer, 2005; Padmakumar *et al.*, 2005; Crisp *et al.*, 2006).

1.6 Aim of the work

Knowledge about SUN domain containing proteins is restricted to lower eukaryotes including fission yeast and *C. elegans* indicating functions in nuclear migration and anchorage whereas very little is known about SUN domain proteins in higher eukaryotes. Do mammalian SUN domain containing proteins share similar functions as their lower eukaryotic orthologues? Are they also involved in nuclear migration? Do they form similar ONM-INM complexes in higher eukaryotes? These were the main questions that we were trying to address in the current PhD thesis. To answer these questions we applied a combination of biochemical, cell biological and genetic approaches. Firstly, we examined the tissue and subcellular distribution of Sun1 in mouse and human. Secondly, we investigated the mobility and stability of Sun1 full length and various Sun1 domains by monitoring their NE dynamics using the iFRAP methodology. Furthermore, we addressed also the NE targeting mechanism of Sun1 by performing localization studies on various Sun1 domains, which were fused to GFP. Thirdly, we applied a combination of yeast two-hybrid, RNAi and biochemical methods to investigate the possible self-interaction of Sun1, and interactions between Sun1, Sun2 and KASH domain proteins. Lastly, in order to reveal the Sun1 functions at the NE, we generated and characterized stably transfected HaCaT cells expressing a dominant negative Sun1 polypeptide.

2. Results

2.1 Characterization, distribution and functional analysis of Sun1

2.1.1 Sun1 is the closest orthologue of *C. elegans* UNC-84 in mouse

UNC-84 is a nuclear envelope protein that is required for nuclear migration and nuclear anchoring during *C. elegans* development (Malone *et al.*, 1999). The UNC-84 protein contains 1111 amino acids, and is composed of an N-terminal nucleoplasmic domain, one predicted transmembrane domain and a conserved C-terminal SUN domain. Current studies in *C. elegans* show that UNC-84 links the nucleus to the cytoskeleton by mediating interactions

Ce UNC-84	YALESSCGAVVSTRCSETYKSYTRLEKFWDIPIIYFHYS PRVVIQRNSKSLFPGECDCEK	998
Mm Sun1	FALSSCGSILSTRCSETYETRTALLSLFCVPLWYFSQSPRVVIQP---DIYPGNCWAFK	801
Mm Sun2	YALESSCGASVISTRCSETYETRTALLSLFCIPLWYHSQSPRVILQP---DVHPGNCWAFQ	587
Mm Sun3	YALRSAGASVI EAGTSESYKNNKAKRYLQHCIGFLNYEMP PDMLLQP---DVHPGNCWAFQ	146
Mm SPAG4	YALSSVFCASIDLEKTSDDYEDQNTAYFQNRLSFQNYARPPSVILEP---DVFPNCWAFE	317
Mm SPAG4L	FALRSIECASIDFEHTSATYNHDKRARSYQNWIRLWNYAQP PDVILEP---NVTPGNCWAFQ	228
Ce UNC-84	ESRCYIAVELSHFIDVSSISYBHGSEVAPEGNRS SAPKCVLWWAYKQIDDLNSRLLIED	1058
Mm Sun1	CSQCYLWVRLSMKIYPTTFIMBHIPKTLSPKGNIS SAPKDFAVYCLETEYQEEG-QPLGR	860
Mm Sun2	CPDGFVWVRLSARIRPTAVTLEHWPKALSPNSTISSAPKDFATFCFDEDLQQEG-TLLGT	646
Mm Sun3	CSQCHILIKLARKIIPAVTMBHISEKVSPPS GNIS SAPKDFSVYCVMMKKCEEE-IFLCQ	205
Mm SPAG4	EDRCQVWIRLPGHVQLSDITLQHPPTVAHTGGAS SAPKDFAVYGLQADDE-TE-VFLCK	375
Mm SPAG4L	SDRCQVTIRLAQKVYLSNITLQHIPKTIISLSCSLDTAPKDFVIYCLESLPR-EE-VFLCA	286
Ce UNC-84	YTYDLDCEPPLQFFLAKHRPDPVVKFVLEVTSNYCAP-FTCLYRLRVHCKVWVQV-----	1111
Mm Sun1	FTYDQECDSLQMFHTLERPDQAFQIWE LRVL SNQCHPEYTCLYRFRVHCEPIQ-----	913
Mm Sun2	FATDQDEEPIQTFYFQASKMATYQVWELRILTMQCHPEYTCLYRFRVHCEPAH-----	699
Mm Sun3	FITYNKMEATIQTFELQNEASESLCWLQIL SNQCHPKYTCLYRFRVHCIPSDYT-----	260
Mm SPAG4	FIFDVQKSETQTFHLQNDPPSAF PKVKIQIL SNQCHPRFTCLYRFRVHCVRTSEWADDNA	435
Mm SPAG4L	FIFQPE-NIIQTFQLQNLPRSEAAWKVKIS SNQCNPRFTCMYRFRVHGSVTPPKDSHLE	345

Figure 2.1. Sun1 is the closest orthologue of Ce UNC-84 in mice. A blast search using the SUN domain of Ce UNC-84 (CAA94142) identified five SUN domain containing protein sequences in the mouse genome, namely Sun1 (BC048156), Sun2 (AY682987), Sun3 (AK132922), SPAG4 (CAM46026) and SPAG4L (AY307077). The alignment was done with the program BioEdit. Identical amino acids are shown in black and similar residues in gray. Mm Sun1, Mm Sun2, Mm Sun3, Mm SPAG4 and Mm SPAGL share 47.8%, 39.8%, 32% 28% and 27% identity to Ce UNC-84 SUN domain, respectively. Ce: *C. elegans*; Mm: *Mus musculus*; SPAG4: sperm associated antigen 4; SPAG4L: sperm associated antigen 4 like protein.

with the ONM proteins ANC-1 and UNC-83. These interactions are proposed to be mediated by the SUN domain. In an effort to identify SUN domain containing proteins in higher eukaryotes, we used the UNC-84 SUN domain sequences and performed a BLAST search in the mouse database, and identified five SUN domain containing proteins (Fig. 2.1).

The *Sun1* gene is located in the mouse chromosomal locus 5G.2, whereas *Sun2* maps at the chromosomal locus 15E.2. The other three SUN domain containing proteins are named Sun3 (located in chromosome 11), sperm associated antigen 4 (SPAG4) and SPAG4 like protein (both located in chromosome 2). Mouse Sun1 and Sun2 display 65% identity and 81% homology in their SUN domain. The SUN domain of mouse Sun1 shares 47.8% identity and 63% similarity to that of *C. elegans* UNC-84, whereas mouse Sun2 shares 39.8% identity and 59% similarity to the SUN domain of *C. elegans* UNC-84. Sun3, SPAG4 and SPAG4 like protein are small proteins less than 500 amino acids and share lower identities with UNC-84.

Ce UNC-84	YALESSCGAVVSTRCS ETYKSYTRLEKFWDIPIYYFHYSPRVVIQRNSKSLFPGECUCFK	998
Hs Sun1	FALESCGGSSILSTRCS ETYE TRTALMSLFGIPLWYFSQSPRVVIQP--DIYPCNCWAFK	699
Hs Sun2	YALESCGASVITSTRCS ETYE TRTALLSLFGIPLWYFSQSPRVVILQP--DWHPGNCWAFK	605
Ce UNC-84	ESRFTIAYELSHFDVSSISYEHIGSEVAPFCNBSAPKGVLVWAYKQIDDLNSRVLIQD	1058
Hs Sun1	GSQGYLVVRLSMMIHPPAAFTLEHIPTLSPTCNISSAPKDFAVYCLENEYDEEG-QLLGQ	758
Hs Sun2	CPQCFAYVRLSARIRPTAVTLEHVPEALSPNSTISSAPKDFAIKGFDEDLQDEG-TLLGK	664
Ce UNC-84	YTYDLDGPPLOFFLAKHKP--DFPVKFWLEWTSNYG--APFTCLYRLRVHCKVWQV	1111
Hs Sun1	FTYDQDGEESLQMFQALKRPDDTAFQIVELRIFSNWGHPEYTCLYRFRVHGE PVK-	812
Hs Sun2	FTYDQDGEPLQTEHFQAPT-MATYQWVELRILTNWGHPEYTCLYRFRVHGE PAH-	717

Figure 2.2. Alignment of *C. elegans* UNC-84 and *Homo sapiens* Sun1 and Sun2 SUN domains. The SUN domain of *C. elegans* UNC-84 was aligned with human Sun1 (KIAA0810) and Sun2 (NM015374) SUN domains. The alignment was done with BioEdit. Identical amino acids are shown in black and similar residues in gray. SUN domains of human Sun1 and human Sun2 display 48% and 39% identity to that of *C. elegans* UNC-84, respectively. Ce: *C. elegans*; Hs: *H. Sapiens*.

In addition, human Sun1 and Sun2 were also aligned with *C. elegans* UNC-84 (Fig. 2.2). Similarly, human Sun1 displays 48% identity and 64% similarity to the SUN domain of UNC-84. Human Sun2 displays 39% identity and 58% similarity to the SUN domain of UNC-84. Consequently, Sun1 is the closest orthologue of *C. elegans* UNC-84 in mouse and human.

2.1.2 Phylogenetic tree of SUN domain containing proteins

A phylogenetic analysis of SUN domain proteins from *H. sapiens*, *M. musculus*, *C. elegans*, *D. discoideum* and *S. pombe* shows that *H. sapiens* Sun1, Sun2 and *M. musculus* Sun1, Sun2 are closely related to each other. In contrast, the sequences of *H. sapiens* Sun3, SPAG4 and *M. musculus* Sun3, SPAG4, SPAG4L are more distantly related to Sun1 and Sun2. *C. elegans* UNC-84 shares higher homology to *H. sapiens* Sun1 than *H. sapiens* Sun3 to Sun1. *D. discoideum* Sun1 is closer to the human and mouse proteins than *C. elegans* matefin and *S. pombe* Sad1 (Fig. 2.3). It is evident from this evolutionary tree that there is a high degree of sequence conservation between mouse and human.

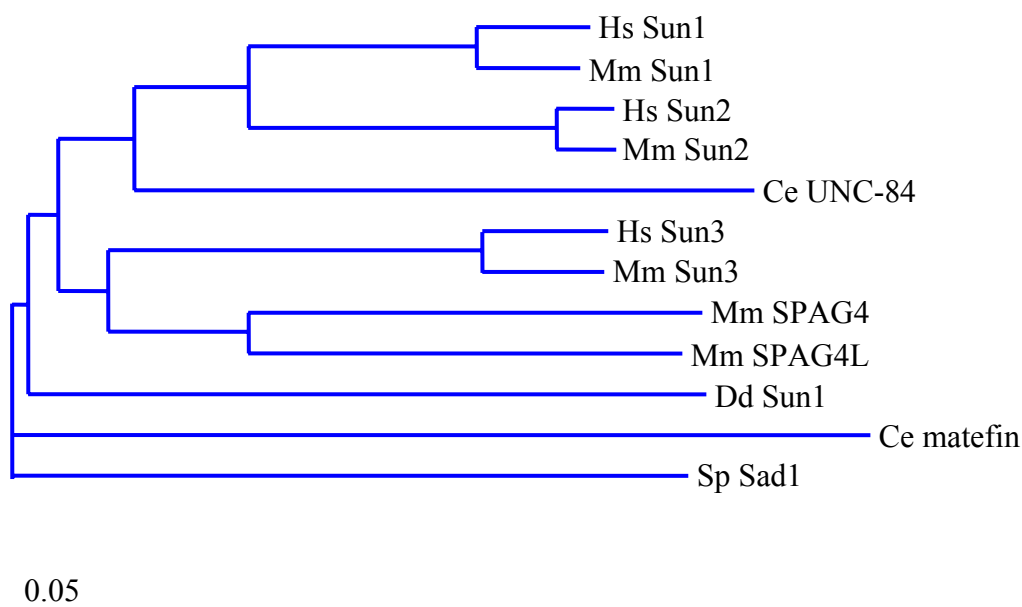


Figure 2.3. Phylogenetic relationships of SUN domain proteins. Hs: *Homo sapiens*, Mm: *Mus musculus*, Ce: *Caenorhabditis elegans*, Dd: *Dictyostelium discoideum*, Sp: *Schizosaccharomyces pombe*. Hs Sun1, Sun2 and Mm Sun1, Sun2 are closely related and forms a subgroup. Hs Sun3 and Mm Sun3, SPAG4, SPAG4L form a more ancient and distinct subgroup. The scale bar indicates genetic distance and is equivalent to 5% diversity. The evolutionary tree was generated using AlignX of Vector NTI program.

2.1.3 Sun1 is broadly expressed in mice

To study the tissue distribution of mouse Sun1, we employed an RT-PCR approach. Total RNA was isolated from multiple wild-type mouse tissue samples and subjected to reverse transcription. The same amount of cDNA obtained from each tissue was used as template for the following PCR analysis. To investigate the Sun1 expression profile, we designed two distinct pairs of primers. One resides in the N-terminus (5'NT/3'NT; amplifying the coding sequence of residues 22-163), whereas the other set is in the C-terminus (5'CT/3'CT; amplifying the coding sequence of residues 748-887). The primer sequences were listed in materials and methods. With the C-terminal primers, a 400-bp product was amplified from all the mouse tissue samples. This is consistent with the northern blot analysis of mRNA from multiple mouse tissues (Crisp *et al.*, 2006), indicating that Sun1 is ubiquitously expressed, suggesting thus that Sun1 may play an essential role in mice. Mouse GAPDH primers were used as positive controls. Interestingly, using N-terminal primers, PCR products were only amplified from brain, kidney, testis, skin and skeletal muscle, but not from heart, liver and lung, suggesting the existence of alternatively spliced isoforms of Sun1 in those tissues (Fig. 2.4). These data are also supported by the examination of the EST-database using Sun1 sequences as a query, indicating that Sun1 exists in multiple, alternatively spliced isoforms. The northern blot analysis of mRNA from multiple mouse tissues revealed at least four or five discrete Sun1 transcripts in different tissues (Crisp *et al.*, 2006). In summary, Sun1 is broadly expressed in many tissues and is encoded by a gene, which gives rise to many splicing variants.

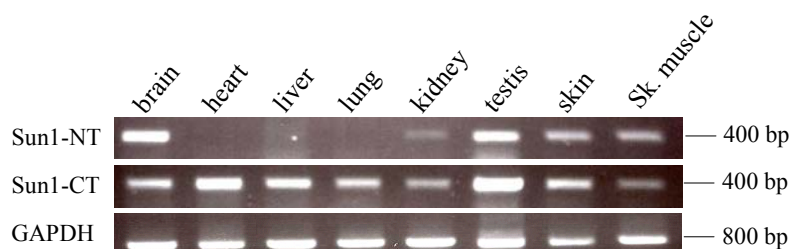


Figure 2.4. Mouse Sun1 mRNA is broadly expressed in various tissues. Total RNA isolated from each tissue was subjected to RT-PCR amplification using the 5'NT/3'NT or 5'CT/3'CT primers, respectively. All RT-PCR products were analyzed by agarose gel electrophoresis and visualized by ethidium bromide staining. GAPDH was used as control.

2.1.4 Subcellular localization of endogenous human Sun1

Endogenous human Sun1 was detected in human keratinocyte HaCaT cells by indirect immunofluorescence experiments using two different polyclonal antisera, which were kindly provided by Dr. Joseph Gotzmann (Biocenter, Vienna). One antibody is designed against the very N-terminus of Sun1 (termed 281; against polypeptides: MDFSRLHMYSPPQC), whereas the other one is directed against the C-terminus of Sun1 (termed 282; against polypeptides: RVDDPQDVFKPTTSR). Staining of both reagents indicates that Sun1 is localized largely to the nuclear envelope (Fig. 2.5, arrowheads) and colocalizes with the inner nuclear membrane protein emerin (Fig. 2.5 right panel). Thus, Sun1 is a nuclear membrane protein. Permeabilization studies employing digitonin revealed that Sun1 is an inner nuclear membrane protein (Padmakumar *et al*, 2005). As shown in Figure 2.5, the antiserum 282 stained only the nuclear envelope, whereas the antiserum 281 stained in addition also the cytoplasm (arrows). Therefore, for all other further studies we used preferentially the 282 antiserum.

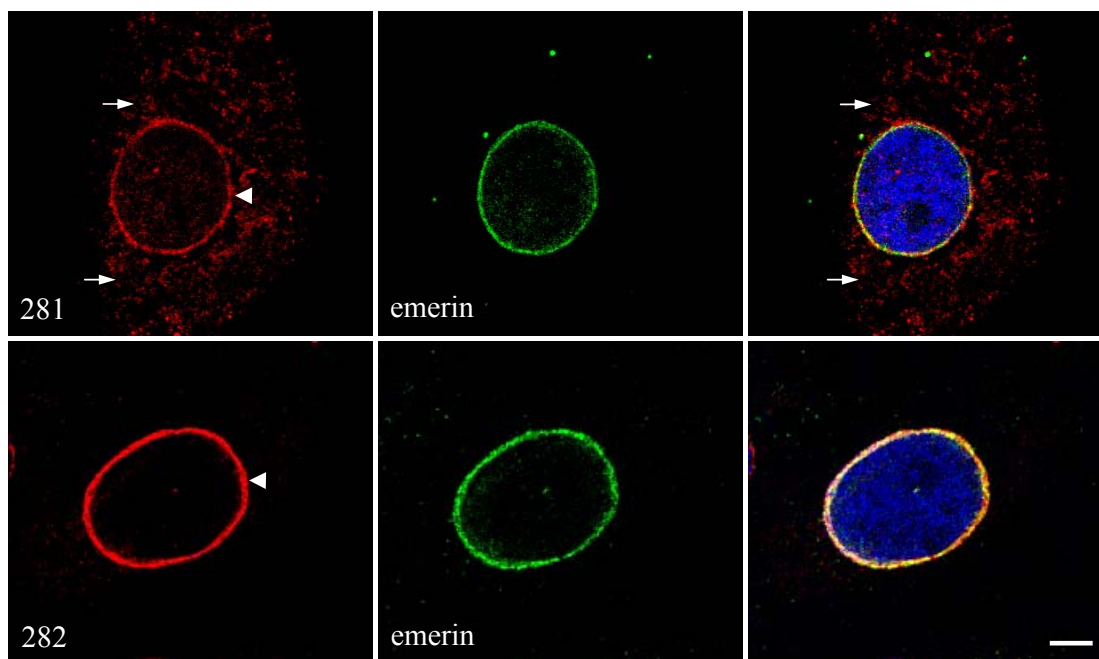


Figure 2.5. Endogenous human Sun1 localizes to the nuclear membrane in HaCaT cells. HaCaT cells were fixed with paraformaldehyde and stained with antibodies against the N-terminus (281) and the C-terminus of Sun1 (282), respectively. Emerin was stained by emerlin specific antibodies and DAPI was used for nuclear staining. The secondary antibodies used for 281 and 282 were conjugated with Alexa 568 and for emerlin were conjugated with Cy3. The cells were observed using the confocal microscope. Bar=6 μ m.

2.1.5 Domain analysis of Sun1

The mouse *SUN1* gene is located in the mouse chromosomal locus 5G.2, spanning 49 kb and is encoded by 25 exons. A schematic representation of the intron and exon organization of mouse Sun1 is represented in Figure 2.6A. *SUN1* codes for a 100 kDa protein (accession No. BC048156) and is composed of 913 amino acids. The protein was predicted to have three putative transmembrane domains (358-383, 386-407 and 413-531 aa) located approximately in the middle of the protein, using the Tmpred software (Hofmann & Stoffel, 1993). The SMART program predicted a ZnF-C2H2 domain (183-205 aa) at the N-terminus of the protein. The C-terminus of the protein contains two coiled-coil domains (492-527 and 563-632 aa). The last 175 amino acids form the evolutionarily conserved SUN domain (738-913

aa), which is highly homologous to *C. elegans* UNC-84. The region between the transmembrane and the SUN domain was divided into two subdomains, SD1 (432-632 aa) and SD2 (633-737 aa) for functional tests. SD1 contains the putative coiled-coils whereas SD2 does not contain any known structural features (Fig. 2.6B).

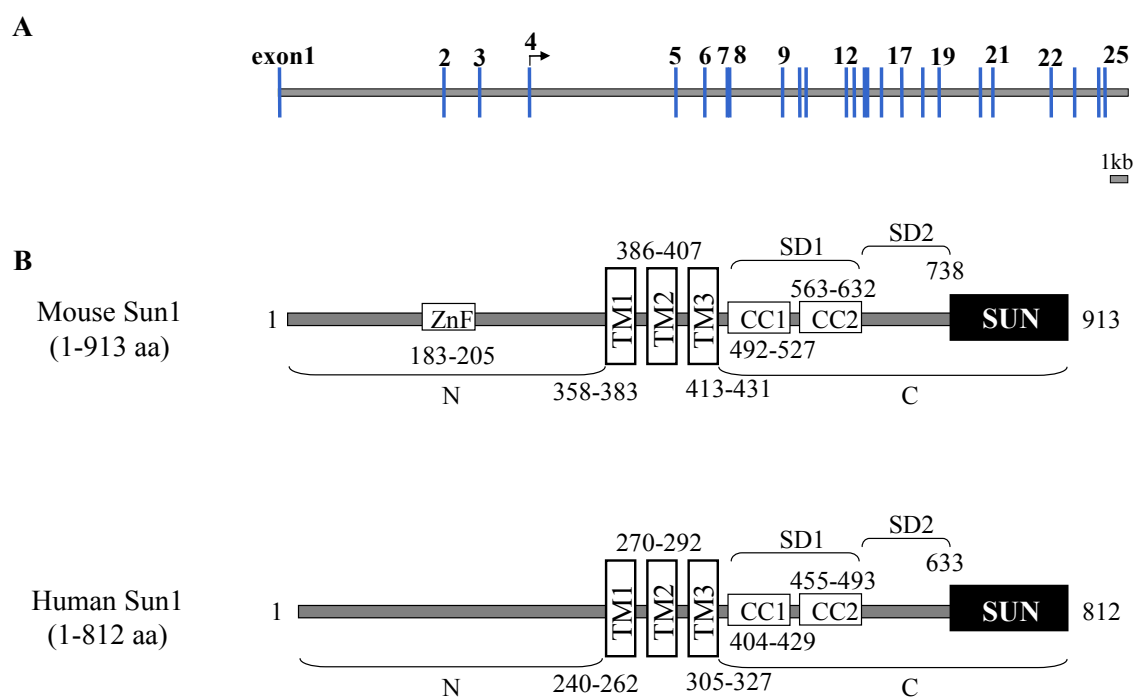


Figure 2.6. Genomic organization of mouse *SUN1* and domain architecture of mouse and human Sun1. (A) Stick diagram illustrating the genomic organization of the mouse *SUN1* locus. Numbered vertical blue bars denote exons, yellow bars between the blue bars represent introns. The start codon is denoted by arrow. The diagram is drawn to scale. Bar=1 kb (B) The domain architecture of mouse and human Sun1 were predicted by the computer program SMART (Simple Modular ARchitecture Research Tool) and TMpred (a transmembrane domain prediction software) program. Mouse Sun1 has three transmembrane domains in the middle of the protein. The N-terminus of the protein has a ZnF-C2H2 domain and the C-terminus has two coiled-coil domains. The C-terminal end of the protein is the evolutionarily homologous SUN domain. Human Sun1 shares the same domain architecture with mouse Sun1 except for the ZnF domain. The numbers below and above the schematic indicate amino acid positions of the Sun1 protein sequence.

Human Sun1 is a protein of 812 amino acids with a predicted mass of about 90 kDa. The domain structure of human Sun1 is identical to that of mouse, except that it lacks the

proposed zinc-finger motif (Fig. 2.6B). The whole protein sequence of human Sun1 shares about 69 % identity and 77 % similarity to that of mouse Sun1.

2.1.6 Sun1 has three transmembrane domains

Tmpred software predicted three transmembrane domains for mouse Sun1. However, other programmes like SMART revealed only two transmembrane domains, especially the first transmembrane domain (358-383 aa) was ambiguous. In order to illuminate the real transmembrane domain structure of Sun1, various constructs expressing EGFP fusion proteins containing the entire Sun1 N-terminus and the first (Sun1-1TM-N) or the first two transmembrane domains (Sun1-2TM-N) were made (Fig. 2.7A). Constructs were transiently transfected into COS7 cells and the transfected cells were examined by direct immunofluorescence. Sun1-2TM-N, which contains at least one real transmembrane domain, was localized to the nuclear membrane in transfected cells as shown in Figure 2.7B lower panel. Similarly to Sun1-2TM-N transfected cells, Sun1-1TM-N localized also to the nuclear membrane (Fig. 2.7B higher panel). The nuclear envelope localization of Sun1-1TM-N and Sun1-2TM-N are indicated by arrows. Thus, both fusion proteins have the ability to localize to the nuclear envelope suggesting that the first transmembrane domain is indeed a transmembrane domain. Haque *et al.* (2006) showed that the Sun1 N-terminus interacts with nuclear lamin A *in vitro*. This combined with our data, which show that Sun1 has three transmembrane domains and is able to span the inner nuclear membrane three times, suggests that the Sun1 N-terminus resides in the nucleoplasm, whereas the C-terminus is situated in the perinuclear space. Interestingly, a similar domain topology has been proposed for UNC-84 and matefin in *C. elegans* (Starr & Han, 2003; Fridkin *et al.*, 2004) and Sun2 in human (Hodzic *et al.*, 2004).

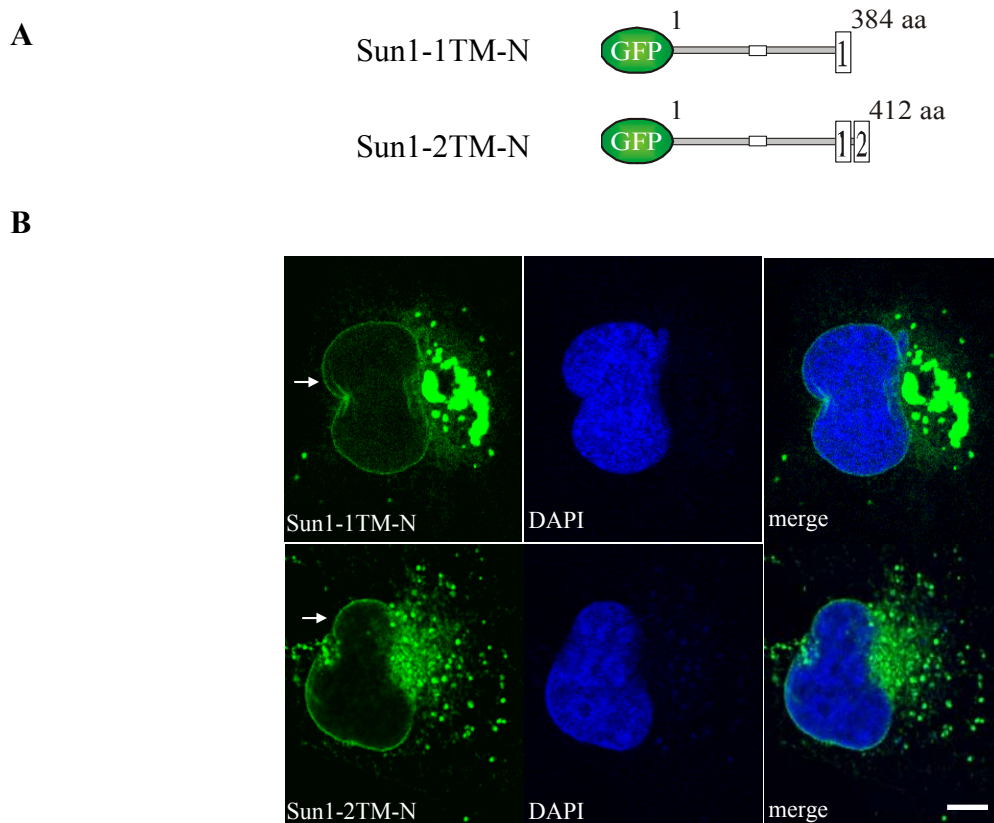


Figure 2.7. Sun1-1TM-N and Sun1-2TM-N localize to the nuclear envelope in COS7 cells. (A) Schematic GFP mouse Sun1 N-terminal constructs used in transfection experiments. Green oval indicates GFP and numbered boxes indicate transmembrane domains. (B) COS7 cells were transiently transfected with the appropriate plasmids and cells were subjected to direct fluorescence microscopy. DAPI was used to stain the nuclei. Images were taken with a confocal microscope. Bar =10 μ m.

2.1.7 Sun1 dynamics at the nuclear envelope

Sun1 is an inner nuclear membrane (INM) protein, and the N- and C-termini of Sun1 can be recruited to the NE, independently (Padmakumar *et al.*, 2005). It has been proposed that integral INM proteins are retained at the INM by forming stable interactions with other INM proteins, the nuclear lamina or chromatin (Ohba *et al.*, 2004). Therefore the N- and C-termini of Sun1 are likely to have distinct interactions at the nuclear envelope. Such interactions can be reflected by the kinetic properties of the protein. To investigate more accurately the kinetic properties of Sun1 full-length and the Sun1 N- and C-termini at the nuclear envelope, we performed inverse fluorescence recovery after photobleaching experiments (iFRAPs).

iFRAPs are more suitable to analyze binding interactions than classical FRAPs because the free pool of the tagged protein is bleached away, allowing precise measurement of the fluorescence changes of only the bound molecules. In an iFRAP, the entire cellular fluorescence is photobleached except for a small nuclear membrane region of interest containing the unbleached tagged proteins (Fig. 2.8). The dissociation of the tagged protein from the nuclear membrane is then reflected by the loss of fluorescence from this region over time monitored by confocal microscopy. The dissociation kinetics reflects the stability of the protein at the nuclear envelope.

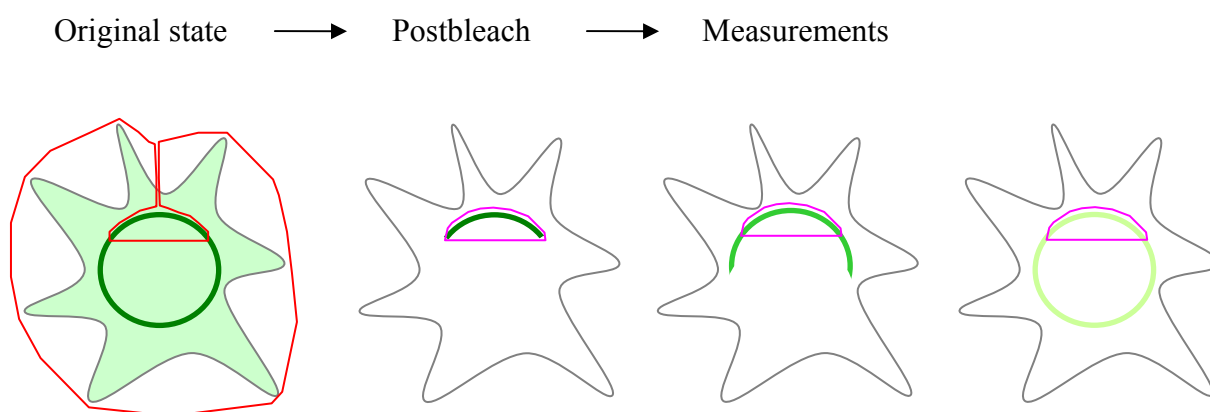


Figure 2.8. Presentation of the iFRAP technique. The scheme depicts the different stages of a typical cell with nucleus (dark green circle) and cytoplasm (light green) in iFRAP. Bleached region is marked by the red boundary. All of the fluorescence of the cell is bleached except for a small region of interest (pink boundary). The postbleach images are analyzed to display the loss of fluorescence from the unbleached region.

To estimate the binding ability of distinct domains of Sun1, GFP-tagged Sun1 full-length and various N- and C-terminal polypeptides containing different functional domains (Fig. 2.9) were used in iFRAPs. As depicted in Figure 2.9, GFP-tagged Sun1 full-length, Sun1-2TM-N, Sun1-TM-C, Sun1-TM-SD1, 2 and Sun1-TM-CC- Δ SUN were transiently transfected in HeLa cells. All fusion proteins are nuclear membrane associated. Figures 2.10A, 2.11A and C, 2.12A and C, show single iFRAP experiments for Sun1 full-length and for four structurally distinct Sun1 GFP-fusions with different dynamic behaviors. At least four similar experiments

were performed for each GFP-tagged protein and were averaged to generate the mean fluorescence decays plotted in Figure 2.10B, 2.11B and D, 2.12B and D.

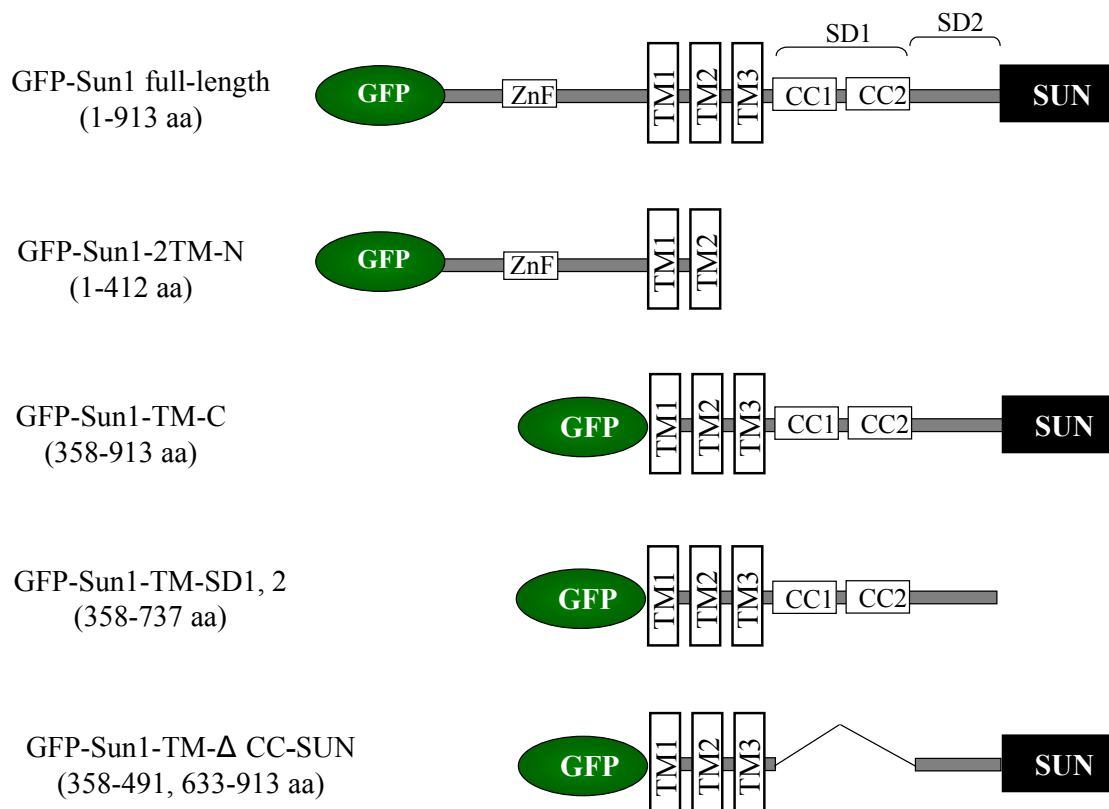


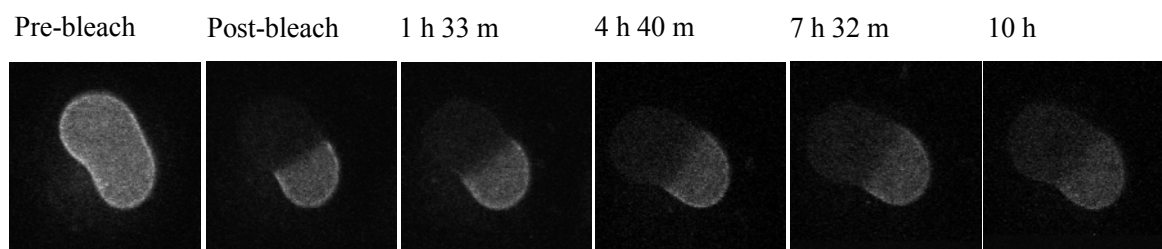
Figure 2.9. Schematic of GFP-Sun1 and different N-/C-terminally truncated Sun1 constructs, which were employed in the iFRAP assays. The GFP part is indicated by green ovals. Sun1 amino acid residues fused to GFP are indicated by numbers. Domain labeling is shown as in Figure 2.6. The constructs were transfected into HeLa cells by FUGENE 6 to determine the dynamics of Sun1 at the nuclear envelope. GFP: green fluorescent protein; ZnF: zinc finger; TM: transmembrane domain; CC: coiled-coil domain; SUN: Sad1/UNC-84 homology domain.

2.1.7.1 iFRAPs of GFP-Sun1 full-length

Similar to endogenous Sun1 protein, GFP-Sun1 full-length mostly localized to the nuclear membrane in transfected cells. The whole cell except 1/3 of the nuclear envelope region was bleached. The fluorescence within this region of interest (ROI) was then followed every 3 minutes over a period of up to 10 hours. To calculate the loss of fluorescence attributed to the imaging process alone, the sum of pixel intensities was also calculated for the

entire cell. This was used to normalize the fluorescence intensity for each ROI. The fluorescent signal of GFP-Sun1 full-length dropped very slowly, and had a residence time of more than 10 hours (Fig 2.10). This indicates that a large proportion of Sun1 at the nuclear membrane is immobile, at least within the time frame of these experiments.

A



B

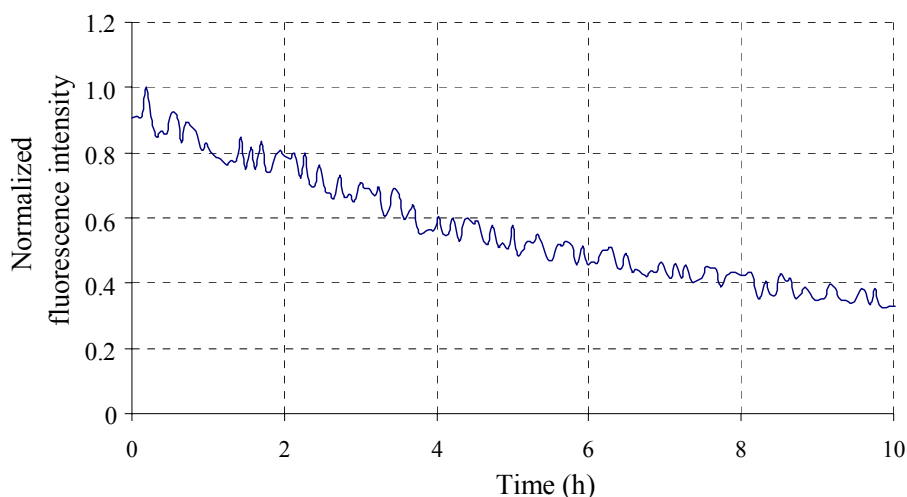


Figure 2.10. GFP-Sun1 full-length dynamics at the nuclear envelope. (A) HeLa cells expressing GFP-Sun1 were imaged before and after photobleaching of the entire nucleus, with the exception of a small region of the nuclear envelope. The loss of fluorescent signal was monitored using time-lapse microscopy. (B) Corresponding plots of fluorescence decay kinetics from the unbleached region of iFRAP experiments of GFP-Sun1. Six individually transfected cells were measured. The experiments were performed on a customized LSM510 confocal microscope using a 40 x 1.3 NA oil objective and a completely open pinhole.

2.1.7.2 iFRAPs of GFP-Sun1-2TM-N and GFP-Sun1-TM-C

GFP-Sun1-2TM-N and GFP-Sun1-TM-C have the ability to localize to the nuclear envelope. In many cases we also observed substantial accumulation of the fusion proteins in the ER as shown in the pre-bleach images of Figure 2.11A and 2.11C (arrows). GFP-Sun1-

2TM-N had a residence time of 35 min and GFP-Sun1-TM-C had a residence time of 29 min (Fig. 2.11). Thus, both constructs display a significantly reduced stability when compared to full-length Sun1. These results suggest that both N- and C- termini of Sun1 are required for the stability of Sun1 at the nuclear envelope.

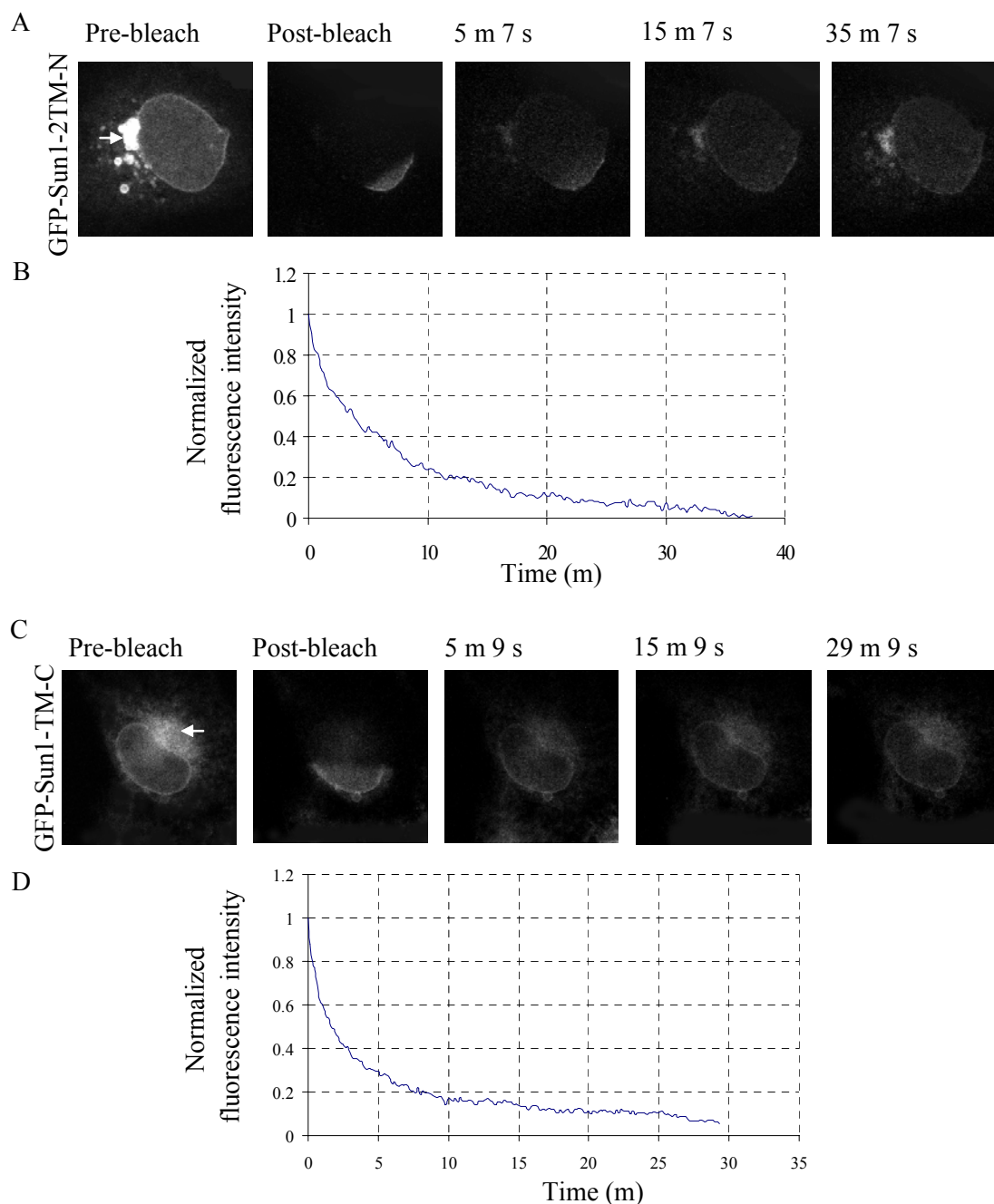
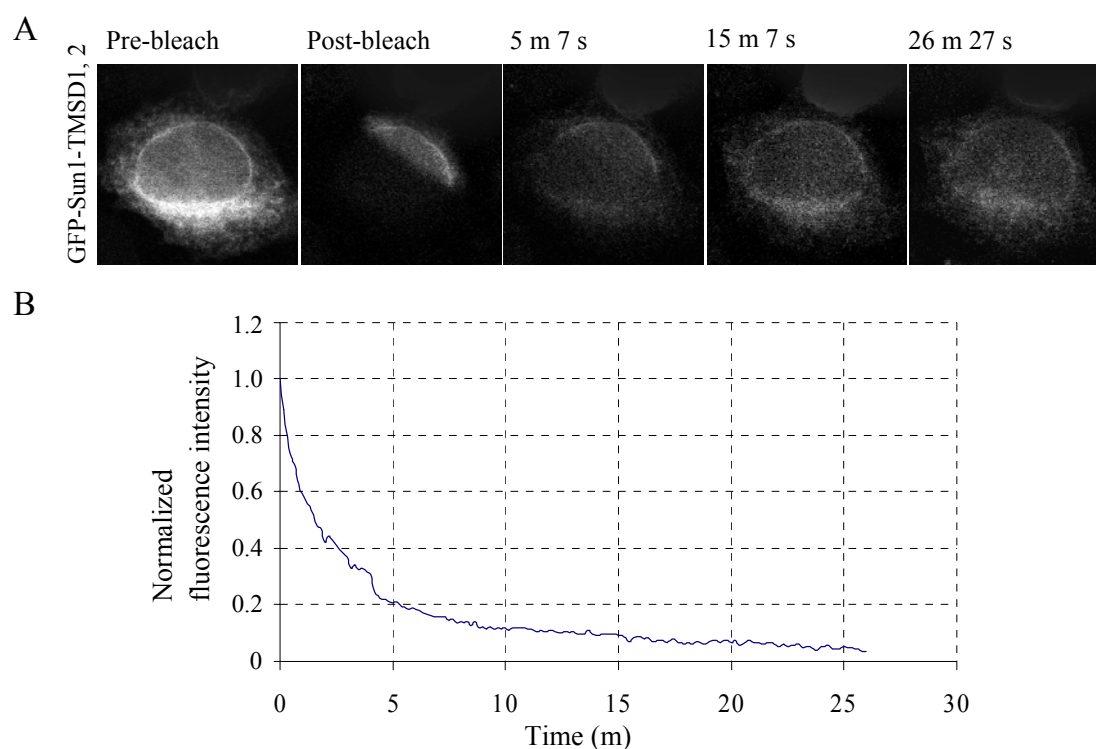


Figure 2.11. GFP-Sun1-2TM-N and GFP-Sun1-TM-C dynamics at the nuclear envelope. (A) and (C) Selected images of iFRAPs in GFP-Sun1-2TM-N and GFP-Sun1-TM-C transfected cells, respectively. Arrows indicate the accumulation of the GFP-fusions in the ER. (B) and (D) Corresponding plots of fluorescence decay kinetics from the unbleached region of iFRAP experiments of GFP-Sun1-2TM-N and GFP-Sun1-TM-C. Four individual cells for each construct were analyzed.

2.1.7.3 iFRAPs of GFP-Sun1-TM-SD1, 2 and GFP-Sun1-TM- Δ CC-SUN

GFP-Sun1-TM-SD1, 2 and GFP-Sun1-TM- Δ CC-SUN are clearly associated with the nuclear membrane and the ER membrane as represented in the pre-bleach images in Figure 2.12A and C. GFP-Sun1-2TM-SD1, 2 had a residence time of about 26 min (Fig. 2.12A and 2.12B), which is slightly faster than that of GFP-Sun1-TM-C. However, when iFRAP was applied to cells expressing GFP-Sun1-TM- Δ CC-SUN, the major fraction of the fluorescence signal for GFP-Sun1-TM- Δ CC-SUN dropped rapidly within 2 min and GFP-Sun1-TM- Δ CC-SUN had a residence time of ~8-10 min (Fig. 2.12 C and D), which is much lower than that of GFP-Sun1-TM-C and GFP-Sun1-TM-SD1, 2. The fast drop-down of the fluorescence signal of GFP-Sun1-TM-C, GFP-Sun1-TM-SD1, 2 and GFP-Sun1-TM- Δ CC-SUN within the first 10s after bleaching may be due to the migration of unbound GFP molecules in the unbleached ER region. GFP-Sun1-TM-SD1, 2 which contains the coiled-coil domains and lacks the SUN domain is more stable than GFP-Sun1-TM- Δ CC-SUN which contains the SUN domain but lacks the coiled-coil domains, suggesting that the SUN domain of Sun1 may have a more



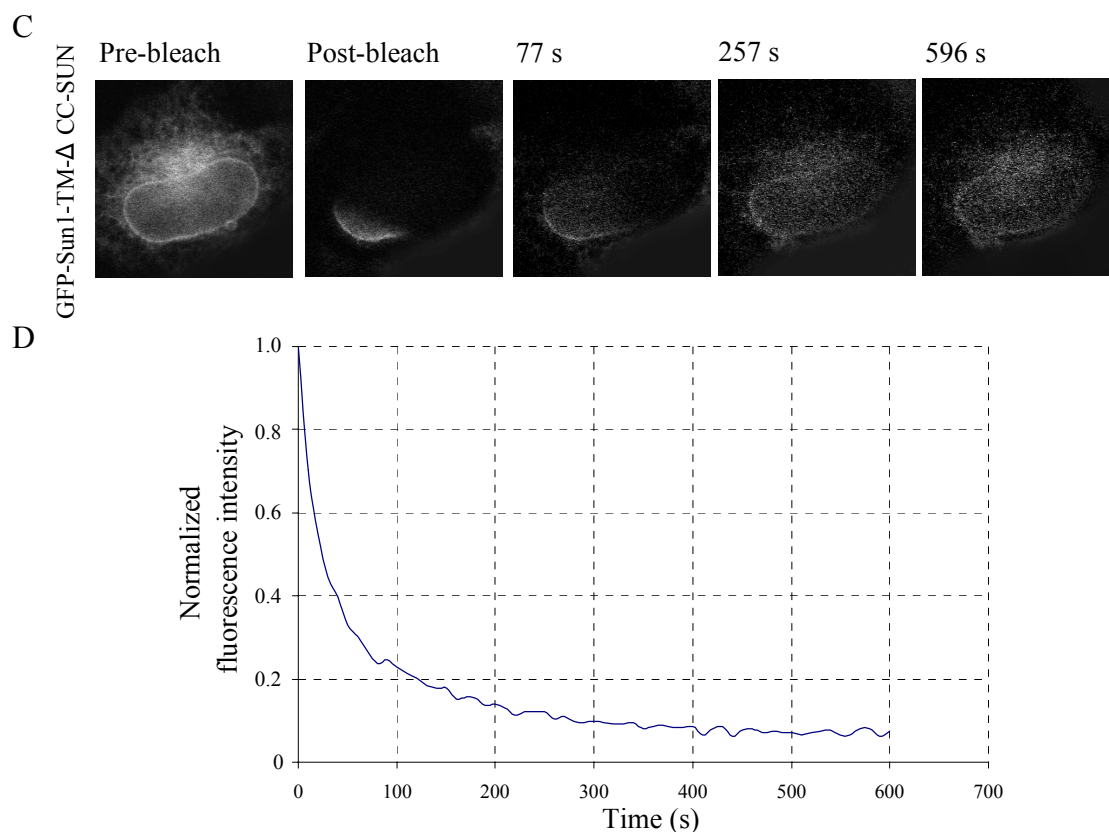


Figure 2.12. GFP-Sun1-TM- Δ CC-SUN dynamics at the nuclear envelope. (A) and (C) Selected images of iFRAPs of GFP-Sun1-TM-SD1, 2 and GFP-Sun1-TM- Δ CC-SUN transfected cells, respectively. (B) and (D) Corresponding plots of fluorescence decay kinetics from the unbleached region of iFRAP experiments of GFP-Sun1-TM-SD1, 2 and GFP-Sun1-TM- Δ CC-SUN. Four individual GFP-Sun1-TM-SD1, 2 transfected cells and six GFP-Sun1-TM- Δ CC-SUN transfected cells were investigated by iFRAPs.

dynamic binding at the nuclear membrane in comparison to the N-terminal domain and the C-terminal coiled-coil domains. Moreover, the coiled-coil domains appear to be important for Sun1 NE dynamics suggesting that these domains may have additional binding partners at the nuclear envelope.

In summary, as shown in Table 1, GFP-Sun1 full-length has a residence time of more than 10 hours in iFRAPs, indicating that Sun1 is an immobile protein closely associated with the nuclear envelope. GFP-Sun1-2TM-N and GFP-Sun1-TM-C have residence times of 35 minutes and 29 minutes respectively, which are much more mobile than GFP-Sun1 full-length, suggesting that the stability of Sun1 at the nuclear envelope requires both Sun1 N- and C-

termini. GFP-Sun1-TM-SD1, 2, which contains the coiled-coil domains, has a residence time of 26 minutes that is slightly faster than GFP-Sun1-TM-C. However, GFP-Sun1-TM- Δ CC-SUN, which contains only the SUN domain, migrated much faster than other GFP-Sun1 fusions and it has a residence time of 8-10 minutes. Thus, the Sun1 coiled-coil domains may be significant nuclear envelope retention domains.

Table 1. GFP-tagged Sun1 dynamics at the NE

Sun1 fusion proteins	Residence time in iFRAPs
GFP-Sun1 full-length	More than 10 hours
GFP-Sun1-2TM-N	~35 minutes
GFP-Sun1-TM-C	~29 minutes
GFP-Sun1-TM-SD1, 2	~26 minutes
GFP-Sun1-TM- Δ CC-SUN	~8-10 minutes

Table 1. Dynamics of GFP-tagged Sun1 fusions at the nuclear envelope. HeLa cells were transiently transfected with GFP fusion constructs and examined 48 hours after transfection. iFRAPs were performed on a customized LSM510 confocal microscope. Most cellular fluorescence was bleached using full laser power and leaving only a fraction (typically 10–20%) of the nuclear envelope unbleached. Post-bleach images were then acquired for up to 10 hours at regular time intervals, depending on the dynamics of the GFP fusion proteins. In iFRAPs, GFP-Sun1 full-length has a residence time of more than 10 hours. GFP-Sun1-2TM-N, GFP-Sun1-TM-C and GFP-Sun1-TMSD1, 2 reside at the NE ~35, ~29 and ~26 minutes, respectively. GFP-Sun1-TM- Δ CC-SUN has a residence time of 8-10 minutes.

2.1.8 Sun1 interacts with chromatin

The iFRAPs on Sun1 full-length suggest that Sun1 is a stable integral protein at the nuclear envelope. Although Sun1 interacts with lamin A, the presence of lamin A/C is not required for Sun1 nuclear envelope localization (Haque *et al.*, 2006). Therefore, Sun1 was proposed to bind to other nuclear factors. Many INM proteins like emerin, LAP2, MAN1 or lamin B receptor, interact with chromatin-associated proteins or bind directly to DNA, providing a membrane anchor important for chromatin organization (Wolff *et al.*, 2001; Cai *et al.*, 2001; Lin *et al.*, 2000; Ye *et al.*, 1997). Sun1 is also an INM protein with its N-terminus exposed to the nucleoplasm. Interestingly mouse Sun1 contains a predicted zinc finger DNA-

binding motif. Therefore, a similar interaction between Sun1 and chromatin may exist. In order to test whether Sun1 interacts with chromatin, we carried out chromatin immunoprecipitation assays (ChIP). Formaldehyde cross-linked chromatin extracts from sonicated HaCaT cells were incubated with Sun1 antibodies (Sun1 281) and after immunoprecipitation, the proteins were removed by proteinase K treatment. The precipitated DNA was analyzed by PCR using a set of primers binding to the 5' UTR of GAPDH. Antibodies against RNA polymerase II were used as positive control and an unrelated antibody (negative IgG) was used as a negative control. As depicted in Figure 2.13, the DNA fragment was coimmunoprecipitated by Sun1 antibodies but not with the negative control IgG antibodies. Our results indicate thus, that Sun1 is able to interact with chromatin.

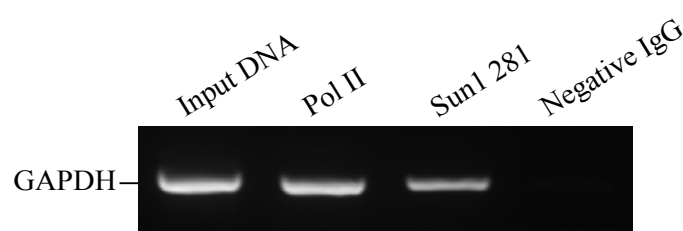


Figure 2.13. Sun1 interacts with chromatin in HaCaT cells. HaCaT cell lysates were sheared by sonication and used in chromatin immunoprecipitation assays in the presence of N-terminal Sun1 polyclonal antibodies (281). Primers binding to exon 1 of the *GAPDH* gene (for primer sequences please see materials and methods) were designed and used for detection of immunoprecipitated DNA. An unrelated antibody (negative IgG) was used for a control immunoprecipitation. An antibody against RNA polymerase II (Pol II) was used as a positive control. Input DNA was isolated genomic DNA from the sheared HaCaT cell lysates, which was used to test the designed primers.

2.1.9 Sun1 oligomerizes via its coiled-coil domains

The results of the above iFRAP experiments suggested that the Sun1 coiled-coil domains may be a significant nuclear envelope retention domain. Coiled-coils have traditionally been recognized as an oligomerization unit in a large number of proteins (Burkhard *et al.*, 2001). Thus, one attractive mechanism would be that oligomerization of the GFP-fusion protein with the endogenous Sun1 leads to the retention of the GFP-fusion protein at the NE. To

investigate whether the predicted coiled-coils within the C-terminus of Sun1 are required for oligomerization, biochemical studies were performed.

The cDNA sequence encoding mouse Sun1 SD1, 2 (residues 432-737), which contains the Sun1 coiled-coil domains were amplified by PCR, and cloned into pGEX4T-1 vector and expressed in *E. coli* as GST fusion protein (GST-SD1, 2) and purified by affinity chromatography with Glutathione Sepharose 4B under native conditions. Thrombin digestion of GST-SD1, 2 generated the GST-free Sun1 SD1, 2 polypeptides (Fig. 2.14). The purified SD1, 2 was used for *in vitro* Native-PAGE and cross-linking assays.

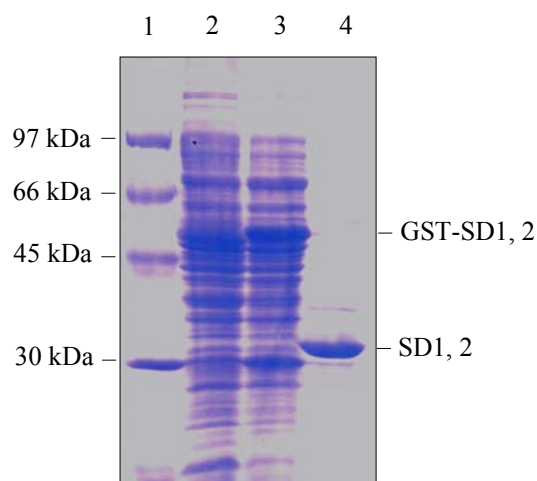


Figure 2.14. Purification of mouse Sun1 SD1, 2 from *E. coli*. 1. Standard low molecular weight markers 2. Cell lysate of uninduced bacterial host DH5 α 3. Cell lysate of IPTG induced bacteria, which expressed GST-SD1, 2 fusion protein. 4. Purified SD1, 2 fraction after thrombin digestion. Samples were loaded on a 12 % polyacrylamide gel and stained by Coomassie blue.

SDS-PAGE analysis of the purified SD1, 2 demonstrated that under reduced conditions the protein behaves as a monomer (32 kDa) (Fig. 2.15A). To examine whether SD1, 2 oligomerizes under native conditions, we performed Native-PAGE analysis, which is essentially used to determine native masses and oligomeric states. Purified SD1, 2 was mixed with 2 x native sample buffer and loaded into the native gel without heating. BSA was used as the standard. The gel was run at 4°C and subsequently stained with Coomassie Blue. By

Native-PAGE we indeed observed a dimer band (64 kDa) and an additional tetramer band migrating as a 130 kDa protein (Fig. 2.15B).

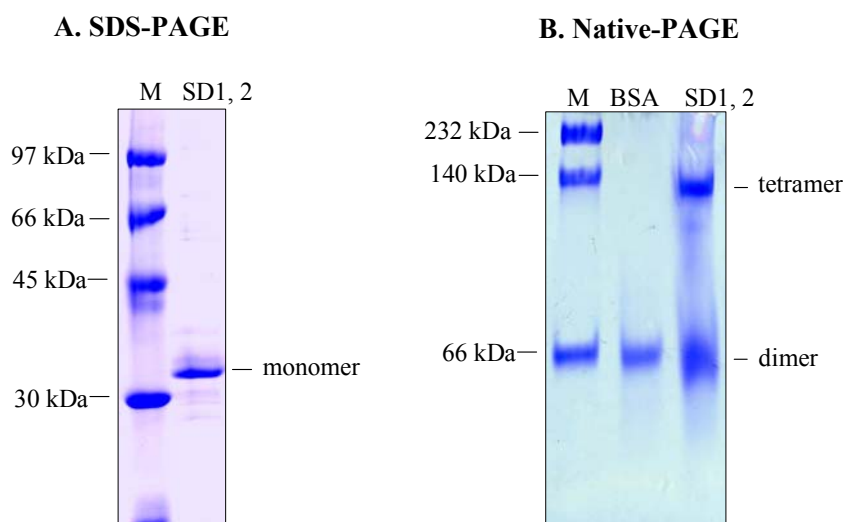


Figure 2.15. The purified mouse Sun1 SD1, 2 forms dimers and tetramers under native conditions. (A) Purified SD1, 2 recombinant protein was supplemented with SDS sample buffer containing β -mercaptoethanol and subjected to SDS-PAGE using a 12% SDS-polyacrylamide gel. M, standard low molecular weight marker proteins; SD1, 2, purified SD1, 2 fraction of mouse Sun1 under reduced conditions. (B) Native-PAGE. Just before gel loading, the purified SD1, 2 was supplemented with blue native sample buffer lacking SDS and β -mercaptoethanol. The samples were loaded on a 10% native-polyacrylamide gel. After electrophoresis, the gel was visualized by Coomassie staining. M, native molecular weight marker; SD1, 2, purified SD1, 2 fraction under native conditions. BSA was loaded as control. BSA; Bovine serum albumin.

In addition to Native-PAGE analysis, we also performed chemical cross-linking experiments to provide additional evidence for the oligomerization of the Sun1 coiled-coil domains. The purified Sun1 SD1, 2 proteins were submitted to cross-linking using various concentrations of glutaraldehyde. The cross-linked samples were then analysed by SDS-PAGE. Without glutaraldehyde treatment, only the monomer band was observed. While the purified SD1, 2 proteins were treated with the cross-linking reagent, a dimer and tetramer bands were evident on the Coomassie stained gels. Furthermore, the relative amount of the monomer was reduced, indicating that the SD1, 2 fractions containing coiled-coils forms

dimers or oligomers *in vitro* (Fig. 2.16A). In contrast, when we performed a similar assay using BSA as negative control, no higher mass polypeptides were detected in the samples treated with the glutaraldehyde cross-linking reagent (Fig. 2.16B).

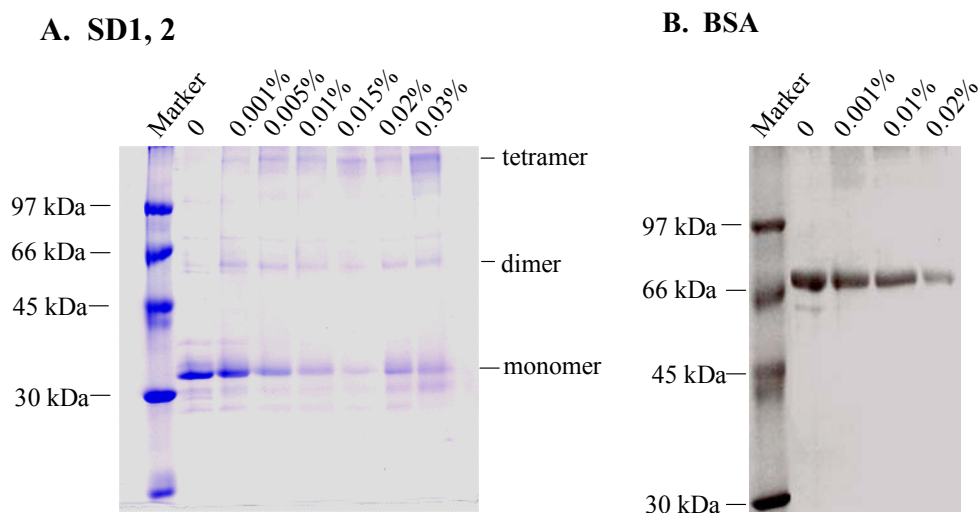


Figure 2.16. The Sun1 SD1, 2 oligomerizes when cross-linked with glutaraldehyde. (A) Equal amounts of the purified mouse Sun1 SD1, 2 were cross-linked with 0.001%-0.03% glutaraldehyde for 30 minutes at room temperature, respectively. Reactions were terminated by addition of SDS sample buffer. The samples were loaded on a 12 % SDS gel and stained by Coomassie Blue. (B) As a negative control, BSA was cross-linked with 0.001%-0.02% glutaraldehyde and examined by SDS-PAGE analysis.

To further corroborate our *in vitro* results, we performed GST pull-down assays. For this we fused GST to the coiled-coil domains of Sun1 (GST-Sun1-SD1; 432-632 aa) to pull down ectopically expressed GFP-Sun1-SD1, 2 (432-737 aa) fusion proteins from COS7 cell lysates (Fig. 2.17A). The GFP-Sun1-SD1, 2 fusions lack the transmembrane domain and localize diffusely in the cytoplasm (data not shown). As anticipated GST-Sun1-SD1 was able to precipitate GFP-Sun1-SD1, 2 from COS7 cell lysates (Fig. 2.17C). In contrast to GST-Sun1-SD1, no interaction with GFP-Sun1-SD1, 2 was observed for GST alone (Fig. 2.17C). To confirm that coiled-coil domains indeed oligomerizes with itself but not with the SD2 domain, GFP-Sun1-SD2 (432-491, 633-737 aa) was constructed, expressed in COS7 cells and used in GST pull-down assays. As shown in Figure 2.17C, there is no interaction between GST-Sun1-SD1 and GFP-Sun1-SD2.

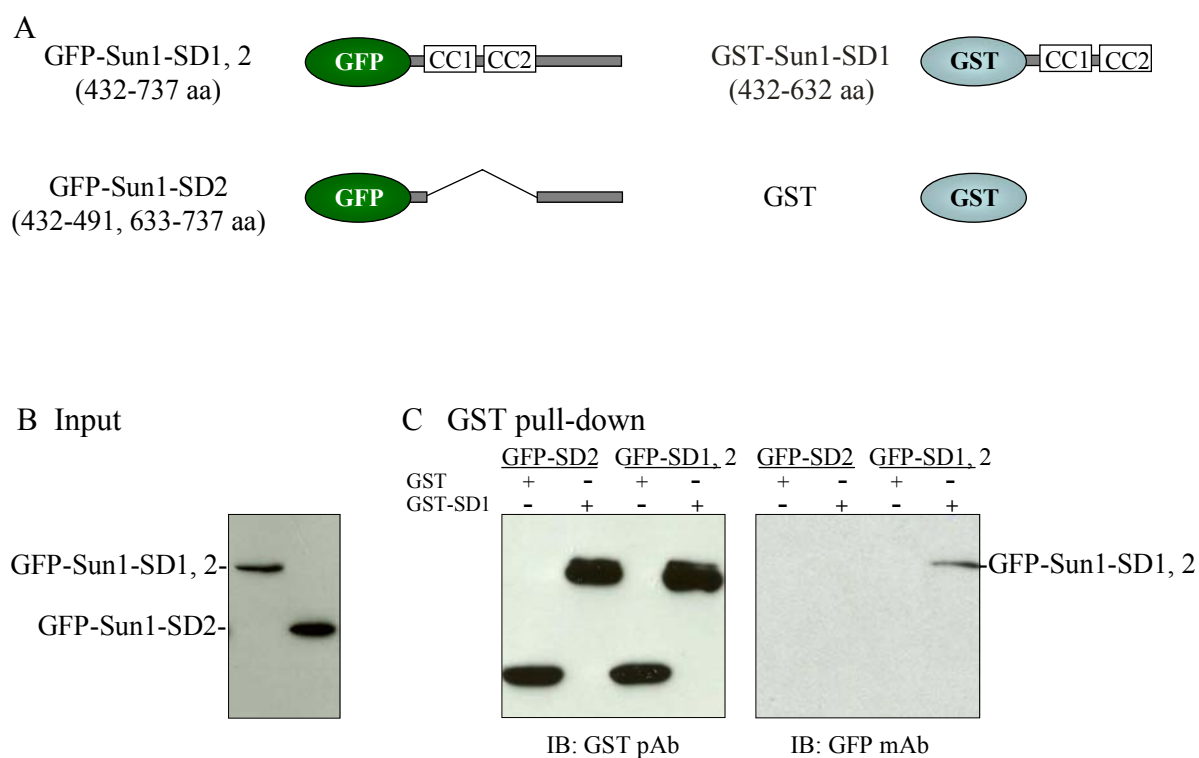


Figure 2.17. The Sun1 coiled-coil domain self-associates. (A) Schematic representation of the GFP-Sun1-SD1, 2, GFP-Sun1-SD2, and GST-SD1 fusion proteins. GFP is indicated by a green oval and GST is indicated by a cyan oval. CC1 and CC2 are predicted coiled-coils. (B) COS7 cells were transiently transfected with GFP-Sun1-SD1, 2 and GFP-Sun1-SD2, respectively. The cell lysates were analyzed by immunoblotting using anti-GFP antibodies. A 66 kDa band representing GFP-Sun1-SD1, 2 and a 42 kDa band representing GFP-Sun1-SD2 were detected. (C) COS7 cell lysates expressing the GFP-Sun1-SD1, 2 or GFP-Sun1-SD2 were incubated with the immobilized GST-SD1 as indicated and GST as control. Specifically bound proteins (pellet of the pull-down assays) were subjected to SDS-PAGE followed by western blot analysis using GST-specific antibodies. The same membrane was later stripped and submitted to anti-GFP immunoblotting.

Collectively the Native-PAGE, cross-linking and GST pull-down analysis indicate that the mouse Sun1 coiled-coil domains oligomerize *in vitro*. Mouse Sun1 is highly homologous to human Sun1 and both proteins share identical domain structures. Thus, human Sun1 may also form oligomers via the coiled-coil domains. Therefore, we tested the oligomerization of the human Sun1 coiled-coil domains *in vivo*, by means of a yeast two-hybrid system analysis. For that, the coiled-coil domains were fused with GAL4 DNA-binding domain in the

pGBKT7 vector (BD-hSun1-CC, 404-493 aa) and GAL4 transcription activation domain in the pGADT7 vector (AD-hSun1-CC, 404-493 aa), respectively (Fig. 2.17A). Figure 2.18B shows that cells cotransformed with pGADT7 and pGBKT7-hSun1-CC, or pGBKT7 and pGADT7-hSun1-CC did not grow on the selection plate and did not secrete β -galactosidase when they grew on the permissive plate (note lack of the blue colour of colonies in the right image). However, cells cotransformed with pGADT7-hSun1-CC and pGBKT7-hSun1-CC grew on the selection plate and in addition, were positive for the β -galactosidase test (blue colonies in the right image). Thus, both human and mouse Sun1 form homo-oligomers through their coiled-coil domains.

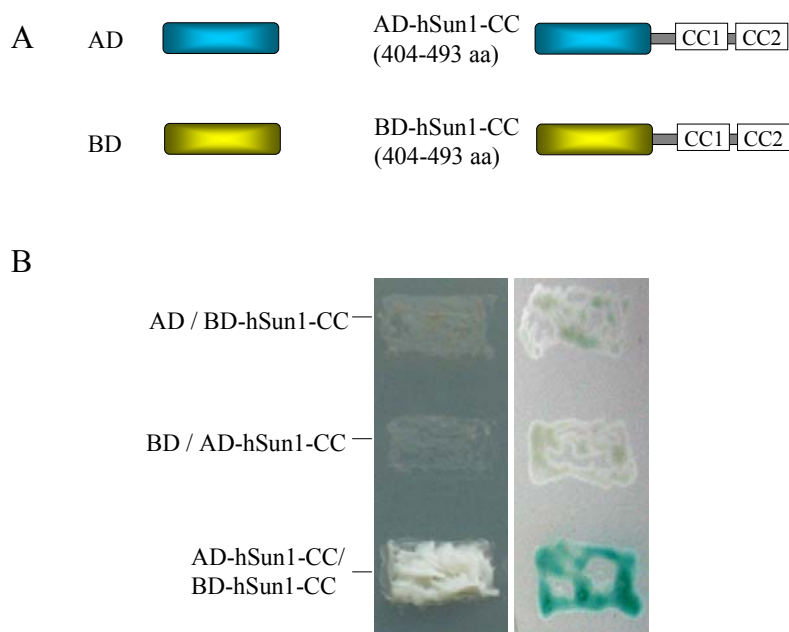


Figure 2.18. The human Sun1 coiled-coil domain interacts with itself *in vivo*. (A) Schematic diagrams of the AD-hSun1-CC and BD-hSun1-CC fusion proteins. AD: GAL4 activation domain (blue bar); BD: GAL4 DNA binding domain (yellow bar). CC1 and CC2: coiled-coils of human Sun1. (B) Yeast two-hybrid assays demonstrate that the coiled-coils of human Sun1 interact with each other. The empty BD and AD plasmids were used as negative controls. Y190 yeast cells were cotransformed with pGADT7/pGBKT7-hSun1-CC, pGBKT7/pGADT7-hSun1-CC or pGADT7-hSun1-CC/pGBKT7-hSun1-CC. The interaction was monitored by growth on SD-Trp-Leu-His (60 mM 3AT) plate (left panel). An X-Gal assay was also performed to confirm the interaction (right panel).

2.1.10 Sun1 forms SDS-resistant dimers under non-reducing conditions

To gain further insights into the oligomerization mechanism of Sun1, we next focused our studies on the full-length Sun1 protein. For this we transfected C-terminal V5-tagged human Sun1 full-length into COS7 cells and analyzed the cell lysates by anti-V5 western blotting. Interestingly, we observed that Sun1 forms SDS-resistant dimers under non-reducing conditions. Without heating and in the absence of DTT in the COS7 lysates, monomer, dimer and tetramer bands were detected even under high SDS conditions (0.5%). In the presence of 100 mM dithiothreitol (DTT), the dimer and the higher molecular mass signals were abolished. Heating of the samples at 70°C or 95°C resulted in a decrease in the intensity of known monomeric signal, through an irreversible aggregation of Sun1-V5 (arrow in Fig. 2.19), a known effect for some transmembrane proteins (Favreau *et al.*, 2001).

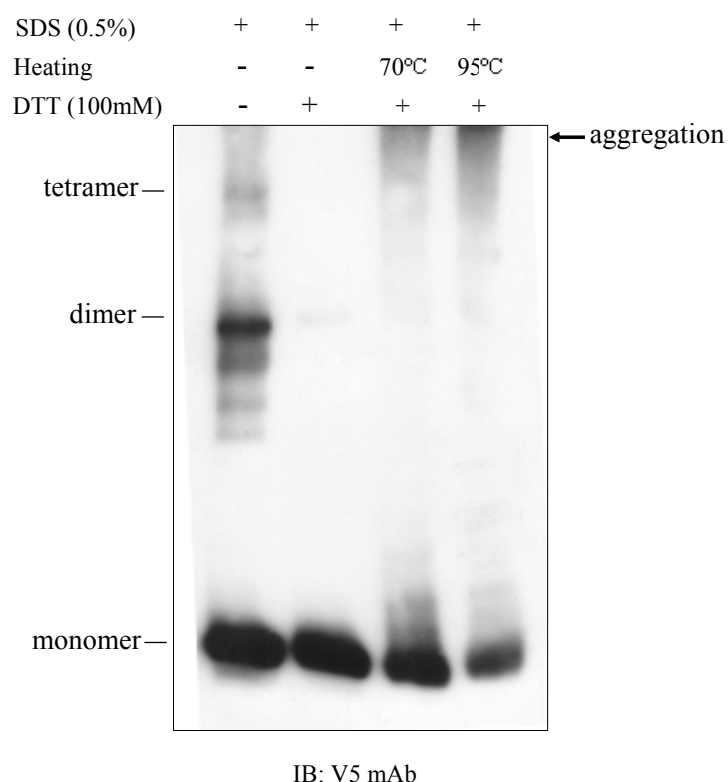


Figure 2.19. V5-tagged human Sun1 full-length forms SDS-resistant dimers under non-reducing conditions. Sun1-V5 was transiently transfected in COS7 cells and the transfected cells were lysed by RIPA buffer. The cell lysates were evenly divided into four portions, and each portion was treated under different experimental conditions as indicated on the top of the blot, then same amount of protein lysates were resolved by 6 % SDS-PAGE and detected by anti-V5 immunoblotting (IB) analysis.

2.1.11 The C-terminal domain of Sun1 forms SDS-resistant dimers under non-reducing conditions through disulfide bond formation

The data presented point out that the V5-tagged full-length human Sun1 protein has the ability to form SDS-resistant dimers under non-reduced conditions, which imply the existence of disulfide bonds between two Sun1 molecules. We know from the Native-PAGE analysis that under native conditions, the purified mouse Sun1 SD1, 2 proteins form tetramers in addition to dimers. Disulfide bonds might be involved in the formation of mouse Sun1 SD1, 2 tetramers. To verify the potential domain mediating the formation the SDS-resistant dimers, we first analyzed the amino acid sequences of Sun1 C-terminal regions. As depicted in Figure 2.20, four conserved cysteine residues are present in the human and mouse Sun1 C-termini. One is located in the SD2 domain (Cys⁵²⁶) the other three conserved cysteine residues (Cys⁶⁵⁷, Cys⁶⁹⁵, Cys⁸⁰⁰) reside in the SUN domain.

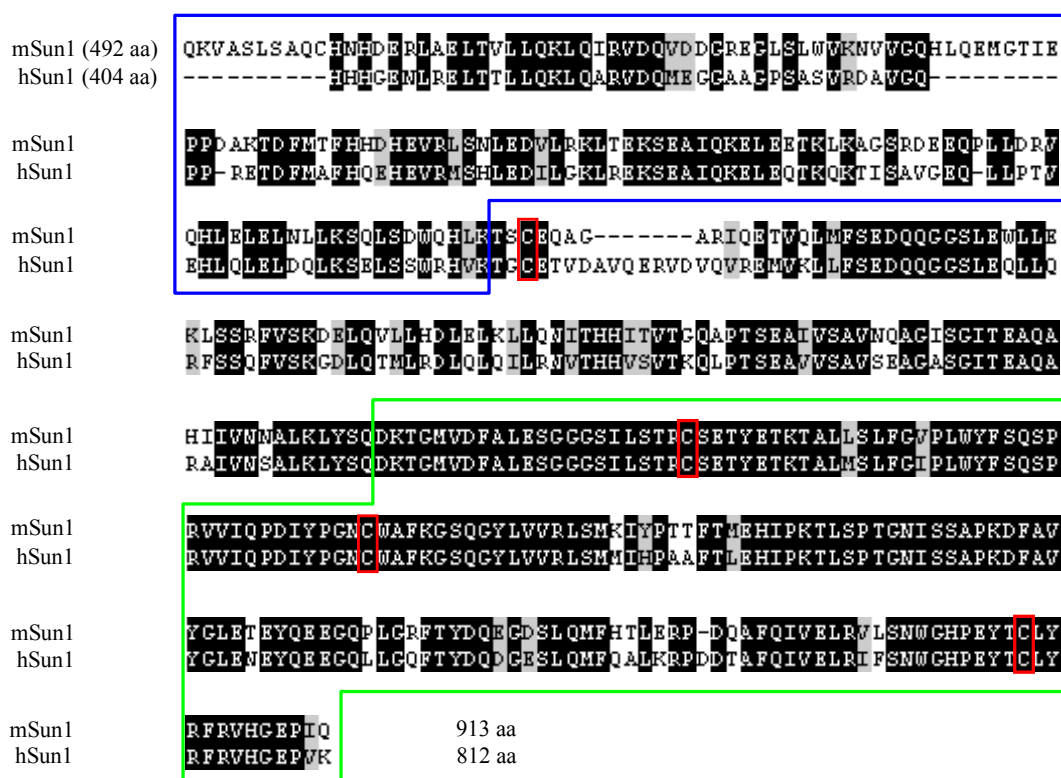


Figure 2.20. Alignment of the mouse and human Sun1C-terminus. Identical residues and conservative substitutions are shown in black and gray, respectively. The conserved cysteine residues are marked by red frames. One is located in SD2 domain and three in the SUN domain. The protein sequences in the blue frame correspond to the mouse and human Sun1coiled-coil domains. The mouse and human Sun1 SUN domain sequences are denoted by the green frame. The amino acids between coiled-coil domain and SUN domain form SD2 domains.

In order to test whether the cysteine in the SD2 domain, the cysteine residues in the SUN domain or the cysteine residues in both SD2 and SUN domain were sufficient to mediate the formation of disulfide linked dimers, two constructs encoding human Sun1 TMC-HA (240-812 aa) which contains all of the four conserved cysteines (Cys⁵²⁶, Cys⁶⁵⁷, Cys⁶⁹⁵, Cys⁸⁰⁰) in the SD2 and SUN domain, and TMSD1, 2-HA (240-632 aa) which contains the cysteine (Cys⁵²⁶) in SD2 domain were generated (Fig. 2. 21A). We choose to use the HA tag, because

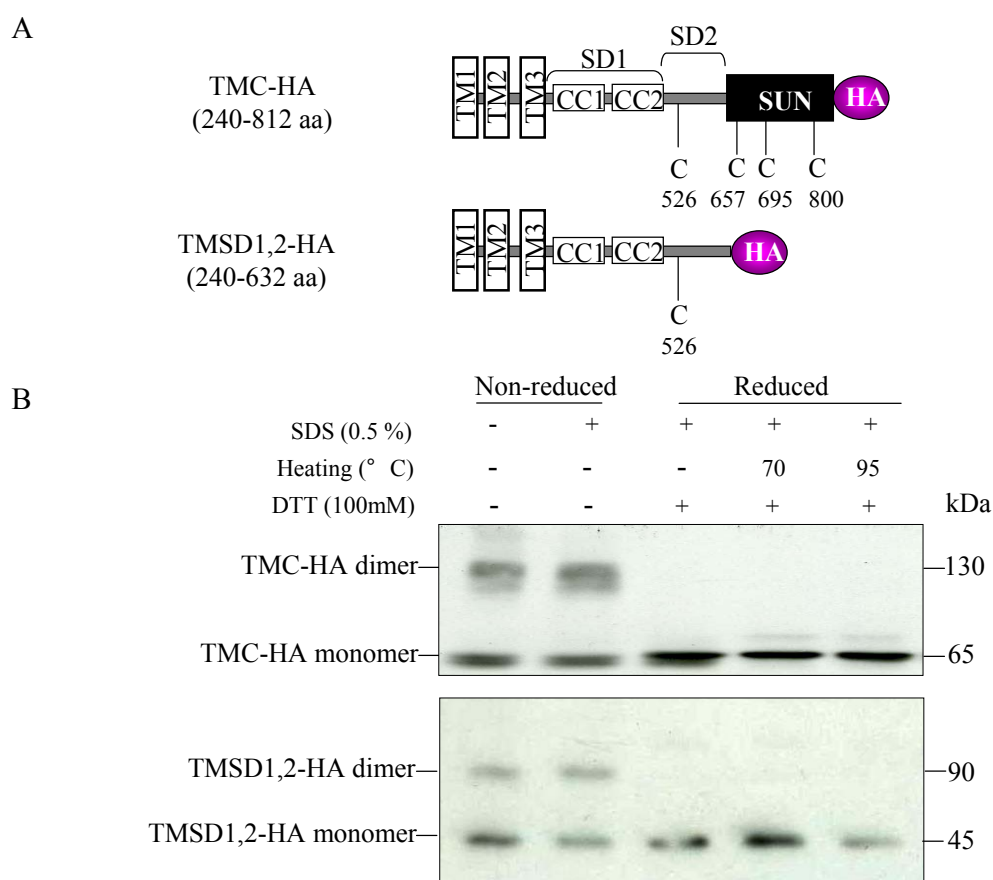


Figure 2.21. The Sun1 C-terminus mediates formation of SDS-resistant dimers. (A) Schematic diagrams for the human Sun1 TMC-HA and TMSD1, 2-HA fusion proteins. HA-tag (pink circle) was added to the C-termini of TMC and TMSD1, 2. Major Sun1 domains are depicted and the positions of the conserved cysteines in SD2 and SUN domains are indicated below the schematic. (B) COS7 cells were transiently transfected with TMC-HA or TMSD1, 2-HA, as indicated on the top of the panel. The cells were lysed by RIPA buffer and treated under different experimental conditions. Both chimeric proteins yield SDS-resistant dimers under non-reduced conditions. The dimers were however absent under reduced conditions (presence of 100mM DTT).

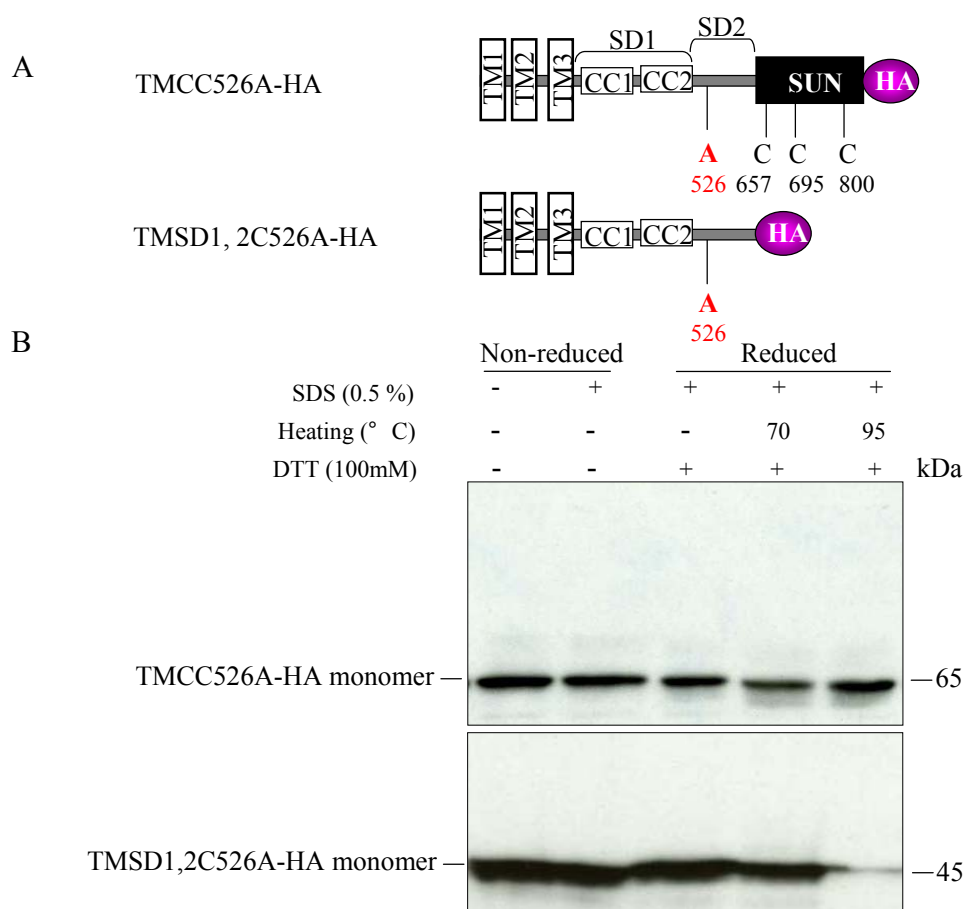


Figure 2.22. Mutation of the cysteine residue 526 in the SD2 domain disrupts formation of Sun1 C-terminal dimers. (A) Schematic representation of TMCC526A-HA and TMSD1, 2-HA fusions. The cysteine in SD2 domain was mutated to an alanine (marked in red). The HA-tags are indicated as pink circles. Cysteins in SUN domain are indicated below the schematic diagrams. (B) COS7 cells were transiently transfected with plasmids encoding TMCC526A-HA or TMSD1, 2-HA. The cell lysates were treated under different experimental conditions (indicated above the western blot) and detected by western blotting using HA specific antibodies.

it is a small peptide of 9 amino acids, which does not contain cysteine residues and does not interact with itself. These two constructs were expressed by transient transfection in COS7 cells. The cells were lysed by RIPA buffer and subdivided into two fractions, which were submitted to non-reduced or reduced conditions. Same amount of proteins from each sample were loaded on a 12% gel and analyzed by SDS-PAGE and concomitant western blotting using V5 antibodies. Under non-reducing conditions, the Sun1 C-terminal dimers were

detectable irrespectively in the absence or presence of SDS in the lysates of either TMC-HA or TMSD1, 2-HA transfected cells. Under reduced conditions, dimer formation was completely abolished (Fig. 2.21B). Thus, the cysteine in the Sun1 SD2 domain seems sufficient for the formation of disulfide bond linked dimers.

To confirm the role of the SD2 domain cysteine residue (Cys⁵²⁶) in the formation of the disulfide bond linked dimers, a mutagenesis study of the Sun1 C-terminus was performed. We generated TMSD1, 2C526A-HA in which Cys⁵²⁶ was replaced with an alanine residue and lacks the SUN domain, and TMCC526A-HA, which contains the same C526A mutation and the SUN domain (Fig. 2.22A). These two constructs were transiently transfected in COS7 cells and the cell lysates were subjected to non-reduced and reduced conditions, and analyzed by western blotting using HA specific antibodies. As shown in Figure 2.22B, when an alanine residue replaced Cys⁵²⁶, no disulfide bond linked dimers were formed by either TMSD1, 2C526A-HA or TMCC526A-HA. In conclusion, the cysteine in the SD2 domain is required for the formation of Sun1 SDS-resistant dimers, whereas, the cysteine residues in the SUN domain of Sun1 are not involved in this process.

2.1.12 Sun1 interacts with Sun2

Human Sun1 and Sun2 share 44% identity and 62% homology to each other. Besides the similarities in their primary amino acid sequences, both proteins share a similar domain organization and an identical topology at the inner nuclear membrane. Similar to Sun1, Sun2 has also two predicted coiled-coil domains, so there is the unexplored possibility that Sun1 and Sun2 might form heterodimers or hetero-oligomers at the INM. To examine whether Sun1 is able to interact with Sun2 at the INM, GFP tagged human Sun1 full-length and V5·6xHis tagged human Sun2 full-length were transiently cotransfected in COS7 cells. The cell lysates were incubated with Ni-NTA agarose beads and the proteins bound to the beads were analyzed by SDS-PAGE and subjected to western blotting with GFP antibodies. GFP, as a negative control, was cotransfected with Sun2-V5·6xHis into COS7 cells. As shown in Figure 2.23, ectopically expressed GFP-Sun1 and Sun2-V5·6xHis were detectable in cotransfected cell lysates. In contrast to GFP alone, GFP-Sun1 was pulled down with the

Sun2-V5-6xHis protein, and was detectable specifically in the pellet fraction. These data indicate thus, that Sun1 and Sun2 interact with each other.

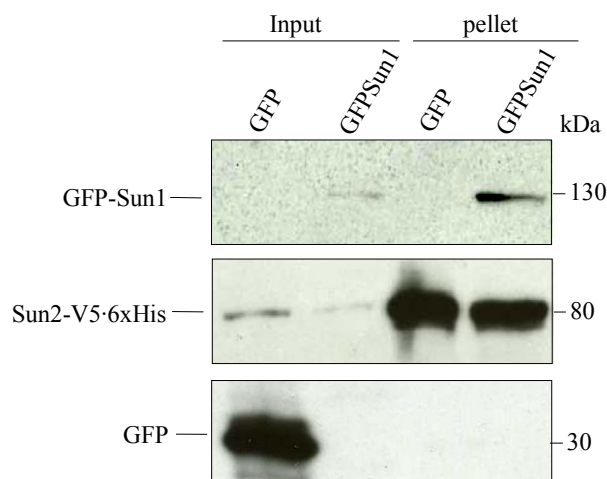


Figure 2.23. Interaction of Sun1 with Sun2 in His-tag pull down assays. Cell lysates were prepared from COS7 cells that had been transiently cotransfected with GFP-Sun1 and Sun2-V5-6xHis or cotransfected with GFP and Sun2-V5-6xHis. The cell lysates were then incubated with Ni-NTA agarose beads. Following extensive washing, the proteins bound to the beads were eluted with 2xSDS sample buffer. The samples were further analyzed by SDS-PAGE and western blotting using specific GFP and V5 antibodies. GFP-Sun1 was pulled down by Sun2-V5-6xHis. Whereas, GFP alone as a negative control, did not show any interactions with Sun2-V5-6xHis.

In order to identify the respective domains involved in the Sun1/Sun2 association *in vivo*, we performed yeast two-hybrid analysis. For this the coiled-coil domains of Sun1 (hSun1-CC) was cloned into pGBKT7 vector and the coiled-coil domains of Sun2 (hSun2-CC) was cloned into pGADT7 vector (Fig. 2.24A). When pGBKT7-hSun1-CC (404-493 aa) and pGADT7-hSun2-CC (400-505 aa) plasmids were cotransformed in a Y190 yeast strain, an interaction between these two proteins was observed in both growth and β -galactosidase activity assays (Fig. 2.24B). Neither growth nor β -galactosidase activity was detected in negative controls using pGBKT7-hSun1-CC with pGADT7 or pGADT7-hSun2-CC with pGBKT7.

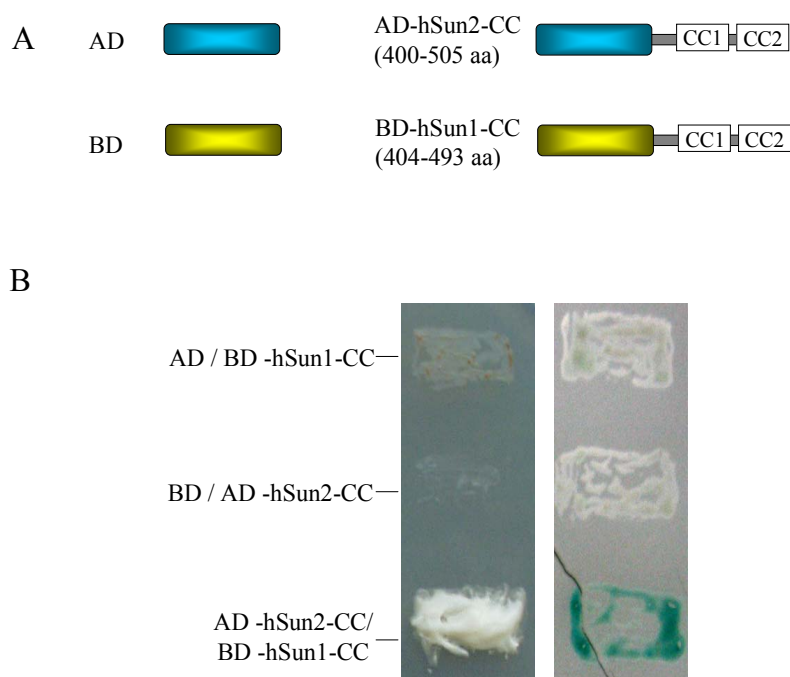


Figure 2.24. Sun1 and Sun2 interact *in vivo* in yeast cells through their respective coiled-coil domains. (A) Schematic showing the fusions used in yeast two-hybrid assays. AD: activation domain (blue bar); BD: DNA binding domain (yellow bar); CC: coiled-coil. (B) The coiled-coil domains of human Sun1 and Sun2 were used in growth and β -galactosidase assays for GAL4 reporter gene expression. Empty binding domain vector pGBKT7 or activation domain vector pGADT7 was cotransformed with pGADT7-hSun2-CC or pGBKT7-hSun1-CC, respectively, as negative controls.

2.1.13 Sun1 is required for proper Nesprin-2 NE localization

In order to determine the *in vivo* functions of Sun1, we silenced specifically the protein in HaCaT cells by siRNA. Sun1 knockdown studies were performed by employing a mixture of two independently expressed siRNAs targeting specifically the N-terminus of Sun1. For more information about the RNAi-competent plasmids pJG173 and pJG174 please see Materials and Methods. pJG173 and pJG174 transiently transfected HaCaT cells were subjected to immunofluorescence studies using Sun1 antibodies in order to verify the efficacy of the Sun1 knockdown (Fig. 2.25). Many transfected cells displayed a reduced Sun1 staining (Fig. 2.25A, D, G; asterisks), while the lamin A/C staining was still observed at the nuclear envelope (Fig. 2.25B; asterisks), suggesting therefore that Sun1 is not essential for lamin A/C localization. In sharp contrast, however, in Sun1 knockdown cells (Fig. 2.25 D-I) the Nesprin-

2 staining pattern was either very faint or absent using both N-terminally (Fig. 2.25E; asterisks) and C-terminally (Fig. 2.25H; asterisks) directed Nesprin-2 antibodies. In summary, our data show that the proper localization of Nesprin-2 at the NE requires Sun1, proposing that Sun1 may directly or indirectly interact with Nesprin-2.

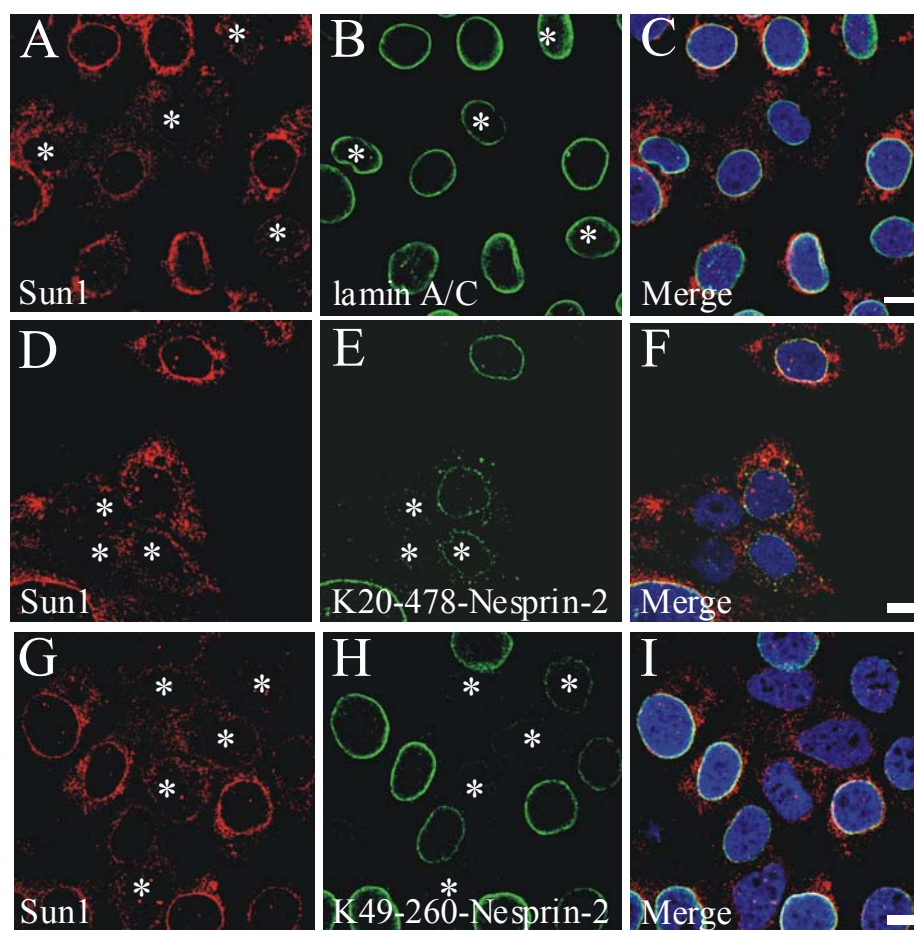


Figure 2.25. The Nesprin-2 localization is affected in cells where Sun1 expression has been silenced by siRNA. HaCaT cells were transiently transfected with a combination of plasmids (pJG173/174) encoding siRNAs targeting hSun1. The distribution of Sun1 (panel A, D and G), lamin A/C (panels B) and Nesprin-2 (panel E and H) was investigated by indirect immunofluorescence in knockdown cells (indicated by asterisks). In Sun1 knockdown cells, the lamin A/C localization remained unaltered (B), whereas Nesprin-2 staining was either absent or reduced (asterisks in panels E, H). DNA was stained by DAPI. The images shown were taken by confocal microscopy and merged to visualize colocalization (panels C, F, I). Bar=10 μ m.

2.1.14 Sun1 affects the nuclear envelope localization of emerin and LAP2 β

Previous data by Libotte *et al.* (2005) in our laboratory indicated that the emerin localization at the nuclear envelope is dependent on Nesprin-2. Therefore we anticipated disturbed emerin localization in the Sun1 knockdown cells. Indeed when Sun1 knockdown cells (Fig.2.26A, asterisks) were subjected to indirect immunofluorescence using anti-emerin antibodies we found that emerin is delocalized partially or completely from the nuclear envelope (Fig.2.26B, asterisks). Interestingly, the distribution pattern of LAP2 β was also perturbed in Sun1 knockdown cells. While in Sun1 expressing cells (Fig. 2.26D, arrows), LAP2 β staining was confined at the nuclear envelope (Fig. 2.26E, arrows), in Sun1 knockdown cells (Fig. 2.26D, asterisks) strong LAP2 β staining was observed inside the nucleus (Fig. 2.26E, asterisks). Thus, the absence of Sun1 in HaCaT cells affects nuclear envelope composition.

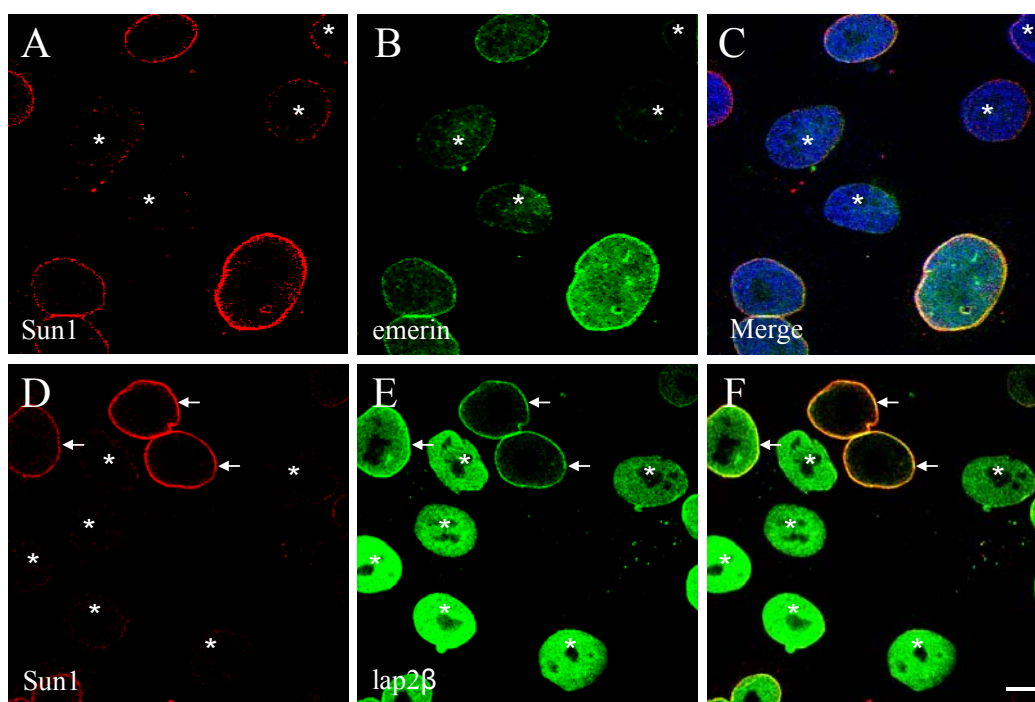


Figure 2.26. The localization of emerin and lap2 β is affected in cells where Sun1 expression has been silenced by siRNA. HaCaT cells were transiently transfected with a combination of plasmids (pJG173/174) encoding siRNAs targeting hSun1. The distribution of Sun1 (panel A and D), emerin (panel B) and lap2 (panel E) was investigated by indirect immunofluorescence in knockdown cells (indicated by asterisks). In Sun1 knockdown cells, the emerin staining was either absent or reduced, whereas lap2 was mislocalized in the nucleus. DNA was stained by DAPI. The images shown were taken by confocal microscopy and merged to visualize colocalization (panels C and F). Bar=10 μ m.

2.1.15 The luminal domain of Nesprin-1 interacts with the SD2 domain of Sun1

Nesprins (Nesprin-1, Nesprin-2) localize to the nuclear envelope via their C-terminal transmembrane domain and a stretch of 30 highly conserved amino acids situated in the perinuclear space, termed as luminal domain (Padmakumar *et al.*, 2005). The luminal domain (LD) of Nesprin-1 shares 80% identity with the LD of Nesprin-2. Similar to Nesprins, the C-terminus of Sun1 is located in the perinuclear space as well (Padmakumar *et al.*, 2005). Inspired by the identical topology of the Sun1, Nesprin C-termini, and more importantly by the documented Sun1 dependency for proper Nesprin localization at the nuclear envelope, we next investigated whether Sun1 interacts *in vivo* with Nesprin.

Constructs		-Trp-Leu-His +3AT(60mM)	X-gal
BD-LN1	AD-SD1, 2	+++	++++
BD-LN1	AD-SD1	-	-
BD-LN1	AD-SD2	+++	++++
BD-LN1	AD	-	-
BD	AD-SD1	-	-
BD	AD-SD2	-	-
BD	AD	-	-

Figure 2.27. Yeast two-hybrid experiments demonstrate that the Sun1-SD2 fragment binds to Nesprin-1. The first column shows the identity and different combinations of plasmids used for the yeast two-hybrid assays. The second column shows the result of growth of yeast cells on SD-Trp-Leu-His+3AT (60 mM) plates. The symbol “+++” was given when the growth was high and optimal. The symbol “-” was assigned when there was no growth. The third column shows the result from the X-gal assay. “++++” symbol was assigned when the intensity of the blue colour was high and “-” when there was no blue colour development.

In order to define and characterize the interacting domains in detail, we performed yeast two-hybrid experiments. The last 30 amino acids of mouse Nesprin-1 were fused in frame to the binding domain (BD) of Gal4 (BD-LN1). Two different C-terminal Sun1 fusion constructs with the activation domain (AD) of Gal4 were made: AD-SD1 (amino acids 432-632, containing two coiled-coil domains) and AD-SD2 (amino acids 633-737, the small region between the second coiled-coil domain and SUN domain). To determine which part of Sun1 interacts with the BD-LE fusion, these constructs were cotransformed into Y190 yeast

cells and a β -galactosidase activation assay was performed. Our results revealed an interaction between BD-LE and Sun1-SD2, whereas controls stayed negative (Fig. 2.27). The Nesprin-1 binding site therefore lies between amino acids 632-738 of the Sun1 molecule.

2.1.16 Construction of a Sun1 C-terminal dominant negative construct

The direct association of the Sun1 and Nesprins C-termini in the perinuclear space suggests the presence of a molecular link, which integrates the nucleoplasm with cytoplasmic structures. Furthermore, this contact may be necessary to structurally link the outer nuclear membrane and inner nuclear membrane to each other. Such views are very attractive and supported by current literature which indicates that in Sun1 and Sun2 double RNAi-treated cells, the outer nuclear membrane was clearly dilated with obvious expansion of the perinuclear space (Crisp *et al.*, 2006). Many Nesprins and SUN proteins and isoforms exist in human and mouse, suggesting a functional redundancy. In order to elucidate the biological significance of the Nesprin/SUN association we choose a dominant negative approach, which is more powerful than ablating individual proteins. For this, the entire C-terminus of Sun1 without the transmembrane segment (Sun1-C, 432-913 aa) was fused with a GFP-tag. To introduce this fusion into the ER lumen and the perinuclear space, we fused the signal peptide sequence of Torsin A onto the N-terminus of GFP-Sun1-C (Fig. 2.28A). SPGFP-Sun1-C was first transiently transfected in HaCaT cells, where Nesprin-2 is highly expressed. In transfected cells, SPGFP-Sun1-C was found to accumulate intracellularly within the peripheral ER and the perinuclear space. Examination of the distribution of Nesprin-2 in transfected HaCaT cells revealed that Nesprin-2 was completely eliminated from the nuclear envelope (Fig. 2.28B upper panel, transfected cells are indicated by arrows and untransfected cells are indicated by arrowheads). To demonstrate the effect of SPGFP-Sun1-C on the distribution of Nesprin-1, the same construct was transiently transfected in primary human fibroblasts. Untransfected human fibroblasts displayed clear nuclear envelope staining of Nesprin-1 (Fig. 2.28B lower panel, arrowheads), whereas in transfected cells, Nesprin-1 was totally absent from the nuclear envelope (Fig. 2.28B lower panel, arrows). Thus, in summary

SPGFP-Sun1-C fusion exerts dominant negative effects on Nesprins, displacing both Nesprin-1 and Nesprin-2 isoforms from the nuclear envelope.

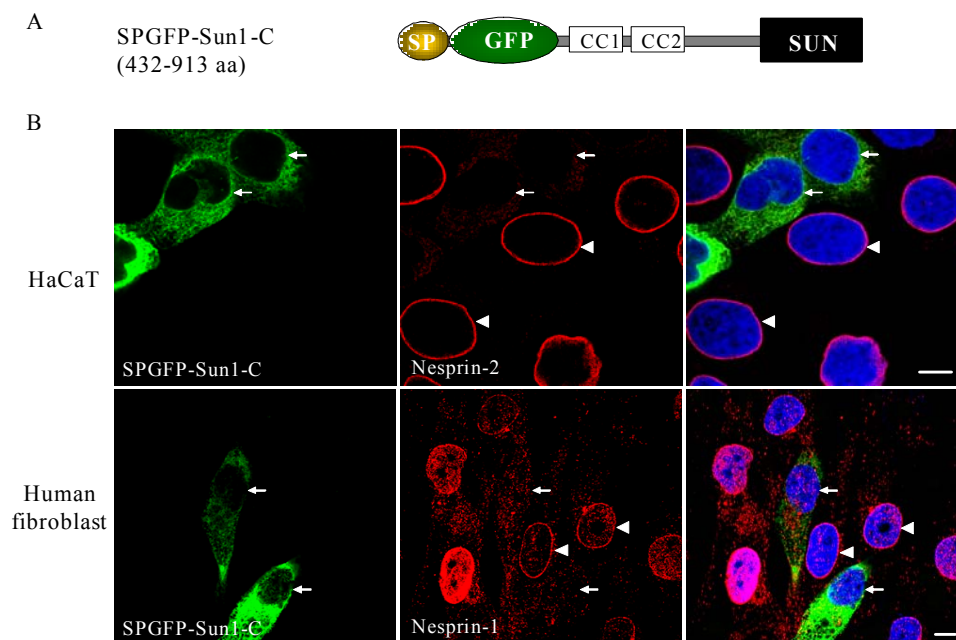


Figure 2.28. SPGFP-Sun1-C affects Nesprin-1 and Nesprin-2. (A) Schematic model of SPGFP-Sun1-C. A signal peptide sequence (SP, yellow circle) and a GFP-tag (green oval) were added to the entire C terminus of Sun1. Major Sun1 domains are indicated. (B) HaCaT cells (higher panel) and primary human fibroblasts (lower panel) were transiently transfected with SPGFP-Sun1-C plasmids. The distribution of Nesprin-2 and Nesprin-1 was investigated by indirect immunofluorescence using pAbK1 antibodies against C-terminal Nesprin-2 and SecII antibodies against C-terminal Nesprin-1. In SPGFP-Sun1-C transfected cells, both Nesprin-2 and Nesprin-1 were lost from the nuclear envelope. Untransfected cells are indicated by arrowheads and transfected cells are indicated by arrows. DNA was stained by DAPI. The images shown were taken by confocal microscopy and merged to visualize colocalization. Bar=10 μ m.

2.1.17 Characterization of HaCaT cells stably transfected with SPGFP-Sun1-C

To better analyze the effects of SPGFP-Sun1-C in transfected cells, we generated stable HaCaT cell lines overexpressing SPGFP-Sun1-C. Three independent positive clones (clone #1, #3, #7) were isolated. Since clone #1 and #3 have similar GFP expression levels, they were used for further studies. These two clones were checked by direct immunofluorescence microscopy and western blotting. SPGFP-Sun1-C stainings of clones #1 and #3 are shown in

Figure 2.29A indicating similar GFP intensities. Furthermore, western blot analysis indicates that SPGFP-Sun1-C expressing #1 and #3 clones express a similar amount of the expected ~87 kDa GFP-fusion (Fig. 2.29B).

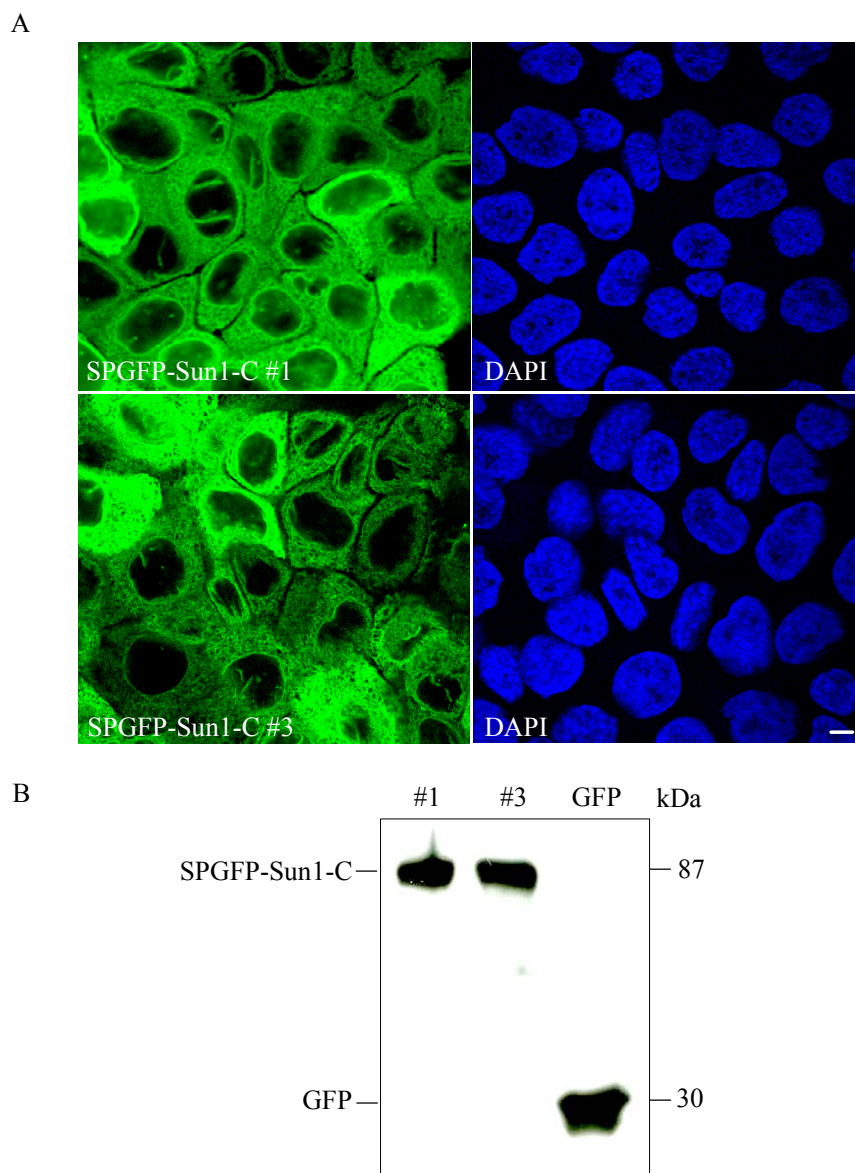


Figure 2.29. Generation of SPGFP-Sun1-C stably transfected HaCaT cell clones. (A) #1 and #3 of SPGFP-Sun1-C stable cells were investigated by direct immunofluorescence. Cells were counter stained by DAPI. The images shown were taken by confocal microscopy. Bar=10 μ m. (B) As expected, 87 kDa bands were observed by western blot analysis of cell lysates of SPGFP-Sun1-C stably transfected HaCaT clones #1 and #3, using GFP antibodies. Cell lysate of GFP transiently transfected HaCaT was loaded as a control.

2.1.18 Nesprin-2 isoforms are mislocalized in SPGFP-Sun1-C stably transfected HaCaT cells

To obtain side-by-side comparisons with wild-type HaCaT cells, the SPGFP-Sun1-C stably transfected HaCaT cells were mixed together with wild-type HaCaT cells in equal proportions and plated onto the same coverslip. *Nesprin-2* codes for at least eight isoforms. In

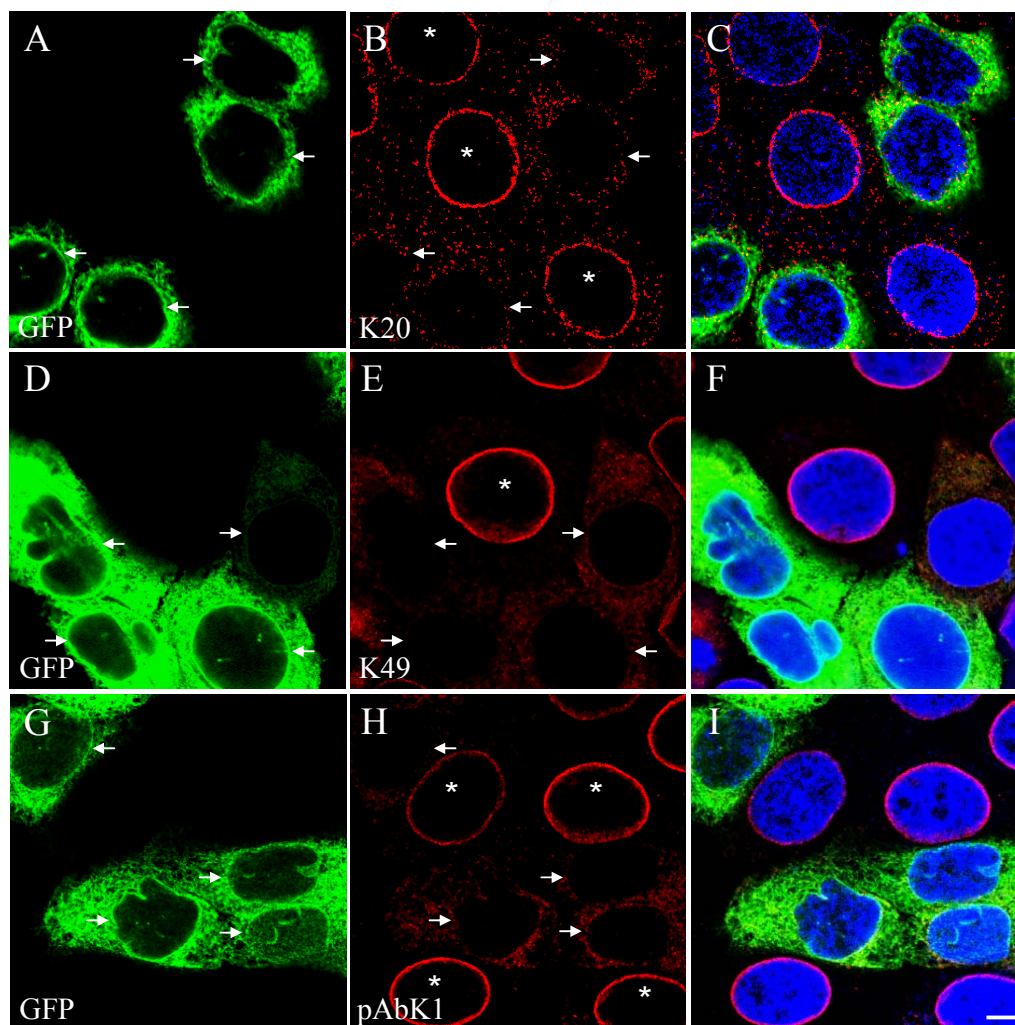


Figure 2.30. Mislocalization of Nesprin-2 in SPGFP-Sun1-C expressing cells as examined using three different Nesprin-2 antibodies. SPGFP-Sun1-C #1 cells were mixed with wild-type HaCaT cells (1:1), fixed by paraformaldehyde and investigated by three different Nesprin-2 antibodies. (A-C) The mixed cells were stained by mAb K20-478 (K20), the monoclonal antibodies recognizing the NH2 terminal ABD domain of Nesprin-2. (D-F) The cells were stained by mAb K49-260 (K49), the monoclonal antibodies recognizing the C-terminus of Nesprin-2. (G-I) The C-terminal polyclonal antibodies pAbK1 of Nesprin-2 were used for the immunostaining. Arrows indicate SPGFP-Sun1-C expressing cells and wild-type HaCaT are marked with asterisks. All the cells were counter stained by DAPI. The images shown were taken by confocal microscopy. Bar=10 μ m.

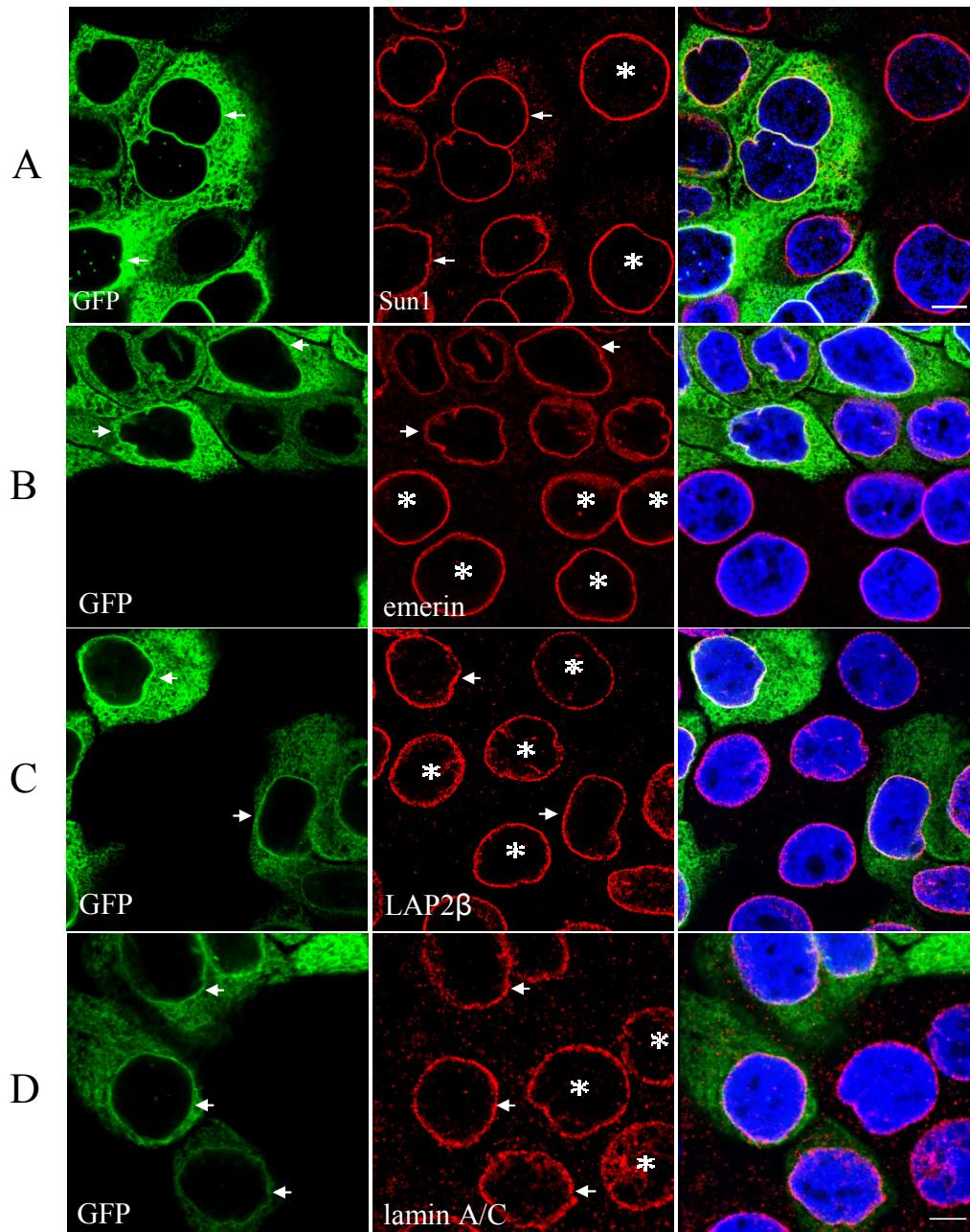


Figure 2.31. The staining pattern of endogenous Sun1, emerin, LAP2 β and lamin A/C is unaffected in SPGFP-Sun1-C stably transfected HaCaT cells. SPGFP-Sun1-C #1 cells were mixed with wild-type HaCaT cells (1:1) and investigated using Sun1 (A), emerin (B), LAP2 β (C) and lamin A/C (D) specific antibodies. Arrows and asterisks indicate SPGFP-Sun1-C cells and wild-type HaCaT cells, respectively. DAPI was used to visualize DNA. The images shown were taken by confocal fluorescence microscopy. Bar=10 μ m.

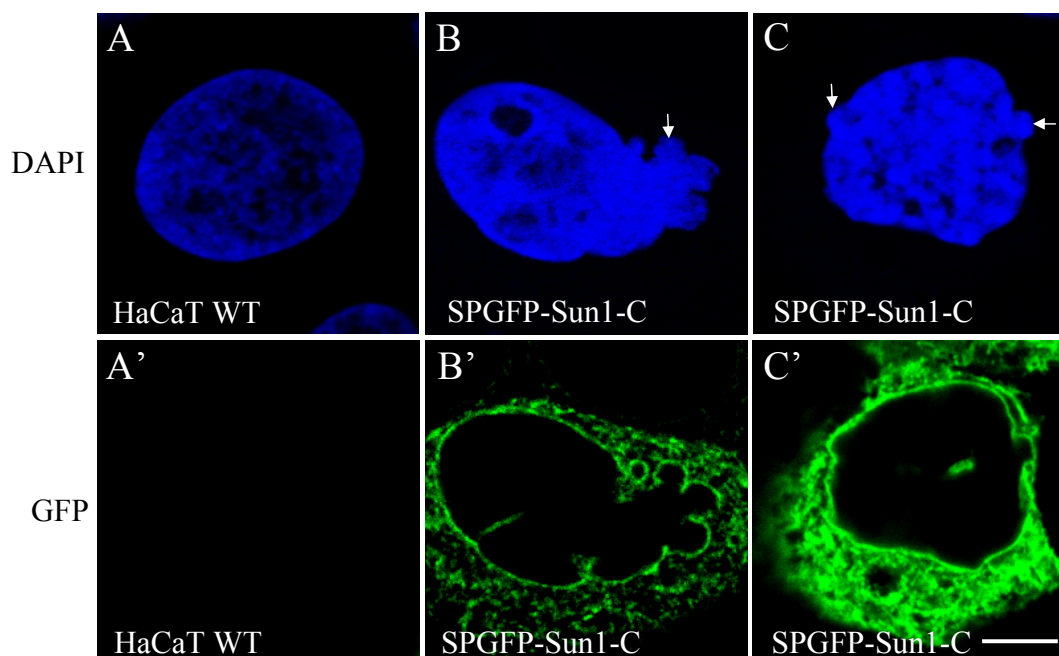
order to demonstrate the absence of all Nesprin-2 isoforms from the nuclear envelope, in SPGFP-Sun1-C expressing cells we employed three different Nesprin-2 specific antibodies, named mAb K20-478 (K20), mAb K49-260 (K49) and rabbit polyclonal Nesprin-2 pAbK1 (pAbK1). K20 is a monoclonal antibody recognizing the N-terminus of human Nesprin-2. pAbK1 and K49 are polyclonal and monoclonal antibodies respectively, against the last two C-terminal spectrin repeats of human Nesprin-2. All three Nesprin-2 antibodies displayed a similar pattern and stained specifically the nuclear envelope in wild-type HaCaT cells (Fig. 2.30B, E, H, asterisks). Whereas, in SPGFP-Sun1-C stably transfected cells no Nesprin-2 was detected on the nuclear envelope by any one of the three antibodies (Fig. 2.30, arrows).

We then examined whether SPGF-Sun1-C affects the localization of endogenous Sun1. For this we performed an immunofluorescence analysis using the Sun1 specific antibodies. However, no difference was observed between the staining of Sun1 in wild-type and SPGFP-Sun1-C stably transfected HaCaT cells (Fig. 2.31A). Surprisingly, also the localization pattern of emerin and LAP2 β in SPGFP-Sun1-C cells was not distinguishable from wild-type. In both cell-types emerin and LAP2 β staining was confined at the nuclear envelope (Fig. 2.31B and C). Similarly, the lamin A/C staining pattern remained unchanged in SPGFP-Sun1-C stably transfected cells (Fig. 2.31D). Thus, SPGFP-Sun1-C expressing cells are Nesprin deficient cells.

2.1.19 Nuclear shape changes in SPGFP-Sun1-C cells

Data from our laboratory (Libotte *et al.*, 2005) indicate a major scaffolding and structural function for Nesprins at the nuclear envelope. Therefore we examined whether the absence of Nesprins affected the nuclear structure of the SPGFP-Sun1-C expressing cells. The labeling of nuclei by DAPI revealed dramatic changes in nuclear morphology in SPGFP-Sun1-C stably transfected HaCaT cells. Nuclei of wild-type HaCaT are roughly circular or slightly ovoid (Fig. 2.32A), whereas cells stably expressing SPGFP-Sun1-C had a significantly increased fraction of highly elongated (Fig. 2.32B) or irregularly shaped (Fig. 2.32C) nuclei and nuclei exhibiting major membrane blebbing when compared to wild-type HaCaT cells

(Fig. 2.32B and C, arrows). The percentage of abnormal shape nuclei was 10.3% for wild type HaCaT, and 32.5% for SPGFP-Sun1-C stably transfected cells (Fig. 2.32D).



D

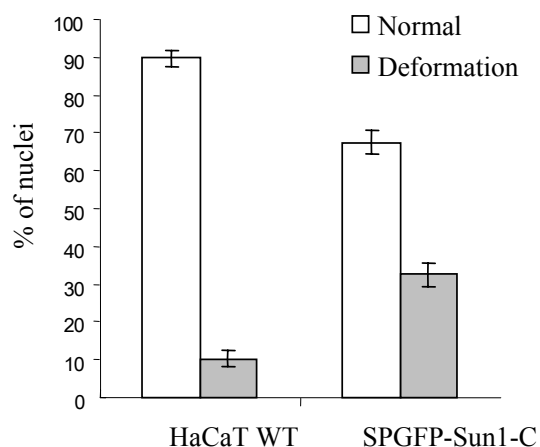
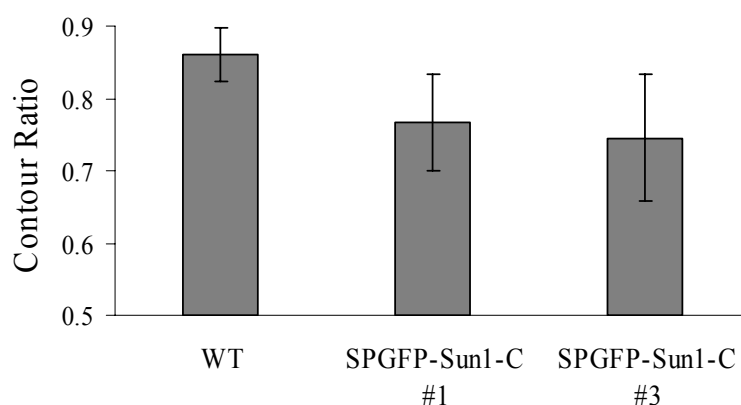


Figure 2.32. SPGFP-Sun1-C stably transfected HaCaT cells have misshapen nuclei. (A-C) DAPI labeled nuclei of wild-type HaCaT and SPGFP-Sun1-C stably transfected cells. The nuclear membrane blebs are indicated with arrows. The images were taken by confocal microscopy. Bar=10 μ m. (B) The percentage of abnormally shaped nuclei was significantly increased in stably transfected cells. The percentage of abnormal shape nuclei was 10.3 \pm 2.36% for wild-type HaCaT, 32.5 \pm 3.12% for SPGFP-Sun1-C stably transfected cells. $P < 0.001$ for SPGFP-Sun1-C transfected cells compared to wild-type HaCaT cells.

To assess the degree of irregular nuclear shape more quantitatively, we measured nuclear cross-sectional area and perimeter of DAPI stained nuclei and computed the nuclear contour ratio ($4\pi \times \text{area}/\text{perimeter}^2$) (Goldman *et al.*, 2004), which yields a quantitative measure of nuclear roundness. For a circular shape that maximizes the area-to-perimeter ratio the contour ratio has a value of 1, whereas more convoluted outlines lead to smaller values. We found that wild-type HaCaT had a contour ratio of 0.86, whereas the contour ratio for SPGFP-Sun1-C #1 and #3 were 0.76 and 0.74, respectively ($P < 0.001$ for both SPGFP-Sun1-C #1 and #3 compared to wild-type HaCaT) (Fig. 2.33). Thus SPGFP-Sun1-C stably transfected cells had a significantly lower mean contour ratio compared to wild-type cells. Taken together, SPGFP-Sun1-C stably transfected cells serving as Nesprin deficient cells have misshapen nuclei, therefore Nesprins probably are major determinants of the nuclear shape in HaCaT cells.



Cell Line	Contour Ratio		P Value
	Mean	\pm SD	
HaCaT WT	0.86	0.03	
SPGFP-Sun1-C #1	0.76	0.06	5.33E-43
SPGFP-Sun1-C #3	0.74	0.08	3.02E-41

Figure 2.33. Contour ratio of HaCaT wild-type and SPGFP-Sun1-C stably transfected cells. Two clones (#1 and #3) of SPGFP-Sun1-C stably transfected cells were used for the measurement of contour ratio. Both of them have a significantly decreased contour ratio compared to wild-type cells (contour ratio 0.86 ± 0.03 for wild-type, 0.76 ± 0.06 for #1, 0.74 ± 0.08 for #3). P values were calculated relative to HaCaT wild-type. For each cell-type, the area and perimeter of 200 cells were measured. SD: standard deviation.

2.1.20 Proliferative ability of SPGFP-Sun1-C stably transfected cells

To evaluate the effect of the nuclear envelope defects observed in SPGFP-Sun1-C stably transfected cells on cell proliferation, we analyzed the proliferative ability of SPGFP-Sun1-C stably transfected cells. 1×10^5 cells of each stable clones #1 and #3, and the control wild-type HaCaT were seeded and every 48 hours the cells were trypsinized and counted for a period of 8 days to generate cell growth rates. The growth curves in Figure 2.34 shows that both SPGFP-Sun1-C stable clones #1 and #3 exhibited a remarkably decreased proliferation when compared with control HaCaT cells after 8 days growing under same conditions.

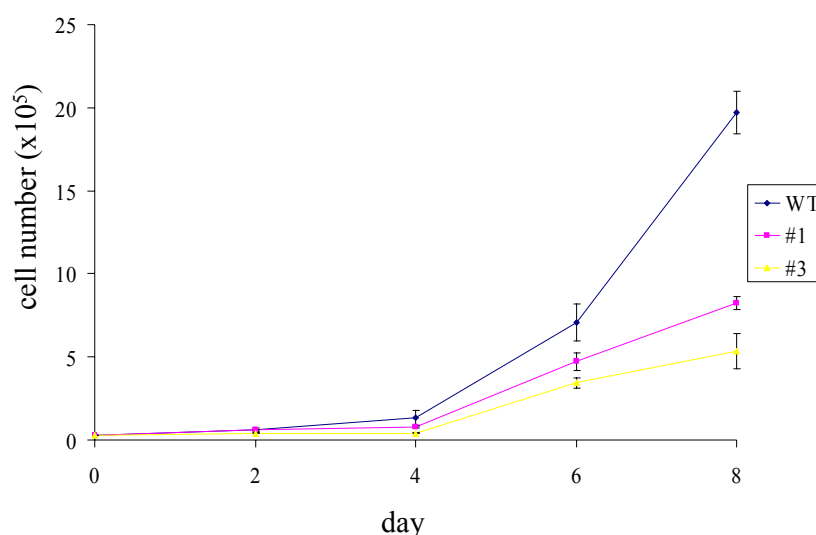
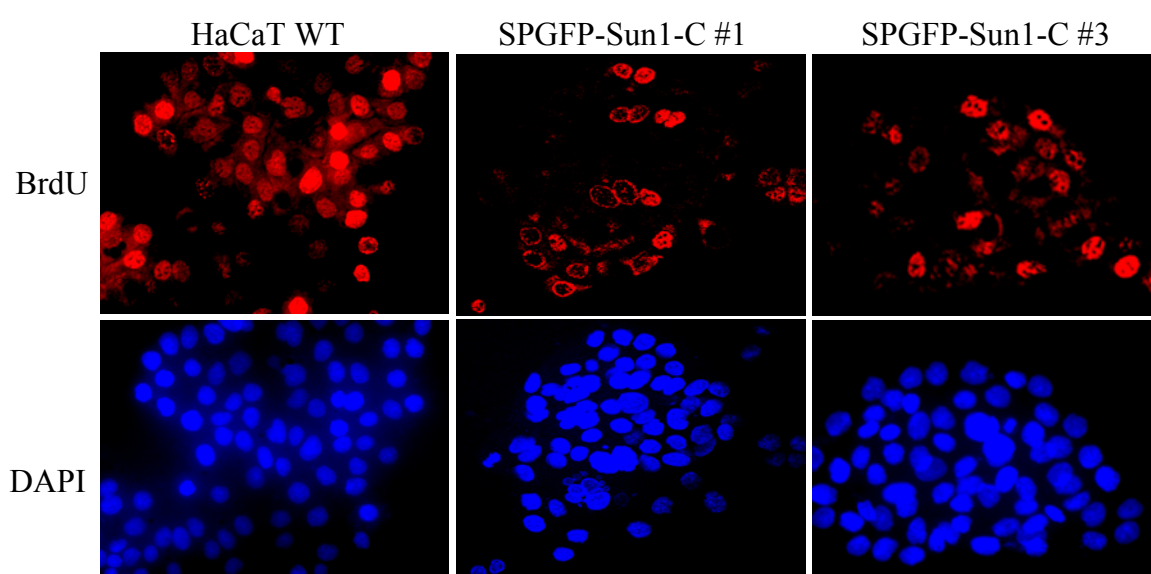


Figure 2.34. SPGFP-Sun1-C stably transfected cells grew slower than HaCaT wild-type cells. Two clones (#1 and #3) of SPGFP-Sun1-C stably transfected cells and wild-type HaCaT were used for the generation of the growth curve. Cells were seeded at an initiative density of 1×10^5 cells/plate, with duplicate plates for each cell line. Both of the mutant cell lines showed significantly reduced growth rates compared to wild-type cells.

Cellular proliferation requires the replication of genomic DNA. Thus, monitoring DNA synthesis is an indirect parameter of cell proliferation. 5'-bromo-2'-deoxyuridine (BrdU) can incorporate into genomic DNA instead of thymidine during DNA synthesis in replicating cells. Cells that have incorporated BrdU can be easily detected using a monoclonal antibody against BrdU. To further strengthen and confirm our data, we next examined BrdU incorporation. Wild-type HaCaT cells and SPGFP-Sun1-C stable clones #1 and #3 were

grown for 2 hours in the presence of BrdU, and subsequently prepared for immunofluorescence analysis using BrdU antibodies. Triplicate counting of 300 cells for each cell line was performed. BrdU staining showed that SPGFP-Sun1-C #1 and #3 have less BrdU positive cells than wild-type HaCaT (Fig. 2.35A). About 57 % of control HaCaT cells were positively stained by BrdU antibodies, whereas 37 % of #1 cells and only 31 % of #3 cells incorporated the nucleotide analogue (Fig. 2.35B).

A



B

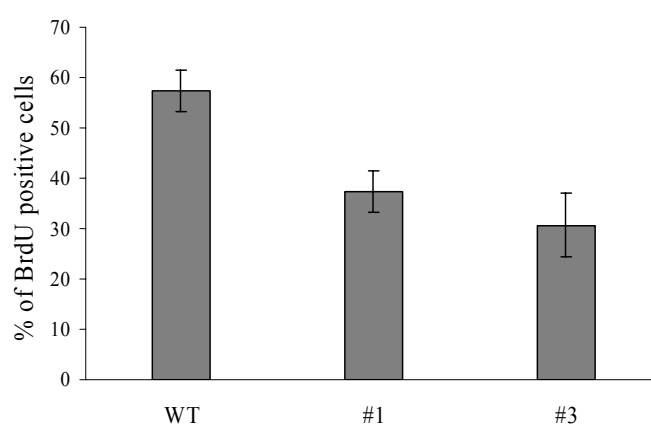


Figure 2.35. BrdU incorporation in HaCaT wild type and SPGFP-Sun1-C stably transfected cells. Two stable clones (#1 and #3) of SPGFP-Sun1-C transfected cells and HaCaT wild type were used for BrdU incorporation. Cells were incubated with BrdU for 2 hrs and processed for immunofluorescence as described in Materials and Methods. Fraction of BrdU incorporation is $57 \pm 4\%$ for wild-type, $37 \pm 4\%$ for #1, $31 \pm 6\%$ for #3. P values were calculated relative to HaCaT wild type. $P < 0.05$

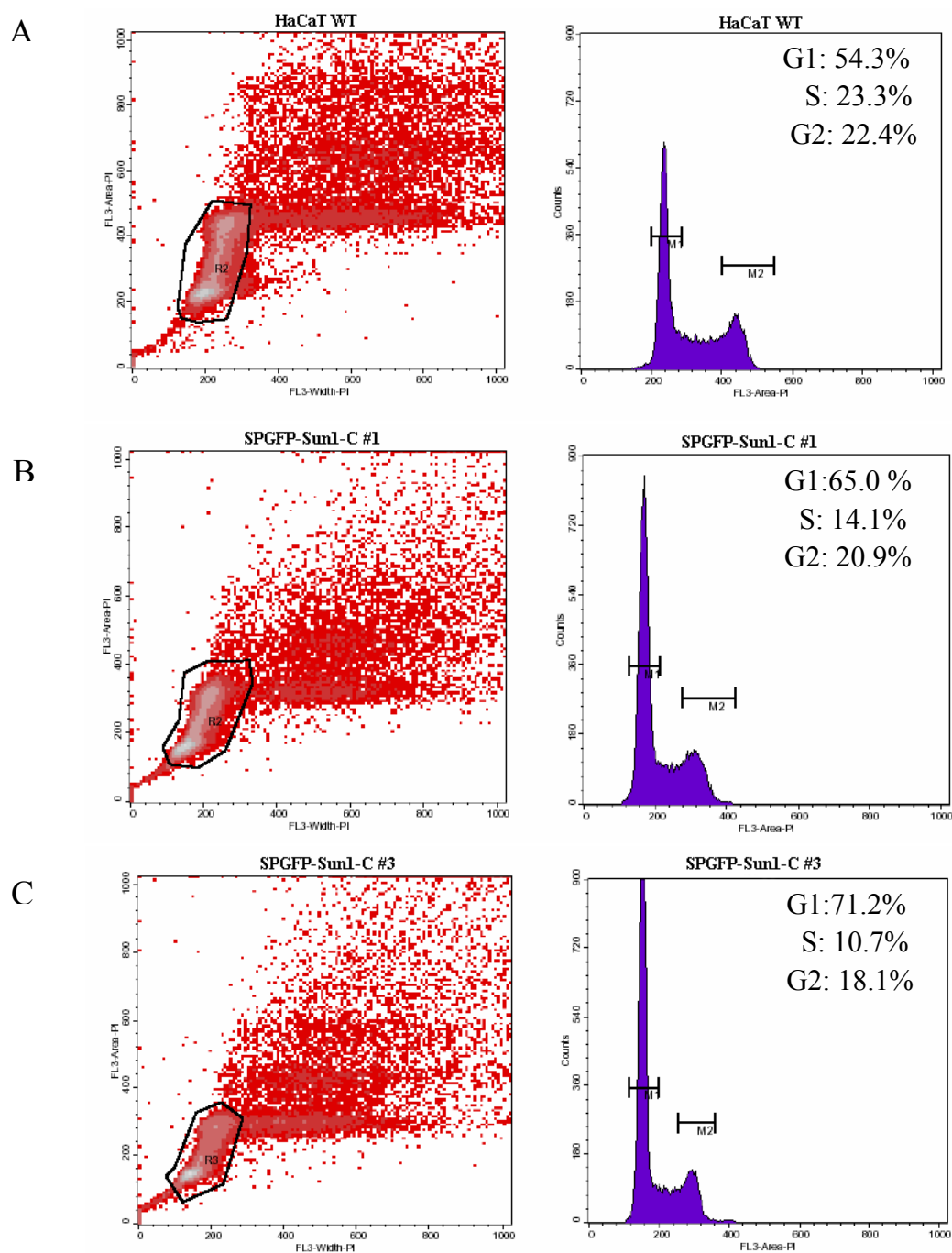


Figure 2.36. Flow cytometric analysis of HaCaT wild-type and SPGFP-Sun1-C stably transfected cells. Propidium iodide staining was performed on stable clones SPGFP-Sun1-C #1, SPGFP-Sun1-C #3 and HaCaT wild-type cells and samples were analyzed by flow cytometry using a FACS equipment. The fluorescence intensity is relevant to the DNA quantity. The first diagram (A, B, C left) shows the fluorescence intensity of the cells. In the second diagram (A, B, C right) the number of the cells in each phase of the cell cycle was represented. 1×10^4 cells were analyzed for each cell line.

Meanwhile, flow cytometry analysis was performed to SPGFP-Sun1-C stable cells and Wild-type HaCaT. The cells were first stained by propidium iodide and subsequently analyzed by a cytofluorimeter. For wild-type HaCaT, 54.3% cells were in G1 phase, 23.3% in S phase and 22.4% in G2 phase (Fig. 2.36A). For SPGFP-Sun1-C #1, 65% cells were in G1 phase, 14.1% in S phase and 20.9% in G2 phase (Fig. 2.36B). While for #3, 71.2% cells were detected in G1 phase, 10.7% and 18.1% cells were in S and G2 phase, respectively (Fig. 2.36C). Thus, there is a significant decrease in replication phase S of both SPGFP-Sun1-C stable clones in comparison to the wild-type cells. The percentage of cells in G1 phase was also remarkably increased. These data suggest that SPGFP-Sun1-C could lead to an arrest of cells in G1 phase, a delayed transition into S phase and eventually restraining proliferation of cells.

2.1.21 Senescence analysis of SPGFP-Sun1-C stably transfected cells

Decline in the growth rate is also associated with cell senescence (Campisi J, 2003). A biological marker of senescence is the expression of a specific isoenzyme of β -galactosidase, which is referred to as senescence-associated β -galactosidase (SA- β -gal) (Dimri GP *et al.*, 1995; Wang X *et al.*, 2004). Therefore we examined SA- β -gal activity in stably transfected cells to investigate whether cellular senescence was induced in SPGFP-Sun1-C stable transfected cells. The cells were fixed with 2% formaldehyde/0.2% glutaraldehyde at room temperature and incubated with fresh prepared SA- β -Gal staining solution at 37°C (no CO₂) for 12 hours. The stained cells were observed under bright field microscopy. Zmpste24 deficient fibroblasts at passage 6, in which β -galactosidase was highly expressed (Varela I *et al.*, 2005), were used as positive control. In wild-type HaCaT, about 6 % cells were positive stained for β -galactosidase at pH 6.0 (Fig. 2.37B, E). Whereas in SPGFP-Sun1-C #1 and #3, about 13 % and 15 % cells expressed β -galactosidase, respectively (Fig.2.37C, D, E). More than 90 % of Zmpste24^{-/-} fibroblasts were positively stained (Fig. 2.37A, E). The percentage of SA- β -gal positive cells in SPGFP-Sun1-C stable clones was slightly increased (6±1.4 for wild-type, 13±2.8 for #1, and 15±4.2 for #3; P>0.05 for wild-type vs. #1 and #3).

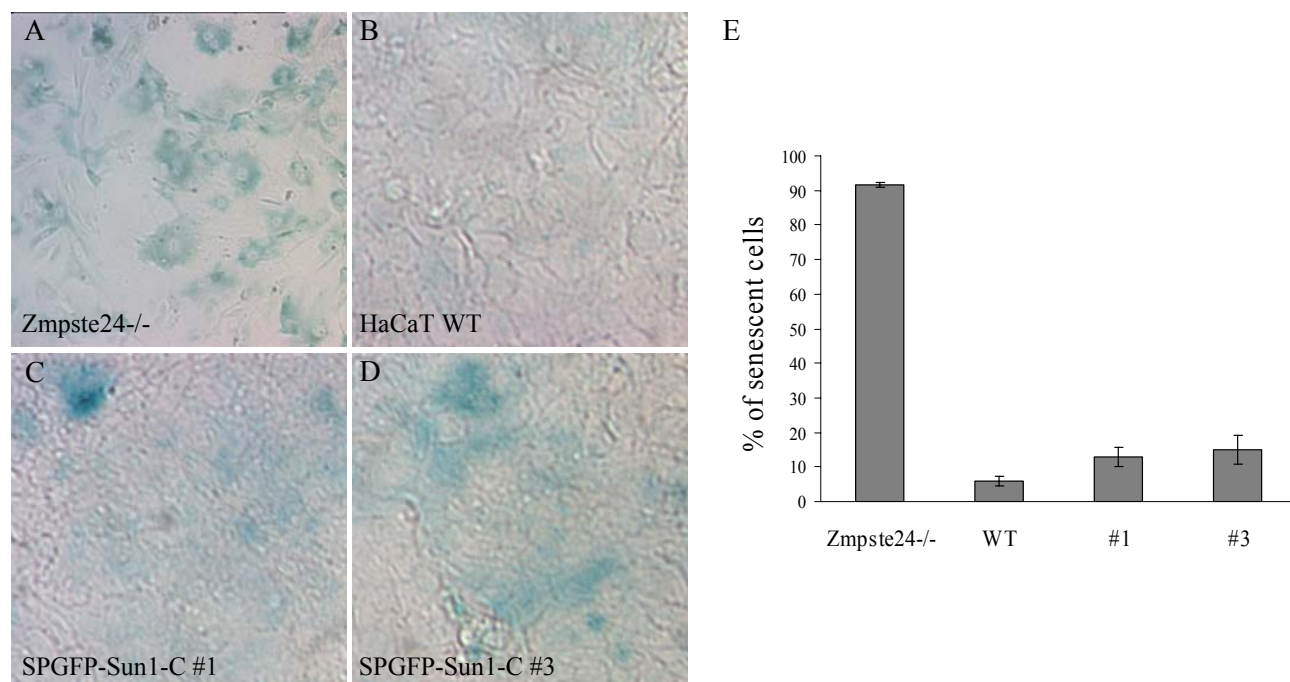


Figure 2.37. Senescence-associated β -gal staining of HaCaT wild type and SPGFP-Sun1-C stably transfected cells. Cells were fixed 5 min with 2% formaldehyde/0.2% glutaraldehyde at room temperature and incubated at 37°C (no CO₂) with fresh prepared SA- β -Gal staining solution. Positive control Zmpste24 deficient cells at passage six (A), HaCaT wild-type (B), SPGFP-Sun1-C #1 cells (C) and SPGFP-Sun1-C #3 cells (D) were viewed under bright field microscopy at 40 x magnification when staining is detectable. (E) Percentage of senescent cells in each cell strain (200 cells were counted duplicate).

2.1.22 The expression level of E-cadherin is increased in SPGFP-Sun1-C stably transfected cells

Many studies have demonstrated physical connections between the plasma membrane, cytoskeleton and nucleoskeleton (Maniotis *et al.*, 1997; Lammerding *et al.*, 2004; Broers *et al.*, 2004). In addition, the presence of Nesprin isoforms at the plasma membrane and focal adhesions suggests a role of Nesprins in cell adhesion (Zhen *et al.*, 2002; Zhang *et al.*, 2005). Therefore, we investigated the cadherin junction formation in SPGFP-Sun1-C cells, which are Nesprins deficient cells. Interestingly, we observed that the expression level of E-cadherin

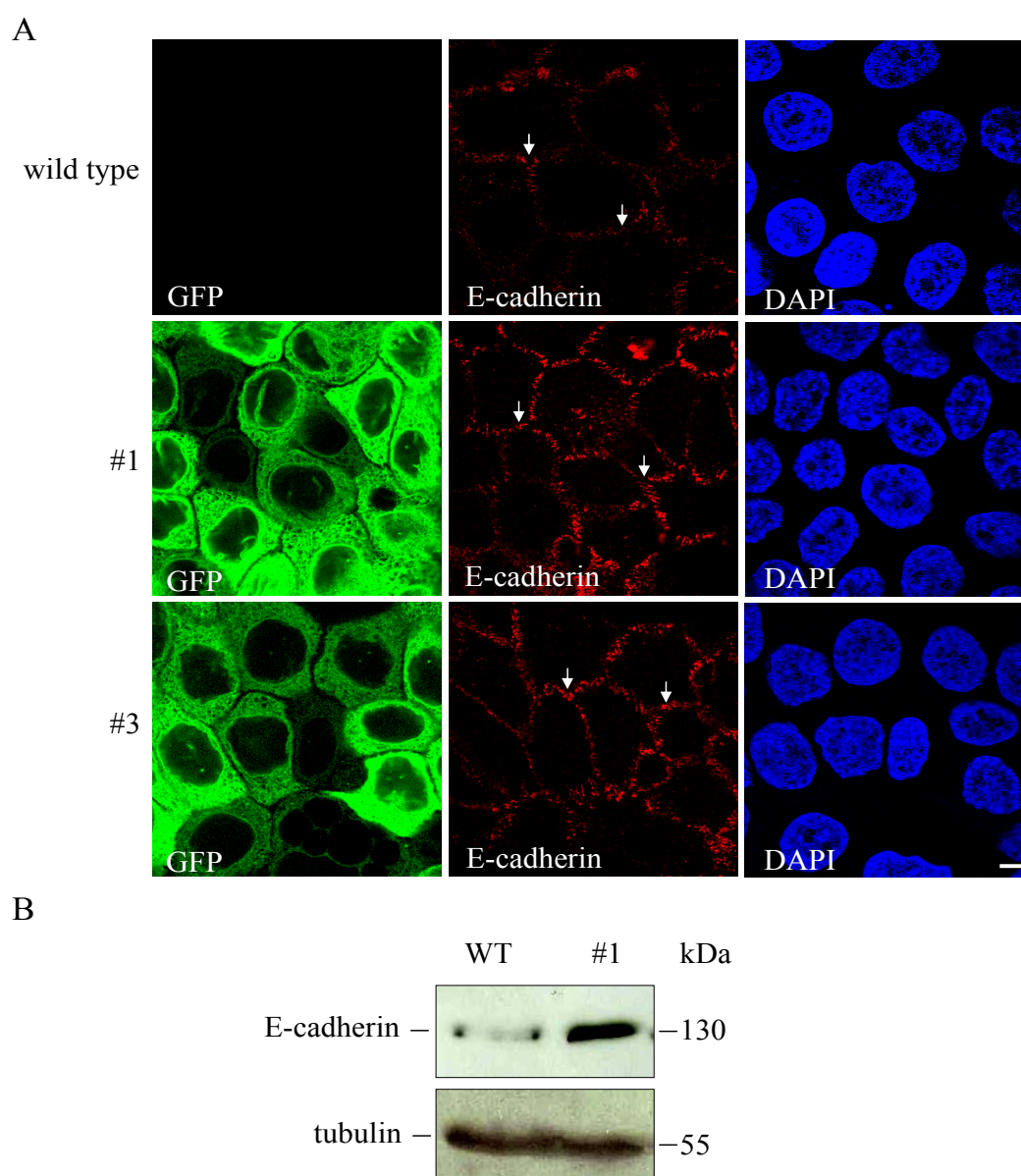


Figure 2.38. Increased expression of E-cadherin in SPGFP-Sun1-C stably transfected HaCaT cells. (A) Wild-type HaCaT, SPGFP-Sun1-C #1 and SPGFP-Sun1-C #3 cells were subjected to immunofluorescence and stained by E-cadherin specific antibodies. Arrows indicate the cell-cell contacts. DAPI was used to visualize DNA. The images shown were taken by confocal fluorescence microscopy. Bar=10 μ m. (B) Western blot analysis of wild-type and SPGFP-Sun1-C #1 using E-cadherin and tubulin antibodies indicated that the expression level of E-cadherin was increased in SPGFP-Sun1-C cells. Tubulin levels indicate equal loading..

was increased in SPGFP-Sun1-C stably transfected cells compared to wild-type cells. As shown in Figure 2.38A, the intracellular localization of E-cadherin was characterized by

immunofluorescence microscopy. In controls, E-cadherin was stained mainly at the cell-cell contact regions (Fig. 2.38A higher panel, indicated by arrows). However, the signal was significantly increased in SPGFP-Sun1-C stable cells (Fig. 2.38A, arrows in middle and lower panels). Western blot analysis indicated that the expression level of E-cadherin was apparently increased in SPGFP-Sun1-C stable cells (Fig 2.38B). The result was consistent with the data from the immunofluorescence analysis.

2.2 Generation of a Nesprin-1 knock-in mouse model

2.2.1 Knock-in strategy and ES clone screening

The mammalian Nesprins (Nesprin-1/-2/-3) are broadly expressed multifunctional proteins (Padmakumar *et al.*, 2004; Zhang *et al.*, 2001; Wilhelmsen *et al.*, 2005), anchored in the nuclear membrane through their highly conserved C-terminal KASH domain (Zhang *et al.*, 2001; Mislow *et al.*, 2002; Warren *et al.*, 2005). Through alternative transcriptional initiation, termination and splicing, *Nesprin-1* and *Nesprin-2* genes gives rise to many protein isoforms that vary markedly in domain architecture and size (Zhen *et al.*, 2002; Padmakumar *et al.*, 2004). The orthologues of Nesprins in *C. elegans* and *D. melanogaster* have been implicated in cytoskeleton dependent processes such as nuclear anchorage and migration (Starr & Han, 2002; Starr & Han, 2003; Rosenberg-Hasson *et al.*, 1996; Yu *et al.*, 2006). However, the exact functions of Nesprins remain largely unknown. Nesprin-1 and -2 were reported directly to associate with emerin and lamin A/C (Zhang *et al.*, 2005). Emerin mutations give rise to Emery-Dresifuss muscular dystrophy (Fairley *et al.*, 1999), whereas lamin A/C mutations cause various clinical disorders, collectively known as “laminopathies” (Broers *et al.*, 2004; Burke & Stewart, 2002; Broers *et al.*, 2006). These particular associations suggest that Nesprins might contribute to genetic disorders. Indeed recently, Gros-Louis *et al.* found that mutations in *Nesprin-1* gene lead to a newly discovered form of autosomal recessive cerebellar ataxia in human, which has the prototypic feature of impaired walking with a lack of coordination of gait and limbs (Gros-Louis *et al.*, 2007).

Genetic mouse models are powerful tools for investigating the functional aspects of a protein and its potential association to human diseases. In order to study the biological function and monitor the tissue distribution pattern of Nesprin-1, we decided to generate knock-in mice in which the KASH domain of Nesprin-1 were ablated and replaced in frame by the reporter EGFP gene. This approach would ensure the absolute mislocalization of all Nesprin-1 isoforms containing the KASH domain, which would enable us to better understand the cellular functions of Nesprin-1 and its isoforms at the nuclear envelope.

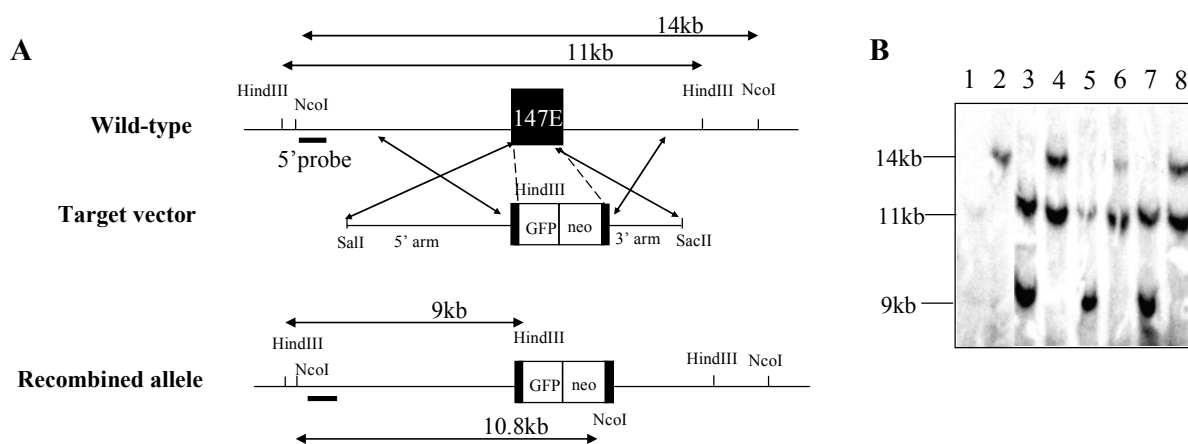


Figure 2.39 Design and generation of Nesprin-1 knock-in ES cell clones. (A) Stick diagram illustrating the partial genomic organization of the *Nesprin-1* (wild-type) locus coding for the KASH domain (black box), targeting vector used, and the desired targeted allele following successful homologous recombination (recombined allele). *Nesprin-1* exon 147 was replaced by reporter EGFP gene (GFP) and neomycin resistance gene (neo). The location of the 5' probe used for Southern blot analysis is indicated. Upon HindIII digestion the wild-type and deleted allele yield fragments of 11 and 9 kb, respectively; upon NcoI digestion the wild-type and deleted allele yield fragments of 14 and 10.8 kb, respectively. (B) Southern blot analysis of genomic DNA from different ES cell clones. Lanes 1, 2: WT genomic DNA digested with HindIII and NcoI, respectively; lanes 3, 4: *Nesprin-1* knock-in clone #43 digested with HindIII and NcoI, respectively; lanes 5, 6: *Nesprin-1* knock-in clone #83 digested with HindIII and NcoI, respectively; lanes 7, 8: *Nesprin-1* knock-in clone #110 digested with HindIII and NcoI, respectively.

The Nesprin-1 gene is located on mouse chromosome 10 and is encoded by 147 exons. Exon 147 codes for the KASH domain of Nesprin-1. The target vector was designed and generated by my former colleague (Padmakumar VC) in the following way: The 5' arm of the

target vector was designed to include 4 kb genomic sequence mostly comprising the intron sequences and the sequences coding for a few amino acids of the last exon until 15 amino acids before the transmembrane domain and is followed by EGFP and the neomycin cassette (NEO), which were cloned in frame to the remaining region of the last exon. The 3' arm containing a 1.9 kb intron sequence was cloned after NEO in the target vector (Fig. 2.39A, Target vector). The 5' probe was generated outside of the 5' arm for selecting site specifically recombined clones (Fig. 2.39A, wild type and recombined allele). The linearized target vector was transfected into embryonic stem (ES) cells from the R1 lineage and selected by G418. As shown in Figure 2.39A, HindIII and NcoI enzymes were used for the screening of the transfected ES clones. HindIII was supposed to give rise to an 11 kb wild-type fragment and a 9 kb recombined fragment. NcoI digestion was proposed to yield a 14 kb wild-type and a 10.8 kb recombined fragment. Three positive ES clones were isolated and confirmed by Southern blot analysis (Fig. 2.39 B).

2.2.2 Generation of Nesprin-1 knock-in chimeric mice

Modified ES cells were introduced into preimplantation mouse blastocysts, by means of ES cell microinjection. The chimeric mice generated, were easily identified by the mosaic pattern of fur colour. Since we know that Nesprin-1 is highly expressed in skin (Padmakumar, Ph.D thesis, 2004), the living animals were imaged using a CCD camera. The chimeric mice emitted a signal that was significantly different from WT mice. In the chimeric mouse, the GFP signal emitted from agouti areas, which develop from the injected ES cells, was more significant than the signal emitted from skin with black fur developing from the recipient's cells (Fig. 2.40).

The generation of chimeric mice is a crucial step in making a genetically altered mouse line. If gametes of a chimera develop from the injected ES cells, the mutant allele present in the ES cells can be vertically transmitted.

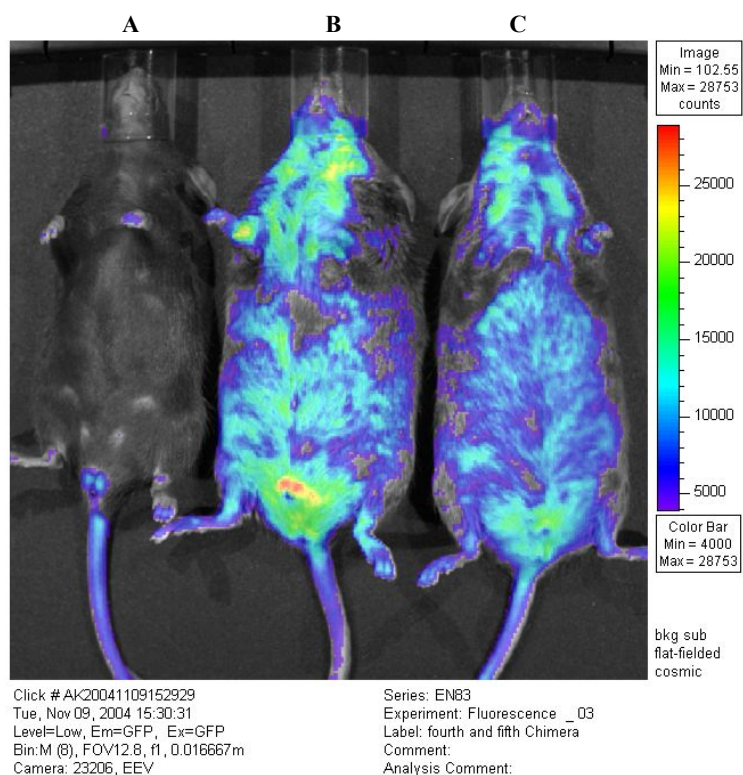


Figure 2.40 Optical charged coupled device imaging of living Nesprin-1 knock-in chimeric mice. (A) Wild type mouse was used as a control. (B and C) Chimeric knock-in Nesprin-1 mice demonstrate expression of GFP in skin.

3. Discussion

3.1 Sun1 and Sun2 proteins display similar topologies at the nuclear envelope

Malone and his colleagues first described the SUN domain in 1999, as an amino acid stretch of about 120 residues in the C terminus of the *C. elegans* UNC-84 protein based on its significant homology to a region in the *S. pombe* Sad1 protein and several uncharacterized mammalian proteins. Genome-database searches indicated that UNC-84 is evolutionarily conserved and that the number of SUN domain proteins has increased over the course of evolution. As shown in the phylogenetic tree, the *S. pombe* genome contains a single SUN domain gene, whereas *C. elegans* has two, and mammals have five paralogues of SUN domain genes namely, *SUN1*, *SUN2*, *SUN3*, *SPAG4* and *SPAG4L*.

Sun1 was first found in a proteomic analysis of the nuclear envelope (Dreger *et al.*, 2001). It is an INM protein (Padmakumar *et al.*, 2005; Crisp *et al.*, 2006) with an N-terminal domain of about 350 amino acids binding to lamin A/C directly (Haque *et al.*, 2006), and a larger C-terminal domain of about 500 amino acids including two predicted coiled-coil domains and the evolutionarily conserved SUN domain. Structural predictions of Sun1 transmembrane domains using the Tmpred software and SMART give slightly different results. Tmpred software predicted three transmembrane domains in Sun1, whereas SMART revealed only two transmembrane domains, in particular the first transmembrane domain was ambiguous. The fact that the Sun1-1TM-N construct containing the ambiguous transmembrane domain could be targeted to the nuclear membrane suggests that mouse Sun1 possesses three closely spaced transmembrane domains between residues 383 and 431, situated approximately in the middle of Sun1. Therefore, Sun1 spans the INM three times, with the N-terminus facing the nucleoplasm and the C-terminus residing in the perinuclear space. In this way, the topology of Sun1 matches that of Sun2 to which it is structurally related (Hodzic *et al.*, 2004).

3.2 Sun1 is a widely expressed INM protein

Sun1 is widely expressed in a variety of tissues, suggesting that Sun1 may play fundamental roles in various cell types. In RT-PCR analysis using N-terminal primers, PCR products were only amplified from brain, kidney, testis, skin and skeletal muscle, but not from heart, liver and lung tissues. This suggests that Sun1 may exist in multiple, alternatively spliced isoforms in different tissues. This conclusion is supported by the examination of Sun1 sequences in the EST-database and northern blot analysis, which reveals at least four or five discrete Sun1 transcripts in different tissues (Crisp *et al.*, 2006). Genetic studies of *Unc-84* in *C. elegans* identified two alternatively spliced products (UNC-84A and UNC-84B) of which only the larger one (UNC-84A) is sufficient to mediate nuclear positioning and rescue the *Unc-84* null-phenotype (Malone *et al.*, 1999). Sun1 interacts with the Nesprin KASH domain via its C-terminus in the nuclear lumen (Padmakumar *et al.*, 2005). *Nesprin-1* and *Nesprin-2* genes give rise to an enormous amount of various isoforms, differing in their expression profile, domain architecture and sub-cellular distribution. The Nesprin isoforms associate with nuclei, mitochondria and the Golgi complex (Gough *et al.*, 2003; Zhang *et al.*, 2005). Smaller Nesprin KASH domain containing isoforms localize at the inner nuclear membrane (Mislow *et al.*, 2002; Zhang *et al.*, 2005). While the respective Nesprin topologies have not been assigned to a particular domain, they may be the result of Sun1 isoform complexity. In such a hypothetical scenario Sun1 isoforms may display different topologies allowing the interaction with various Nesprin isoforms at different organelles. Indeed, a newly generated Sun1 monoclonal antibody in our lab recognized Golgi (made by Martina Munck, 2007). Such thoughts are very attractive considering that the data available for *klarsicht* indicates different roles and different cellular localization for its isoforms. Whereas, KASH domain containing isoforms localize at the nucleus and are required for tethering nuclei in the cytoplasm by linking the ONM directly to the actin cytoskeleton; KASH domain deficient isoforms are required for lipid droplet transport (Starr & Fischer, 2005; Gross *et al.*, 2000).

Indirect immunofluorescence experiments using two polyclonal Sun1 antibodies indicate that Sun1 is largely localized at the NE and colocalizes with the INM emerlin protein. These

data are consistent with the identification of Sun1 and Sun2 proteins in a proteomic screen for NE-specific membrane proteins (Dreger *et al.*, 2001; Schirmer *et al.*, 2003).

3.3 Sun1 displays a low lateral mobility at the NE

The dynamics of Sun1 during interphase have been investigated using inverse fluorescence recovery after photobleaching experiments (iFRAPs). Our results revealed that GFP-Sun1 full-length was immobilized within the nuclear envelope membranes and had a residence time of more than 10 hours – a useful feature for a component possibly involved in nuclear anchorage and migration.

The dynamics of many NE proteins has been characterized by fluorescence recovery after photobleaching (FRAP) assays. Lamin A was shown to move back into the bleach area very slowly, similar to that reported for lamin B1 (>180 min) (Moir *et al.*, 2000). GFP-tagged lamin C expressed in CHO cells has also been reported to show very little recovery after 1 hour (Broers *et al.*, 1999). The slow recovery of lamin A is compatible with its incorporation into stable intermediate filament polymers that exchange subunits very slowly. Most nuclear proteins e.g. transcription factors and even chromatin-associated proteins such as HP1 are very dynamic, recovering into the bleached areas within a few seconds to few minutes (Phair *et al.*, 2004). Even the INM proteins emerin, LAP2 β , and Man1 have recovery halftimes of about 1 minute (Shimi *et al.*, 2004). LBR is more immobile at the NE. More than 60% LBR-GFP fractions reside within the NE membranes 6 min after photobleaching (Ellenberg *et al.*, 1997; Okada *et al.*, 2005). Therefore, Sun1 seems to be one of the most immobile INM proteins described so far. The extensive immobilization of GFP-Sun1 observed from iFRAP experiments suggested a tight binding to fixed structural components of the nucleus or/and retention by assembly into multimeric complexes, which would be expected to result in low diffusion rates. GFP labeled nuclear pore complex components for example, which are known to form oligomeric complexes have been shown to diffuse slowly within the NE (Bucci & Wentz, 1997; Rabut *et al.*, 2004).

The GFP-tagged Sun1 N- (1-407 aa) and C-termini (358-913 aa) localized to the NE independently. Deletion of either N- or C termini resulted however in a partial mislocalization

of Sun1 to ER (Fig. 2.11, arrows). In addition, both chimeric proteins diffused much faster than the full-length protein. These data together suggest that the N- and C-termini of Sun1 have different binding interactions at the NE and that the stability of Sun1 requires both N- and C-termini. It is known that the N-terminus of Sun1 interacts with lamins *in vitro* (Haque *et al.*, 2006), but unlike other INM proteins, the NE localization of Sun1 is lamin A/C and lamin B1 independent (Padmakumar *et al.*, 2005; Hasan *et al.*, 2006), suggesting that Sun1 may interact with additional nuclear components.

The faster dissociation of GFP-Sun1-TM- Δ CC-SUN compared to that of GFP-Sun1-TM-SD1, 2 and GFP-Sun1-Tm-C indicates that the coiled-coil domain is a significant NE retention domain of Sun1. Furthermore, the SUN domain has a more dynamic binding at the nuclear membrane in comparison to the N-terminal domain and the C-terminal coiled-coil domains. Indeed our data indicate that Sun1 forms homo-oligomers and hetero-oligomers with Sun2 via the coiled-coil domains. Therefore, Sun1 and Sun2 can form higher ordered complexes at the NE and interact with other proteins to stabilize the whole complex at the NE. SD2 and SUN domains most probably serve as protein-protein interaction motifs, mediating important SUN related functions such as linking other nuclear proteins including Nesprins to the NE, rather than serve as retention domains. The fact that the Sun1 SD2 domain directly interacts with the Nesprin-1 KASH domain gives rise to the speculation that Sun1 can connect the INM and ONM by providing a perinuclear-tethering device.

3.4 Sun1 oligomerizes via the coiled-coil domains

Genetic evidence indicates that *C. elegans* UNC-84 exists as dimers at the NE (Malone *et al.*, 1999) similar to matefin, another SUN domain protein in *C. elegans* reported to homodimerize (Fridkin *et al.*, 2004). In addition, we observed that the isolated truncated protein of Sun1 polypeptide containing the predicted coiled-coil region can form dimers and tetramers under native conditions or under reduced denature conditions after glutaraldehyde cross-linking. The self-interaction of the coiled-coil region of Sun1 was further confirmed by GST pull-downs and yeast two-hybrid assays. Sun2 also has predicted C-terminal coiled-coil domains and was demonstrated to form homodimers through the N-terminal region and the

coiled-coil domains (Wang *et al.*, 2006). These data together suggest that oligomerization at the NE is a common feature for SUN family members.

V5-tagged full-length Sun1 and HA-tagged C-terminus of Sun1 have the ability to form SDS-resistant dimers under non-reduced conditions, therefore we investigated whether the SDS-resistant Sun1 dimers are due to the formation of disulfide bridges. Indeed, mutagenesis assays demonstrated that the cysteine residue (Cys⁵²⁶) in the Sun1 SD2 domain is responsible for the formation of the SDS-resistant dimers.

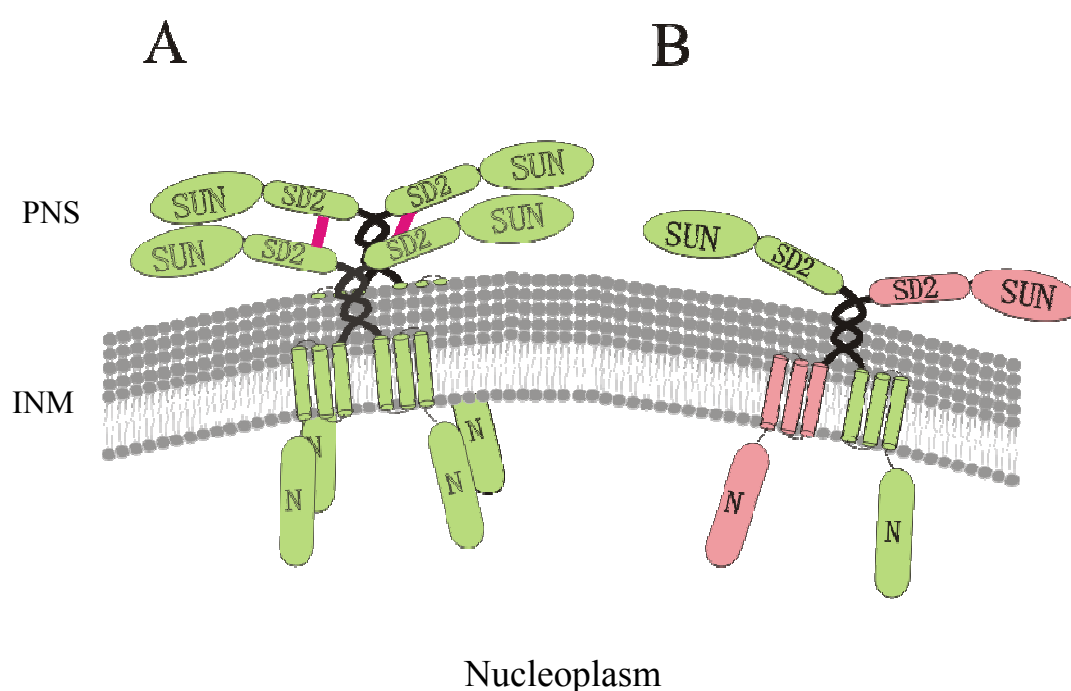


Figure 3.1. Model illustrating the interaction of SUN proteins at the nuclear envelope. (A) Sun1 self-association. Sun1 is composed of a SUN domain, a SD2 domain, a coil-coil domain (black coil), transmembrane domains and an N-terminal nucleoplasmic domain. Two Sun1 proteins can first form a dimer via coil-coil domain, and two dimers can further form a tetramer by disulfide bridges (pink rods) formed in trans between SD2 domains of each dimer. (B) Sun1 and Sun2 interaction. Sun1 (in green) and Sun2 (in pink) are able to form hetero-dimers through their coiled-coil domains.

Therefore, Sun1 can form homodimers via the coiled-coil domains and associate with another Sun1 molecule through disulfide-bond linkage (Fig. 3.1). We demonstrated that Sun1 interacts with Sun2 through their respective coiled-coil domains. Therefore, it is possible that the SUN proteins can form higher ordered complexes around the nuclear envelope and

constitute docking sites for other proteins. The oligomerization of Sun1 may be important for its function at the NE, because each SUN complex could directly anchor two or more binding partners and thereby significantly enhance the mechanical stability of protein complexes that bridge the NE. Furthermore, SUN oligomers could interact with proteins in the same membrane (for example the ONM or the INM), or opposite membranes (the ONM and the INM).

3.5 Sun1 binds to chromatin

Lamin and many lamin binding proteins have the ability to interact with chromatin, providing a membrane anchor important for chromatin organization (Gotzmann & Foisner, 1999). Lamin-B receptor (LBR) forms a complex with histones H3/H4 and heterochromatin protein 1 (HP1) (Polioudaki *et al.*, 2001). Chromatin IPs using a Sun1 specific antibody revealed that human Sun1 also binds to chromatin in ChIP assays.

In *C. elegans*, proper UNC-84 localization requires the nuclear lamina (Lee *et al.*, 2002). In contrast, another *C. elegans* SUN protein, Matefin, localizes to the NE independently of lamin (Fridkin *et al.*, 2004). Recently, mammalian Sun1 has also been shown to localize correctly in the absence of lamin A/C (Padmakumar *et al.*, 2005), and Sun1 depends neither on lamin A/C nor lamin B1 (and likely lamin B2) for INM retention (Hasan *et al.*, 2006).

How mammalian Sun1 is retained in the INM is still an open question. Our result indicates that the interaction between Sun1 and chromatin may confer the NE localization of Sun1 in the absence of A-type lamins. In addition, two more possibilities for Sun1 retention exist. First, Sun1 could bind to DNA directly or indirectly by associating to a DNA-binding protein. This possibility would require a DNA binding domain. Indeed, mouse Sun1 contains a Zn-finger motif within its N-terminal domain. Whether or not this Zn-finger binds to DNA has not been addressed so far. However, even though the overall domain organization of mouse and human Sun1 is similar, human Sun1 does not contain this Zn-finger motif. Therefore, it needs to be experimentally addressed in the future, whether Sun1 binds to DNA directly or not. Second, the Sun1 N-terminus could be recruited to the INM by an interaction with another protein of the INM or the NPC. As we have shown, Sun1 interacts with Sun2.

Sun2 was also identified as a predicted stable component of the nuclear lamina network in a large-scale proteomic analysis of mammalian NE proteins (Schirmer *et al.*, 2003). However, Sun2 was frequently lost from the NE of A-type lamin deficient fibroblasts (Crisp *et al.*, 2006). Sun2 is thus not sufficient to target Sun1 to the NE.

3.6 Sun1 interacts with Nesprins to form a bridge across the NE

Recent focus on NE composition and function has been primarily powered by the unexpected involvement of several NE components and associated proteins in human diseases (Burke *et al.*, 2002). Understanding the pathology of all those diseases requires the identification and functional characterization of all nuclear envelope constituents as a first step, as well as knowledge of the networking interactions that take place at the NE. Towards this end, using both biochemical as well as cell biological data we unravel the first link between an inner nuclear membrane protein (Sun1) and constituents of the outer and inner nuclear membranes (Nesprins).

Genetic studies in *C. elegans* (Starr & Han, 2002) have shown that the SUN domain protein UNC-84 is required for the localization of ANC-1 at the ONM and, in turn UNC-84 requires Ce-lamin for correct NE anchoring (Lee *et al.*, 2002). Although no physical interactions among these proteins have been detected, they have proposed a model in which the luminal domain of UNC-84 forms a complex with the luminal KASH domain of ANC-1. In this way, UNC-84 and ANC-1 would provide a molecular link that spans the perinuclear space (PNS) and connects the actin cytoskeleton to the nuclear lamina. Because similar SUN and KASH domain molecules are widely represented in the animal kingdom, we attempted to determine whether the UNC-84/ANC-1 model was applicable to mammalian systems. We used a combination of RNAi and yeast two hybrid to test this possibility. We found that Sun1 is required for the localization of Nesprin-2 at the NE and that the C-terminal Sun1 SD2 domain is interacting with the conserved luminal KASH domain of Nesprin-1. In addition, overexpressing the C-terminus of Sun1, which resides in the nuclear lumen, caused the loss of both Nesprin-1 and -2 from the NE. Therefore we conclude that the C-terminus of Sun1 interacts with the KASH domain of Nesprin-1 and -2 in the PNS. Unlike other NE proteins,

Nesprins are present on both ONM and INM (Mislow *et al.*, 2002; Zhang *et al.*, 2005; Libotte *et al.*, 2005). The absence of Nesprin-2 staining in Sun1-silenced cells and SPGFP-Sun1-C expressing cells strongly suggests that Sun1 recruits both ONM and INM Nesprin pools through their KASH domains. It should be noted here, that the formation of immobile Sun1 oligomers at the NE, in conjunction with their ability to interact with Nesprins may be the reason for observing endogenous Nesprin-2 proteins as clusters along both sides of the NE (Libotte *et al.*, 2005). The N-terminus of Sun1 interacts directly with the nuclear lamina (Haque *et al.*, 2006) and Nesprins bind to the actin cytoskeleton via their N-terminal actin binding domains (Zhen *et al.*, 2002). Through its direct interaction with both the nuclear lamina and Nesprins, Sun1 therefore forms part of a physical bridge across the NE, linking the nuclear interior to the actin cytoskeleton. Many studies have documented mechanical coupling between the nucleus and the cytoplasm (Maniotis *et al.*, 1997; Lammerding *et al.*, 2004; Broers *et al.*, 2004). Therefore, based on the structural features of the SUN/KASH complex, such associations may be capable of integrating the nucleus into a protein matrix that includes the cytoskeleton, extracellular matrix, and cell–cell adhesion complexes. Whether this connection is able to transduce mechanical signals in response to external stimuli into the nucleus to modulate chromatin organization needs however experimental verification.

In addition to the altered Nesprin-2 localization in Sun1 knockdown cells, the subcellular distribution of emerin and LAP2 β was also influenced, implying that emerin and LAP2 β might associate directly or indirectly with Sun1. In summary, our results suggest a novel Sun1-based mechanism by which Nesprins, emerin and LAP2 β are properly localized to the nuclear membrane. Recent findings emphasized the fundamental functions of emerin, lamins and nuclear envelope proteins in human diseases. Mutations in the human *EMERIN* gene cause the X-linked form of Emery-Dreifuss Muscular Dystrophy, a rare neuromuscular disorder (Emery & Dreifuss, 1966; Wilson, 2000). Mutations in *LAMNA* gene cause diverse tissue-specific disorders, collectively named laminopathies (Wilson, 2000; Broers *et al.*, 2004; Somech *et al.*, 2005). These findings clearly underscore the importance of nuclear envelope and lamina components in a wide range of tissue-specific disorders, but it is still unclear why

and how the lack of nuclear components can cause such effects. The association of Sun1 with lamin A/C and in particular the fact that Sun1 is required for proper emerin localization at the NE implicates the involvement of SUN proteins in human genetic diseases.

3.7 Overexpression of Sun1-C disrupts the SUN-Nesprin linkage across the NE

SPGFP-Sun1-C, the soluble luminal region of Sun1, has the ability to freely diffuse in ER and NE lumen and contains the binding sites of Nesprin-1 and -2 KASH domains. Overexpression of SPGFP-Sun1-C leads to the loss of both Nesprin-1 and -2 from the NE, disrupting the SUN-Nesprin linkage across the nuclear envelope. No effects on other nuclear membrane proteins, however, like endogenous Sun1, emerin, LAP2 and lamins were observed. Therefore the SPGFP-Sun1-C stably transfected cell-line is a Nesprin-deficient cell-line model useful for studying the role and functions of the SUN-Nesprin bridge across the NE.

In our work, we conducted a quantitative comparison between wild-type HaCaT and SPGFP-Sun1-C stably transfected HaCaT cells using a series of experiments. We found that SPGFP-Sun1-C cells, unlike wild type HaCaT, had an abnormal nuclear architecture. More than 30 % of SPGFP-Sun1-C cells display nuclear deformations exhibiting a mean nuclear contour ratio of ~ 0.75 . This value is similar to the one reported for lamin A/C deficient embryonic fibroblasts, which is a paradigm of nuclear structure deformations. A-type lamin deficient embryo fibroblasts have about 37 % irregularly shaped nuclei and a mean contour ratio of about 0.8 (Lammerding *et al.*, 2005). The effect of A-type lamins on nuclear structure and mechanics has also been demonstrated *in vivo* (Nikolova *et al.*, 2004) and *in vitro* (Broers *et al.*, 2004).

Nesprin-1 and Nesprin-2 have been demonstrated to directly associate with actin cytoskeleton (Padmakumar *et al.*, 2004; Zhen *et al.*, 2002). The deletion of the KASH domain of Nesprin-1 abolished the formation of clusters of synaptic nuclei in skeletal muscle (Zhang *et al.*, 2007). These results indicated an essential role of Nesprin in anchorage of nuclei inside

the cell. The nuclear positioning effects are postulated to result from the affected integration of the nuclei to the cytoskeleton due to the absence of the Nesprins. Indeed similar results were obtained for Nesprin orthologues in lower eukaryotes where ANC-1 and MSP-300 mutations affect nuclear positioning in *C. elegans* and *D. melanogaster*, respectively (Starr & Han, 2002; Yu *et al.*, 2006).

However until now there was no evidence that Nesprins have any roles in establishing and maintaining nuclear structure and composition. Here we demonstrated that the loss of both Nesprin-1 and Nesprin-2 from the NE has a severe effect on the morphology of the nuclei, implying that Nesprins are essential proteins for nuclear architecture. It is well known that the lamins have a central role as a load-bearing structure, providing resilience and ability to resist forces of deformation of the nucleus (Broers *et al.*, 2006). Our results indicate that Nesprins can mediate similar functions by reinforcing the nuclear membrane from the cytosolic site. We thus propose two sources of structural platforms counteracting mechanical forces to keep normal nuclei structure, one that comes from the nucleoplasm conferred by lamin and potentially the C-terminal Nesprin variants and the other being provided by Nesprin isoforms localized at the outer nuclear surface. Of course this model needs to be further supported by experiments.

Growth curves showed that SPGFP-Sun1-C cells had a reduced proliferation. BrdU incorporation and cell cycle FACs analysis demonstrated that the percentage of stably transfected cells in the S and G2 phases was lower than that of wild type cells indicating a reduced proliferation for SPGFP-Sun1-C cells. Since Sun1 links Nesprins to A-type lamins, and lamins are well known to have a function in DNA replication and transcription, it is plausible to propose that Nesprins could regulate the cell cycle through lamins. It has been observed that lamins can bind to different transcription regulators. For example, A-type lamins can interact with Rb repressing the activity of the E2F-DP3 transcription factor complex, which is required for the entry into S phase of the cell cycle (Korenjak & Brehm *et al.*, 2005). Interaction of A-type lamins with c-Fos resulted in suppression of AP-1 and a decrease in proliferation in mouse embryonic fibroblasts (Ivorra *et al.*, 2006). There are also reports showing that NE proteins can directly influence the transcription and cell signaling.

For example, GCL is able to inhibit the DP3 subunit of the E2F-DP3 complex independently of Rb (De la Luna *et al.*, 1999). It is also possible that inner nuclear Nesprins could directly regulate cell proliferation.

We observed that the expression level of E-cadherin was increased in SPGFP-Sun1-C stably transfected cells compared to wild type cells. E-cadherin, a Ca^{2+} -dependent transmembrane glycoprotein, plays a key role in the maintenance of intercellular adhesion, regulation of tissue morphogenesis, and cell polarity in epithelial cells, and disruption of E-cadherin expression or function causes invasion and metastasis (Takeichi, 1991; Gumbiner, 1996; Gumbiner, 2005; Wheelock *et al.*, 2003). Therefore, E-cadherin is thought to be an invasion suppressor (Vleminckx *et al.*, 1991; Christofori & Semb, 1999). E-cadherin-mediated cell-cell adhesion plays a critical role in early embryonic development through a mechanism known as EMT (Thiery, 2002). Several molecular mechanisms that up-regulate E-cadherin function have been reported, including gene mutation (Berx *et al.*, 1998), promoter methylation (Graff *et al.*, 2000), and posttranslational modification of the cadherin-catenin complex (Lickert *et al.*, 2000). Which pathway is affected in SPGFP-Sun1-C stably transfected cells still remains elusive. Further investigations are definitely needed to resolve the effects of Nesprins on cell-cell adhesion.

3.8 Proposed roles of Sun1 in higher eukaryotes

Many studies have documented mechanical coupling between the nucleus and the cytoplasm. Maniotis *et al.* (1997) used microneedle-mediated deformation of the cytoplasm of cultured cells to demonstrate mechanical connections between integrins, cytoskeletal filaments, and the nucleoplasm. More recently Lammerding *et al.* (2004) showed that fibroblasts derived from *Lmna*-null mouse embryos have impaired mechanically activated gene transcription. In related studies, Broers *et al.* (2004) have shown that these same cells exhibited reduced mechanical stiffness and perturbations in the organization of the cytoskeleton. The phenotypes displayed by *unc-84* and *Ce-sun1* mutants in *C. elegans* indicate the importance of inner nuclear membrane SUN domain proteins in developmental

processes and that they may play a role in attachment to both the actin and microtubule networks (Malone *et al.*, 1999; Lee *et al.*, 2002; Fridkin *et al.*, 2004).

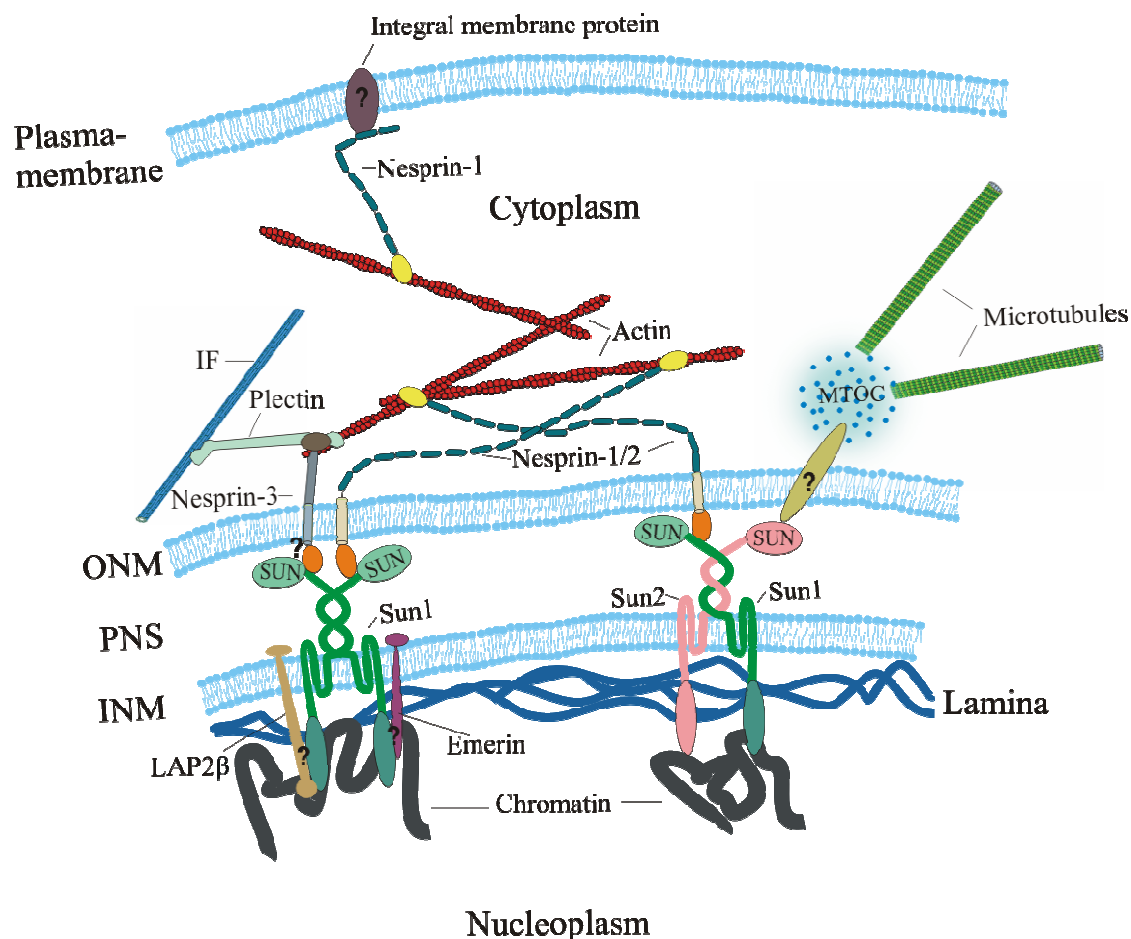


Figure 3.2. Model illustrating mechanical links bridging the nuclear envelope by SUN domain proteins. The scheme depicts (not drawn to scale) the interaction between Sun1 (green), Sun2 (pink) and KASH domain (orange) proteins (Nesprin-1, -2, -3) in the perinuclear space. Sun1 binds to the lamins (blue strands) and chromatin (black) and associates with emerin (purple) and LAP2 β (brown) directly or indirectly. Outer nuclear membrane Nesprin-1 and -2 connect the nucleus to the actin cytoskeleton (red) and Nesprin-3 may associate with Sun1 to connect the nucleus to the intermediate filaments (blue bar) and actin filaments via its interaction with plectin (light blue). SUN domain proteins in *C.elegans* and fission yeast bind to the MTOC or MTOC equivalent structures, therefore in higher eukaryotes SUN proteins may also bind to the MTOC or to microtubules via unknown protein (brown oval with question mark). IF: intermediate filament; ONM: outer nuclear membrane; PNS: perinuclear space; INM: inner nuclear membrane; MTOC: microtubule organizing center. Question marks indicate unknown protein or hypothetical interactions.

On the basis of the currently available data we propose that the existence of the SUN-Nesprin bridge provides a basis for various observations in that it may integrate the nucleus into a protein matrix that includes the cytoskeleton, extracellular matrix, and cell–cell adhesion complexes (Fig. 3.2). This mechanical link may not only provide structural continuity within the cell, but may also directly transduce physical signals from the cytoplasm to the nucleus, facilitating potentially rapid and regionalized gene regulation.

4. Summary

The nucleus is separated from the cytoplasm by a selective structural barrier - the nuclear envelope in eukaryotic cells. The nuclear envelope is composed of inner and outer nuclear membranes (INM and ONM) separated by a perinuclear space (PNS). The specific INM integral proteins interact with the nuclear lamina and are associated with a variety of human diseases, collectively termed nuclear envelopathies. In eukaryotes the SUN domain proteins form a conserved family, the majority of which localize to the INM. UNC-84, which is the first SUN domain protein discovered in *Caenorhabditis elegans*, has been well studied and shown to be involved in nuclear anchorage and migration. Sun1, a novel INM protein, is the closest homolog to *Caenorhabditis elegans* UNC-84 in mammals.

We show that Sun1 is broadly expressed in various mouse tissues. It spans the inner nuclear membrane three times via transmembrane domains with the N-terminus facing the nucleoplasm and the C-terminus residing in the perinuclear space. Like other inner nuclear membrane proteins Sun1 interacts with chromatin. Sun1 proteins are able to form homo-oligomers with a reduced lateral mobility, which are further stabilized by disulfide bonds. Sun1 can also oligomerize with Sun2, another SUN domain paralogous mammalian protein, at the nuclear envelope. The Sun1 C-terminus directly interacts with the KASH domain of Nesprins. These nuclear spectrin repeat containing proteins are able to bind directly to the actin cytoskeleton. Furthermore, we demonstrated that Sun1 is required for the proper nuclear envelope localization of Nesprin-1 and -2 by RNA interference and dominant negative interference studies. Together these data support a model in which SUN proteins tether Nesprins at the envelope via interactions inside the perinuclear space. In this way, SUN proteins and Nesprins form a physical link between the nucleoskeleton and cytoskeleton. We propose that SUN domain proteins by serving as mechanical adaptors and nuclear envelope receptors allow the physical integration and signaling interplay of cytoplasmic and nucleoplasmic compartments.

Zusammenfassung

In eukaryotischen Zellen wird das Nukleoplasma vom Zytoplasma durch die strukturelle und selektive Barriere der Kernhülle getrennt. Die Kernhülle besteht aus einer inneren und einer äußeren Membran (INM und ONM), die durch einen perinukleären Raum (PNS) separiert werden. Spezielle integrale Proteine der INM interagieren mit der Kernlamina und werden mit einer Vielzahl humaner Krankheiten, die allgemein als "nuclear envelopathies" bezeichnet werden, in Verbindung gebracht. In Eukaryonten bilden Proteine mit SUN Domänen eine konservierte Familie, von denen die Mehrheit an der inneren Kernmembran lokalisiert ist. UNC-84 wurde in *Caenorhabditis elegans* als erstes SUN Domänen Protein gefunden.

Eingehende Untersuchungen haben gezeigt, dass dieses Protein an der Verankerung und Migration des Nukleus beteiligt ist. Sun1, ein neues Protein der inneren Kernmembran, besitzt in Säugetieren die größte Ähnlichkeit zum *C. elegans* UNC-84. Menschliches Sun1 wird in verschiedenen Geweben exprimiert. Mit Hilfe von drei Transmembrandomänen wird dieses Protein in der INM spezifisch verankert, wobei der N-Terminus in das Nukleoplasma und der C-Terminus in den perinukleären Raum hineinreichen. Zudem besitzt Sun1 wie auch andere Proteine der INM die Fähigkeit an Chromatin zu binden. Weiterhin konnten wir zeigen, dass Sun1 in der Lage ist, Homo-Oligomere zu bilden, die durch Disulfidbrückenbindungen stabilisiert und somit in ihrer lateralen Beweglichkeit eingeschränkt werden. Sun1 kann außerdem mit Sun2, einem weiteren Säuger Paralog, das ebenfalls an der Kernhülle lokalisiert, Oligomere bilden. Der C-Terminus von Sun1 interagiert direkt mit den KASH Domänen von Nesprinen. Diese Kernhüllenproteine, die eine Vielzahl von Spektrin Domänen aufweisen, können über eine N-terminale Aktin-bindende Domäne an das Aktin-Zytoskelett binden. Im Rahmen dieser Arbeit konnte mittels der RNAi Technik und der Expression dominant negativer Proteine in Zellen gezeigt werden, dass Sun1 für die Lokalisierung von Nesprin-1 und -2 an der Kernhülle verantwortlich ist. Zusammenfassend unterstützen diese Daten ein Modell, in dem SUN Proteine Nesprine durch die Interaktion im perinukleären

Raum an die Kernhülle binden. Auf diese Weise bilden die SUN und die Nesprine Proteine eine physikalische Verknüpfung zwischen dem Nukleo- und Zytoplasma. Dies lässt vermuten, dass SUN Proteine als mechanische Adaptoren und Rezeptoren der Kernhülle fungieren, um die physische Eingliederung und Signaltransduktion zwischen zyto- und nukleoplasmatischen Zellbestandteilen zu ermöglichen.

5. Materials and methods

5.1 Cloning strategies

The appropriate DNA fragments of mouse Sun1 were amplified from IMAGE clone AH48156 by PCR and cloned into pGEMTeasy (Promega) vectors before cloning them in the GFP, GST or yeast two-hybrid vectors. All the GFP fusion proteins generated carry GFP at their N-terminus. GFP-Sun1-1TM-N (aa 1-384), amplified by Ntermouseunc84.5' and NTM1SUN1rev primers and GFP-Sun1-TM-C (aa 358-913), amplified by GFPCT+3TMUNC84.5' and Munc84dsred.3' primers were cloned into the EcoRI/SalI site of EGFP-C2 vector. GFP-Sun1 full-length (aa 1-913), GFP-Sun1-2TM-N (aa 1-412), GFP-Sun1-TM-SD1, 2 (aa 358-737), GFP-Sun1-TM- Δ CC-SUN (aa 358-491, 633-913), GFP-Sun1-SD1, 2 (aa 432-737) and GFP-Sun1-SD2 (aa 432-491, 633-737) were cloned into the EcoRI/BamHI site of the EGFP-C2 plasmid. Sun1 full-length (aa 1-913) was amplified using Ntermouseunc84.5' and Ctermouseunc84.3' primers. Sun1-2TM-N (aa 1-412) was amplified using Ntermouseunc84.5' and Ntermouseunc84.3' primers. Sun1-TM-SD1, 2 was amplified using GFPCT+3TMUNC84.5' and bSUNy2h.3' primers. Sun1-TM- Δ CC-SUN was generated by performing two rounds of PCR. A first round of PCR was performed using the GFPCT+3TMUNC84.5' / Tm3SUN1 rev primers (PCR1) and the DSUN for / bSUNy2h.3' primers (PCR2) on the Sun1 full-length template. The products of PCR1 and PCR2 were mixed and used as the template using the Sun1-TM- Δ CC-SUN with GFPCT+3TMUNC84.5' and bSUNy2h.3' set of primers. Sun1-SD1, 2 was amplified using Ctermouseunc84.5' and bSUNy2h.3' primers. Sun1-SD2 was amplified using Ctermouseunc84.5' and bSUNy2h.3' primers from GFP-Sun1-TM- Δ CC-SUN. GST-SD1, 2 (aa 432-737) and GST-Sun1-SD1 (aa 432-632) were cloned in pGEX4T-1 vector between the EcoRI and XhoI sites. The luminal domain of Nesprin-1 (LDN-1 residues 109-138, BE917568) was amplified from embryonic stem cell genomic DNA and cloned between EcoRI and SalI sites in pGBKT7 (Clontech) vectors. Sun1-SD1 (aa 431-633) and Sun1-SD2 (aa 632-737) were cloned into EcoRI/BamHI-digested pGADT7. SD2 was amplified using u84-D3-for and bSUNy2h.3' primers. SPGFP-

Sun1-C was prepared in the following way: fragments encoding the signal peptide sequence of Torsin A and EGFP were isolated from pcDNAV5HisGFP-hTORA (gift from Dr. William Dauer; Goodchild & Dauer, 2004) plasmid by XhoI/EcoRI digestion and ligated into XhoI/BamHI-digested pcDNA3.1 (-) together with the EcoRI/BamHI-digested Sun1-C fragment, which was isolated from the pEGFPC2-CT plasmid generated previously by Padmakumar Velayuthan Chellammal.

The plasmid pJG128 containing V5-tagged full-length human Sun1 and the plasmid pJG129 containing V5-6xHis-tagged full-length human Sun2 were kindly provided by Dr. Josef Gotzmann (Biocenter, Vienna). hSun1-CC (aa 404-527) was amplified by 5'hSun1CCy2h and 3'hSun1CCy2h primers and cloned into EcoRI/BamHI-cut pGBKT7 and pGADT7. hSun2-CC (aa 400-505) was amplified by 5'hSun2CCy2h and 3'hSun2CCy2h primers and cloned into pGADT7 vector between EcoRI and BamHI sites. hSun1-TM-C (aa 240-812) amplified by 5'hSun1TM1 and 3'hSun1SUN primers and hSun1-TM-SD1, 2 (aa 240-632) amplified by 5'hSun1TM1 and 3'hSun1SD2 primers were cloned in pHA (Roche) vector between the EcoRI and HindIII sites.

5.2 Primer sequences for cloning

Ntermouseunc84.5' primer

CGAATTCATGGACTTTTCTCGGCTGCACACGTAC

Ntermouseunc84.3' primer

CGGATCCCTTGCAAATATTTTGAAGGCACCTGGTAAG

NTM1SUN1rev primer

GTCGACGAAGGTTCCCGAGGCTGCCTT

GFPCT+3TMUNC84.5' primer

CGAATTCGGGTGGTCTGTGGCCGAGGCCGTG

bSUNy2h.3' primer

CGGATCCTTGGGAGTACAGCTTCAGAGCATTG

Munc84dsred.3' primer

CGTCGACAACTGGATGGGCTCTCCGTGGACTC

Ctermouseunc84.5' primer

CGAATTCGTCTCCCTGTGGGGCCAGGGAAACTTC

Ctermouseunc84.3' primer

CGGATCCCTACTGGATGGGC TCTCCGTGGACTC

Tm3SUN1 rev primer

AGCCTGCTGACAGCTGGTCCCCATGTCACTCTCCTG

DSUN for primer

CAGGAGAGTGACATGGGGACCAGCTGTGAGCAGGCT

U84-D3-for primer

GAATTCAAGACCAGCTGTGAGCAGGCTGGGG

5'hSun1CCy2h primer

GAGGAATTCCACCACCATGGTGAGAAT

3'hSun1CCy2h primer

GTAGGATCCGTTTTTTGCTTGGTCTGT

5'hSun2CCy2h primer

GAGGAATTCCAGGAGTCCTTCCAGGAG

3'hSun2CCy2h primer

GTAGGATCCCTACCTGGCCGACTTGCCCT

5'hSun1TM1 primer

TGTAAGCTTCTGGCACATCTGGGCATGTG

3'hSun1SUN primer

GTCGAATTCTTGACAGGTTCGCCATG

3'hSun1SD2 primer

CTGGAATTCAGCTTCAAGGCGCTGTT

5.3 RNA isolation and RT-PCR analysis

Total RNA was extracted from mouse tissues with TRIZOL reagent (Invitrogen Life Technologies, Carlsbad, CA), following the manual's instructions. The concentration of the RNA was measured with a UV spectrophotometer. The quality of the RNA was evaluated by running RNA samples on a 1.2% gel. Two sets of specific primers were designed from published mouse Sun1 DNA sequences (accession No. BC048156) obtained from the NCBI. For the N-terminus: 5'-CGCACTCAGTTCTAGTTACTCG-3' and 5'-TATTTCCACCTTTAAGGTCACC-3' and for the C-terminus: 5'-AGTCTGGAGGTGGCAGCATC-3' and 5'-GCTCTACTATCTGGAAGGCTTG-3'. RT-PCR was performed according to standard protocols. Briefly, total RNA was reverse transcribed using oligo (dT) primers and reverse transcriptase (Invitrogen) according to the manufacturer's instructions. The cDNA (2 µg) was amplified for 35 cycles using the following conditions: 94°C for 30 seconds, 60°C for 45 seconds and 72°C for 1 minute, resulting in a 400-bp cDNA coding for N-terminal Sun1 and C-terminal Sun1 sequence, respectively. GAPDH was amplified as control using GAPDH specific primers 5'-GTCTACATGTTCCAGTATGACTCCACTCACGG-3' and 5'-GTTGCTGTAGCCGTATTCATTGTCATAACCAGG-3'.

5.4 Tissue culture and transfection

COS7 cells were grown as described (Padmakumar *et al.*, 2004). HaCaT cells and human primary fibroblasts were routinely cultivated in DMEM supplemented with 10% fetal calf serum at 37°C in a humidified atmosphere containing 5% CO₂. HeLa cells were grown in DMEM medium supplemented with 10% fetal bovine serum, 2 mM glutamine, 1 mM pyruvate at 37°C, 5% CO₂ and 100% humidity. Tissue culture media, supplements, fetal bovine serum and inhibitors were from Sigma.

COS7 cells were transfected by electroporation (200V, 950 µF; Gene Pulser Xcell, Bio-Rad). HaCaT cells were transfected by using the Amaxa nucleofector technology according to the manufacturer's instructions (Amaxa Biosystems). HeLa and human primary fibroblasts were transfected by FUGENE HD transfection reagent according to the manufacturer's instructions (Roche).

5.5 Establishment of stably transfected HaCaT cell lines

1x10⁶ HaCaT cells were transfected with 5 µg circular SPGFPC plasmid DNA according to the Amaxa manufacture's instructions. Cells were split to 1:10, 1:20, 1:50 into 15 cm plates containing growth medium. Selection was initiated 24 h after electroporation with medium containing 1mg/ml G418 (GIBCO BRL). After approximately 10-15 days, G418 resistant clones were picked using cloning discs (Sigma) and placed first into 24 well plates. When the clones reached around 80% confluence, cells were expanded and placed into 6 well plates and examined using the fluorescence microscope (Olympus). Positive clones were used for further studies.

5.6 Inverse fluorescence recovery after photobleaching experiments (iFRAP)

For live-cell imaging, Hela cells were transiently transfected with GFP fusion constructs using FUGENE 6 transfection reagent and examined 48 hours after transfection. iFRAPs were performed on a customized LSM510 confocal microscope using a 40 x 1.3 NA oil Fluor

objective and a completely open pinhole. Most cellular fluorescence was bleached using full laser power and leaving only a fraction (typically 10–20%) of nuclear envelope unbleached. Post-bleach images were then acquired for up to 10 h at regular time intervals, depending on the dynamics of the GFP fusion proteins. Image acquisition was semi-automated, using a visual basic macro developed for the LSM software that automatically corrected focus fluctuations, tracked moving cells and parallelized image acquisition at multiple locations (Rabut *et al.*, 2004).

Images of iFRAP time series were first registered to correct for cellular movements (translations and rotations) using the TurboReg plugin (<http://bigwww.epfl.ch/thevenaz/turboreg/>) for ImageJ (<http://rsb.info.nih.gov/ij/>). Then, for each time point the average fluorescence intensities of unbleached ($F_u(t)$) and bleached ($F_b(t)$) GFP signal was measured in the respective regions. The background (BG(t))-subtracted intensities were normalized by the corresponding background-subtracted pre-bleach values ($F_u(t_{pre})-BG(t_{pre})$ and $F_b(t_{pre})-BG(t_{pre})$ respectively), and if necessary corrected for acquisition photobleaching. To obtain the dissociation kinetics ($D(t)$), we subtracted the fluorescence of the bleached GFP signal from that of the unbleached GFP signal. Its initial time was set to the time of acquisition of the first post-bleach image (t_{post}) and its initial intensity to 1. The dissociation kinetic is thus given by the formula:

$$D(t-t_{post}) = \frac{\left(\frac{F_u(t)-BG(t)}{F_u(t_{pre})-BG(t_{pre})} - \frac{F_b(t)-BG(t)}{F_b(t_{pre})-BG(t_{pre})} \right)}{\left(\frac{F_u(t_{post})-BG(t_{post})}{F_u(t_{pre})-BG(t_{pre})} - \frac{F_b(t_{post})-BG(t_{post})}{F_b(t_{pre})-BG(t_{pre})} \right)}$$

5.7 Antibodies and immunofluorescence microscopy

Western blotting and immunofluorescence (IF) studies were performed as described (Zhen *et al.*, 2002; Gotzmann *et al.*, 2000).

The following antibodies were used: mouse monoclonal anti-Nesprin-2/NUANCE mAb K20-478 (Zhen *et al.*, 2002), mouse monoclonal anti-Nesprin-2/NUANCE mAb K49-260 (Libotte *et al.*, 2005), rabbit polyclonal Nesprin-2 pAbK1 (1:50 IF, 1:1000 western blotting),

rabbit polyclonal Nesprin-1 SpecII(1:15 IF), mouse monoclonal anti-emerin (1:40 IF, 1:100 western blotting), mouse monoclonal anti-lamin A/C (1:50 IF; JoL2, Chemicon), mouse monoclonal anti-LAP2 β (1:250 IF) (Dechat *et al.*, 1998), mouse monoclonal anti- β -tubulin (1:50 IF, 1:1000 WB; WA3), rat anti-E-cadherin antibody (1:40 IF, 1:500 WB), goat polyclonal anti-GST antibody (Amersham Biosciences), GFP-specific mAb K3-184-2 (Noegel *et al.*, 2004), rat anti-HA antibody, mouse monoclonal anti-V5 antibody (Invitrogen), mouse monoclonal anti-BrdU mAb G3G4 (1:200 IF), unpurified rabbit polyclonal hSun1 281 (1:50 IF; 1:400 western blotting), rabbit polyclonal hSun1 282 (1:50 IF; 1:400 western blotting). Sun1 polyclonal antibodies were produced against two peptides encompassing the first 14 amino acids (MDFSRLHMYSPQ; NP_079430) and amino acids 358-372 (RVDDPQDVFKPTTSR) of human Sun1 to create antisera 281 and 282, respectively (Eurogentec, Belgium). The secondary antibodies used were conjugated with Cy3 (Sigma), TRITC (Sigma) and FITC (Sigma). Samples were analysed by wide-field fluorescence microscopy (DMR, Leica, Bensheim, Germany) or confocal laser-scanning microscopy (TCS-SP, Leica).

5.8 siRNA knockdown of Sun1

The RNA interference-competent vector pSHAG-1 (containing a human U6 promoter fragment; -265 to +1) was constructed in the pTOPO-ENTR/D backbone (Invitrogen), as described (Paddison *et al.*, 2002; http://katahdin.cshl.org:9331/RNAi_web/scripts/main2.pl). Oligonucleotides A and B, encoding a short hairpin RNA, were designed according to the RNAi-retriever protocol at <http://katahdin.cshl.org:9331/homepage/portal/html/protocols/>. For knocking down specifically human Sun1 the following oligonucleotides were used to create vectors pJG173 and pJG174, respectively: Oligo 173A, 5'-CTCGGACAGCATGCTGCAGTTGCTGCAGGAAGCTTGCTGCGGCGACTGCGGCATGTTGTCCGAGCGCTTTTTT-3'; Oligo 173B, 5'-GATCAAAAAGCGCTCGGACAACATGCCGAGTCGCCGAGCAAGCTTCTGCAGCAACTGCAGCATGCTGTCCGAGCG-3'; Oligo 174A, 5'-AGGACGTGACCTGCCTTGACACGTGGTTGAAGCTTGAGCCGCGTGTTAAGGCAGGTCACGTTCTCTGTTTTT-3'; Oligo 174B, 5'-

GATCAAAAAACAGAGAACGTGACCTGCCTTAACACGCGGCTCAAGCTTCAACCA
C GTGTCAAGGCAGGTCACGTCCTCG-3'. Annealed oligonucleotides were cloned into pSHAG-1 by insertion of resulting overhangs into the BseRI/BamHI-sites. The control vector pSHAG-FF1 encoding a shRNA targeting Firefly Luciferase was a kind gift of Greg Hannon (Cold Spring Harbor Laboratory, NY). The integrity of all vectors was verified by sequencing from both ends. Two RNAi-vectors targeting hSun1 were always mixed and used for transient knockdown experiments. The cells were fixed 4 days after the transfection and examined by indirect immunofluorescence.

5.9 Chromatin immunoprecipitation assays (ChIP)

ChIP assays were performed using a ChIP-IT express kit and ChIP-IT control kits (Active motif) as described in the manufacturer's instructions. Briefly, approximately 4.5×10^7 HaCaT cells were fixed by 1% formaldehyde for 10 minutes at room temperature. The fixation reactions were stopped by Glycine Stop-Fix solution. Cells were washed once with ice-cold PBS and collected using ice-cold Cell Scraping Solution. Cells were pelleted by centrifugation and then resuspended in ice-cold Lysis Buffer (supplemented with proteinase inhibitor + PMSF). Samples were incubated on ice for 30 minutes. Nuclei were pelleted and resuspended in the Shearing Buffer. We sheared the DNA to an average length of 200 bp to 1,000 bp. The sheared DNA samples were centrifuged at 10,000 to 15,000 rpm in a 4°C microcentrifuge for 12 minutes. A small aliquot of the sheared chromatin (supernatant) was used for checking the DNA shearing efficiency and DNA concentration. Protein G Magnetic Beads/Sheared Chromatin/Antibody mixtures were incubated on a rolling shaker overnight at 4°C. hSun1, negative Control IgG and an RNA pol II antibody (positive control) were used for ChIP reactions. The DNA/protein complexes were eluted and treated with 0.4 µg/µl proteinase K at 37°C for 1 hour. The proteinase K digestion was stopped and the eluted DNA was immediately processed as a template for further PCR analysis. Eluted DNA from the hSun1 antibody, negative control IgG and RNA pol II antibody and purified DNA from the sheared chromatin, were assessed for the presence of the GAPDH DNA fragments using PCR and the following primers: 5'GAPDH exon1, 5'-GCGCCCCCGGTTTCTATAAATTGAG-3'

and 3'GAPDH exon1, 5'-AGAGAACAGTGAGCGCCTAGTGGCC-3'. 3 µl of each eluted DNA was amplified for 34 cycles using the following conditions: 95°C for 30 seconds, 70°C for 30 seconds and 72°C for 40 seconds.

5.10 Purification of GST fusion proteins and in vitro binding assays

Purification of GST fusion proteins and GST pull-down experiments were performed as described (Dreuillet et al., 2002). For the pull-down assay, transfected COS7 cells were lysed with 50 mM Tris-HCl, pH 7.5, 150 mM NaCl, 1% Triton X-100 and protease inhibitors (Roche). The 100,000 g supernatant of the lysate was incubated with equal amounts of GST fusions and the solutions were incubated at 4°C overnight with GST-sepharose beads on a roller. Samples were centrifuged and the pellets (washed five times with PBS and two times with lysate buffer) and then analyzed by SDS-PAGE and concomitant western blot analysis.

5.11 Native Polyacrylamide Gel-Electrophoresis (Native-PAGE)

Native gels were prepared similar to SDS polyacrylamide gels, except that SDS omitted from the gels and buffers employed. Each sample was mixed with 2 x blue native sample buffer (pH 6.8) containing 20% glycerol and 0.01% bromophenol blue in 125 mM Tris-HCl (pH 6.8) and applied onto the native polyacrylamide gel without heating. Molecular mass marks (Amersham Biosciences) and BSA were used as the standards. The gel was run in the cold room and subsequently visualized by Coomassie Blue staining.

5.12 Chemical Cross-linking Experiments

Cross-linking experiments with the bacterially expressed coiled-coil fraction of mouse Sun1 were performed in a buffer containing 20 mM HEPES, pH 8.0, 150 mM NaCl, 5 mM EDTA, and incubated with 0.001%- 0.03% glutaraldehyde for 30 min at room temperature. SDS sample buffer was added to the reactions, and the samples were resolved by 12% SDS-PAGE gel and stained by Coomassie Blue.

5.13 Yeast two-hybrid assay

Y190 yeast cells were cotransformed with the plasmids and transformants were selected on SD-Trp-Leu plates. Interaction was monitored by growth on plates containing selection media SD-Trp-Leu-His and 60 mM 3-amino 1,2,4-triazole. An X-Gal assay was also performed to confirm the interaction. The protocols for performing the yeast transformation and X-gal assay are described in detail elsewhere (Yeast Protocols Handbook PT3024-1; Clontech).

5.14 Site-directed Mutagenesis

Construction of the point mutant (C526A) in hSun1-TMC-HA and hSun1-TMSD1, 2-HA was done with the QuikChange XL Site-Directed Mutagenesis Kit (Stratagene, La Jolla, CA) as described in the manual. For the generation of C-terminally HA-tagged Sun1-TMCC526A and Sun1-SD1, 2 C526A mutants, pHA-hSun1-TMC and pHA-hSun1-TMSD1, 2 were used as templates for two independent PCRs and the following oligonucleotides as the mutagenic primers:

	tmcDelta526sense:	5'-
	GCGACACGTGAAGACCGGCGCCGAGACAGTGGATGCCGTAC-3'	and
	tmcDelta526antisense:	5'-
	GTACGGCATCCACTGTCTCGGCGCCGGTCTTCACGTGTCGC-3'	

The mutations in Sun1-TMCC526A-HA and Sun1-SD1, 2 C526A-HA were verified by DNA sequencing.

5.15 His-tag pull-down assays

GFP-Sun1 and Sun2-V5·6xHis, or GFP and Sun2-V5·6xHis were transiently cotransfected into COS7 cells. The transfected cells were lysed using lysate buffer (50 mM NaH₂PO₄, 150 mM NaCl, 1% NP-40, 0.5% Na-desoxycholate, pH 8.0). Same amount of proteins from GFP-Sun1 and Sun2-V5·6xHis cotransfected cells, and GFP and Sun2-V5·6xHis cotransfected cells were coupled to Ni-NTA agarose beads (Qiagen, Hilden) by incubation for 4 hours at 4°C in 1 ml of lysate buffer. The Ni-NTA agarose beads were washed 5 times with PBS, and three times with lysate buffer. The beads were precipitated by

centrifugation at 2,000 g, and proteins bound to the beads were eluted with SDS sample buffer, resolved by 12% SDS-PAGE and subjected to western blotting analysis.

5.16 BrdU incorporation

Stably transfected SPGFPC HaCaT cells and control HaCaT cells were plated onto glass coverslips. After 12 hrs, the cells were incubated with 10 µg/ml BrdU (5'-bromo-2'-deoxyuridine) for 2 hrs under growing conditions. BrdU was diluted in cell culture medium. After incubation, the cells were fixed with 3% paraformaldehyde and permeabilized with 0.4 % tritonX-100. To render incorporated BrdU accessible to antibody, the fixed cells were rinsed twice with PBS, incubated in 2 M HCl for 40 min at room temperature and neutralized by three washes of PBS. Then the cells were blocked with blocking buffer for 1 hour. Immunofluorescence was carried out with G3G4 antibody.

5.17 Generation of Growth Curves

The growth rate of stable clones of transfected SPGFP-Sun1-C and control HaCaT cells were generated by seeding cells at a density of 1×10^5 cells/10 cm plate in 10% FCS DMEM (duplicate plates for each cell line). Every 48 hrs, the cells were trypsinized and counted using a cell counter.

5.18 PI/FACS (cell cycle) analysis

Cells were harvested from a 70% confluent 10 cm dish by scrapping and washed once with 5-10 ml PBS. After washing, 5 ml of cold 70% ethanol (-20°C) was immediately applied to the cells and mixed completely. The cells were fixed at 4°C for at least 1 hour by ethanol and after fixation were washed once again with PBS (10ml). Subsequently, the cell pellet was resuspended in 300µl propidium iodide (PI) solution (50µg/ml Propidium Iodide (Sigma) in 38mM NaCitrate, pH 7.4) with 20µl of 10mg/ml RNase. Then the sample was incubated at 37°C for 30-45min in dark. Finally, the cell solution was transferred to FACS tubes and

analyzed a Becton Dickinson Calibur cytofluorimeter. The raw data was further analyzed by a Cellquest Software. Experiments were run in duplicate.

5.19 Senescence-Associated β -Galactosidase Assays

Cells were seeded on cover slips the previous day; the next day cover slips were washed with PBS and fixed 3-5 min with 2% formaldehyde/0.2% glutaraldehyde (or 3% formaldehyde) at room temperature. Cells were washed twice with PBS and then incubated at 37°C (no CO₂) with freshly prepared senescence-associated β -Gal (SA- β -Gal) staining solution: (1 mg/ml 5-bromo-4-chloro-3-indolyl β -D-galactoside (X-Gal), 40 mM citric acid/sodium phosphate pH 6.0, 5 mM potassium ferrocyanide K₄Fe(CN)₆, 5 mM potassium ferricyanide K₃Fe(CN)₆, 150 mM NaCl, 2 mM MgCl₂). The cells were examined under the microscope for staining. Normally, the blue color is observable in 2-4 hrs and maximal in 12-16 hrs. Control HaCaT and SPGFPC stably transfected HaCaT cells were viewed under bright field microscopy at 40x magnification.

5.20 Nuclear shape analysis

To quantify the overall fraction of irregularly shaped or blebbing nuclei, HaCaT wild-type cells and SPGFP-Sun1-C stably transfected clones #1 and #3 were incubated for 30 min with 0.1 μ g/ml DAPI (Molecular Probes) and washed with PBS. For each cell-type, fluorescence images of 200 randomly selected nuclei were acquired at 20x on a microscope (model CTRMIC; Leica) using a DFC350 FX camera (Leica). To quantify the variation in nuclear morphology, we measured nuclear area and perimeter in midsections of the fluorescent nuclei using Leica FW4000 software. From these data, we computed the nuclear roundness or contour ratio ($4\pi \times \text{area} / \text{perimeter}^2$) (Goldman *et al.*, 2004). The contour ratio reaches a maximum value of 1 for a circle and decreases with increasingly convoluted nuclear shapes.

5.21 Statistical analysis

Data are expressed as mean \pm standard deviation (SD). Statistical comparisons were made using unpaired Student's t-tests. A difference was considered significant at a value of $P < 0.05$.

6. References

1. Apel ED, Lewis RM, Grady RM, Sanes JR (2000). Syne-1, a dystrophin- and Klarsicht-related protein associated with synaptic nuclei at the neuromuscular junction. *J. Biol. Chem.* 275: 31986-31995.
2. Berx G, Nollet F, van Roy F (1998). Dysregulation of the E-cadherin/catenin complex by irreversible mutations in human carcinomas. *Cell Adhes. Commun.* 6: 171-184.
3. Bonne G, Di Barletta MR, Varnous S, Becane HM, Hammouda EH, Merlini L, Muntoni F, Greenberg CR, Gary F, Urtizbera JA, Duboc D, Fardeau M, Toniolo D, Schwartz K (1999). Mutations in the gene encoding lamin A/C cause autosomal dominant Emery-Dreifuss muscular dystrophy. *Nat. Genet.* 21: 285-288.
4. Broers JL, Machiels BM, van Eys GJ, Kuijpers HJ, Manders EM, van Driel R, Ramaekers FC (1999). Dynamics of the nuclear lamina as monitored by GFP-tagged A-type lamins. *J. Cell Sci.* 112: 3463-3475.
5. Broers JL, Peeters EA, Kuijpers HJ, Endert J, Bouten CV, Oomens CW, Baaijens FP, Ramaekers FC (2004). Decreased mechanical stiffness in LMNA^{-/-} cells is caused by defective nucleo-cytoskeletal integrity: implications for the development of laminopathies. *Hum. Mol. Genet.* 13: 2567-2580.
6. Broers JL, Ramaekers FC, Bonne G, Yaou RB, Hutchison CJ (2006). Nuclear lamins: laminopathies and their role in premature ageing. *Physiol. Rev.* 86: 967-1008.
7. Bucci M, Wente SR (1997). In vivo dynamics of nuclear pore complexes in yeast. *J. Cell Biol.* 136: 1185-1199.
8. Burkhard P, Stetefeld J, Strelkov SV (2001). Coiled coils: a highly versatile protein folding motif. *Trends. Cell Biol.* 11: 82-88.
9. Burke B, Stewart CL (2002). Life at the edge: the nuclear envelope and human disease. *Nat. Rev. Mol. Cell Biol.* 3: 575-585.
10. Burke B, Ellenberg J (2002). Remodelling the walls of the nucleus. *Nat. Rev. Mol. Cell Biol.* 3: 487-497.
11. Cai M, Huang Y, Ghirlando R, Wilson KL, Craigie R, Clore GM (2001). Solution structure of the constant region of nuclear envelope protein LAP2 reveals two LEM-domain structures: one binds BAF and the other binds DNA. *EMBO J.* 20: 4399-4407.
12. Campisi J (2003). Cancer and aging: rival demons? *Nat. Rev. Cancer.* 3: 339-349.

13. Chikashige Y, Tsutsumi C, Yamane M, Okamasa K, Haraguchi T, Hiraoka Y (2006). Meiotic proteins bqt1 and bqt2 tether telomeres to form the bouquet arrangement of chromosomes. *Cell*. 125: 59-69.
14. Clements L, Manilal S, Love DR, Morris GE (2000). Direct interaction between emerin and lamin A. *Biochem. Biophys. Res. Commun.* 267: 709-714.
15. Crisp M, Liu Q, Roux K, Rattner JB, Shanahan C, Burke B, Stahl PD, Hodzic D (2006). Coupling of the nucleus and cytoplasm: role of the LINC complex. *J. Cell Biol.* 172: 41-53.
16. Christofori G, Semb H (1999). The role of the cell-adhesion molecule E-cadherin as a tumour-suppressor gene. *Trends Biochem. Sci.* 24: 73-76.
17. Cutler DA, Sullivan T, Marcus-Samuels B, Stewart CL, Reitman ML (2002). Characterization of adiposity and metabolism in *Lmna*-deficient mice. *Biochem. Biophys. Res. Commun.* 291: 522-527.
18. Dechat T, Gotzmann J, Stockinger A, Harris CA, Talle MA, Siekierka JJ, Foisner R (1998). Detergent-salt resistance of LAP2alpha in interphase nuclei and phosphorylation-dependent association with chromosomes early in nuclear assembly implies functions in nuclear structure dynamics. *EMBO J.* 17: 4887-4902.
19. De La Luna S, Allen KE, Mason SL, La Thangue NB (1999). Integration of a growth-suppressing BTB/POZ domain protein with the DP component of the E2F transcription factor. *EMBO J.* 18: 212-228.
20. De Sandre-Giovannoli A, Chaouch M, Kozlov S, Vallat JM, Tazir M, Kassouri N, Szepietowski P, Hammadouche T, Vandenberghe A, Stewart CL, Grid D, Levy N (2002). Homozygous defects in LMNA, encoding lamin A/C nuclear-envelope proteins, cause autosomal recessive axonal neuropathy in human (Charcot-Marie-Tooth disorder type 2) and mouse. *Am. J. Hum. Genet.* 70: 726-736.
21. Dimri GP, Lee X, Basile G, Acosta M, Scott G, Roskelley C, Medrano EE, Linskens M, Rubelj I, Pereira-Smith O, Peacocke M, Campisi J (1995). A biomarker that identifies senescent human cells in culture and in aging skin in vivo. *Proc. Natl. Acad. Sci. U S A.* 92: 9363-9367.
22. Dreger M, Bengtsson L, Schoneberg T, Otto H, Hucho F (2001). Nuclear envelope proteomics: novel integral membrane proteins of the inner nuclear membrane. *Proc. Natl. Acad. Sci. USA.* 98: 11943-11948.

23. Dreuillet C, Tillit J, Kress M, Ernoult-Lange M (2002). In vivo and in vitro interaction between human transcription factor MOK2 and nuclear lamin A/C. *Nucleic. Acids Res.* 30: 4634-4642.
24. Drummond S, Ferrigno P, Lyon C, Murphy J, Goldberg M, Allen T, Smythe C, Hutchison CJ (1999). Temporal differences in the appearance of NEP-B78 and an LBR-like protein during *Xenopus* nuclear envelope reassembly reflect the ordered recruitment of functionally discrete vesicle types. *J. Cell Biol.* 144: 225-240.
25. Dwyer N, Blobel G (1976). A modified procedure for the isolation of a pore complex-lamina fraction from rat liver nuclei. *J. Cell Biol.* 70: 581-591.
26. Ellenberg J, Siggia ED, Moreira JE, Smith CL, Presley JF, Worman HJ, Lippincott-Schwartz J (1997). Nuclear membrane dynamics and reassembly in living cells: targeting of an inner nuclear membrane protein in interphase and mitosis. *J. Cell Biol.* 138: 1193-1206.
27. Emery AE, Dreifuss FE (1966). Unusual type of benign X-linked muscular dystrophy. *J. Neurol. Neurosurg. Psychiatry.* 29: 338-342.
28. Eriksson M, Brown WT, Gordon LB, Glynn MW, Singer J, Scott L, Erdos MR, Robbins CM, Moses TY, Berglund P, Dutra A, Pak E, Durkin S, Csoka AB, Boehnke M, Glover TW, Collins FS (2003). Recurrent de novo point mutations in lamin A cause Hutchinson-Gilford progeria syndrome. *Nature.* 423: 293-298.
29. Fairley EA, Kendrick-Jones J, Ellis JA (1999). The Emery-Dreifuss muscular dystrophy phenotype arises from aberrant targeting and binding of emerin at the inner nuclear membrane. *J. Cell Sci.* 112: 2571-2582.
30. Fatkin D, MacRae C, Sasaki T, Wolff MR, Porcu M, Frenneaux M, Atherton J, Vidaillet HJ Jr, Spudich S, De Girolami U, Seidman JG, Seidman C, Muntoni F, Muehle G, Johnson W, McDonough B (1999). Missense mutations in the rod domain of the lamin A/C gene as causes of dilated cardiomyopathy and conduction-system disease. *N. Engl. J. Med.* 341: 1715-1724.
31. Favreau C, Bastos R, Cartaud J, Courvalin JC, Mustonen P (2001). Biochemical characterization of nuclear pore complex protein gp210 oligomers. *Eur. J. Biochem.* 268: 3883-3889.
32. Fischer-Vize JA, Mosley KL (1994). Marbles mutants: uncoupling cell determination and nuclear migration in the developing *Drosophila* eye. *Development.* 120: 2609-2618.

33. Fisher DZ, Chaudhary N, Blobel G (1986). cDNA sequencing of nuclear lamins A and C reveals primary and secondary structural homology to intermediate filament proteins. *Proc. Natl. Acad. Sci. U S A.* 83: 6450-6454.
34. Foisner R, Gerace L (1993). Integral membrane proteins of the nuclear envelope interact with lamins and chromosomes, and binding is modulated by mitotic phosphorylation. *Cell.* 73: 1267-1279.
35. Franke WW, Scheer U, Krohne G, Jarasch ED (1981). The nuclear envelope and the architecture of the nuclear periphery. *J. Cell Biol.* 91: 39s-50s.
36. Franke WW (1987). Nuclear lamins and cytoplasmic intermediate filament proteins: a growing multigene family. *Cell.* 48: 3-4.
37. Fridkin A, Mills E, Margalit A, Neufeld E, Lee KK, Feinstein N, Cohen M, Wilson KL, Gruenbaum Y (2004). Matefin, a *Caenorhabditis elegans* germ line-specific SUN-domain nuclear membrane protein, is essential for early embryonic and germ cell development. *Proc. Natl. Acad. Sci. USA.* 101: 6987-6992.
38. Furukawa K, Hotta Y (1993). cDNA cloning of a germ cell specific lamin B3 from mouse spermatocytes and analysis of its function by ectopic expression in somatic cells. *EMBO J.* 12: 97-106.
39. Gant TM, Harris CA, Wilson KL (1999). Roles of LAP2 proteins in nuclear assembly and DNA replication: truncated LAP2beta proteins alter lamina assembly, envelope formation, nuclear size, and DNA replication efficiency in *Xenopus laevis* extracts. *J. Cell Biol.* 144: 1083-1096.
40. Gerace L, Blum A, Blobel G (1978). Immunocytochemical localization of the major polypeptides of the nuclear pore complex-lamina fraction. Interphase and mitotic distribution. *J. Cell Biol.* 79: 546-66.
41. Gerace L, Burke B (1988). Functional organization of the nuclear envelope. *Annu. Rev. Cell Biol.* 4: 335-374.
42. Goldman RD, Shumaker DK, Erdos MR, Eriksson M, Goldman AE, Gordon LB, Gruenbaum Y, Khuon S, Mendez M, Varga R, Collins FS (2004). Accumulation of mutant lamin A causes progressive changes in nuclear architecture in Hutchinson-Gilford progeria syndrome. *Proc. Natl. Acad. Sci. USA.* 101: 8963-8968.
43. Gorlich D, Kutay U (1999). Transport between the cell nucleus and the cytoplasm. *Annu. Rev. Cell Dev. Biol.* 15: 607-60.

44. Gotzmann J, Foisner R (1999). Lamins and lamin-binding proteins in functional chromatin organization. *Crit. Rev. Eukaryot. Gene Expr.* 9: 257-265.
45. Gough LL, Fan J, Chu S, Winnick S, Beck KA (2003). Golgi localization of Syne-1. *Mol. Biol. Cell.* 14: 2410-2424.
46. Graff JR, Gabrielson E, Fujii H, Baylin SB, Herman JG (2000). Methylation patterns of the E-cadherin 5' CpG island are unstable and reflect the dynamic, heterogeneous loss of E-cadherin expression during metastatic progression. *J. Biol. Chem.* 275:2727-2732.
47. Gros-Louis F, Dupre N, Dion P, Fox MA, Laurent S, Verreault S, Sanes JR, Bouchard JP, Rouleau GA (2007). Mutations in SYNE1 lead to a newly discovered form of autosomal recessive cerebellar ataxia. *Nat. Genet.* 39: 80-85.
48. Gumbiner BM (1996). Cell adhesion: the molecular basis of tissue architecture and morphogenesis. *Cell.* 84: 345-357.
49. Gumbiner BM (2005). Regulation of cadherin-mediated adhesion in morphogenesis. *Nat. Rev. Mol. Cell Biol.* 6: 622-634.
50. Hagan I, Yanagida M (1995). The product of the spindle formation gene *sad1+* associates with the fission yeast spindle pole body and is essential for viability. *J. Cell Biol.* 129: 1033-1047.
51. Haque F, Lloyd DJ, Smallwood DT, Dent CL, Shanahan CM, Fry AM, Trembath RC, Shackleton S (2006). SUN1 interacts with nuclear lamin A and cytoplasmic nesprins to provide a physical connection between the nuclear lamina and the cytoskeleton. *Mol. Cell Biol.* 26: 3738-3751.
52. Harborth J, Elbashir SM, Bechert K, Tuschl T, and Weber K (2001). Identification of essential genes in cultured mammalian cells using small interfering RNAs. *J. Cell Sci.* 114: 4557-4565.
53. Hasan S, Guettinger S, Muehlhaeusser P, Anderegg F, Buergler S, Kutay U (2006). Nuclear envelope localization of human UNC84A does not require nuclear lamins. *FEBS letters.* 580: 1263-1268.
54. Hodzic DM, Yeater DB, Bengtsson L, Otto H, Stahl PD (2004). Sun2 is a novel mammalian inner nuclear membrane protein. *J. Biol Chem.* 279: 25805-25812.
55. Hoger TH, Krohne G, Franke WW (1988). Amino acid sequence and molecular characterization of murine lamin B as deduced from cDNA clones. *Eur. J. Cell Biol.* 47: 283-290.

56. Hoger TH, Zatloukal K, Waizenegger I, Krohne G (1990). Characterization of a second highly conserved B-type lamin present in cells previously thought to contain only a single B-type lamin. *Chromosoma*. 100: 67-69.
57. Hofmann K, Stoffel W (1993). TMbase - A database of membrane spanning proteins segments. *Biol. Chem. Hoppe-Seyler*. 374: 166.
58. Hutchison CJ, Alvarez-Reyes M, Vaughan OA (2001). Lamins in disease: why do ubiquitously expressed nuclear envelope proteins give rise to tissue-specific disease phenotypes? *J. Cell Sci*. 114: 9-19.
59. Hutchison CJ (2002). Lamins: building blocks or regulators of gene expression? *Nat. Rev. Mol. Cell Biol*. 3: 848-858.
60. Ivorra C, Kubicek M, Gonzalez JM, Sanz-Gonzalez SM, Alvarez-Barrientos A, O'Connor JE, Burke B, Andres V (2006). A mechanism of AP-1 suppression through interaction of c-Fos with lamin A/C. *Genes Dev*. 20: 307-320.
61. Jagatheesan G, Thanumalayan S, Muralikrishna B, Rangaraj N, Karande AA, Parnaik VK (1999). Colocalization of intranuclear lamin foci with RNA splicing factors. *J. Cell Sci*. 112: 4651-4661.
62. Jenkins H, Whitfield WG, Goldberg MW, Allen TD, Hutchison CJ (1995). Evidence for the direct involvement of lamins in the assembly of a replication competent nucleus. *Acta. Biochim. Pol*. 42: 133-143.
63. Korenjak M, Brehm A (2005). E2F-Rb complexes regulating transcription of genes important for differentiation and development. *Curr. Opin. Genet. Dev*. 15: 520-527.
64. Laguri C, Gilquin B, Wolff N, Romi-Lebrun R, Courchay K, Callebaut I, Worman HJ, Zinn-Justin S (2001). Structural characterization of the LEM motif common to three human inner nuclear membrane proteins. *Structure*. 9: 503-511.
65. Lammerding J, Schulze PC, Takahashi T, Kozlov S, Sullivan T, Kamm RD, Stewart CL, Lee RT (2004). Lamin A/C deficiency causes defective nuclear mechanics and mechanotransduction. *J. Clin. Invest*. 113: 370-378.
66. Lammerding J, Hsiao J, Schulze PC, Kozlov S, Stewart CL, Lee RT (2005). Abnormal nuclear shape and impaired mechanotransduction in emerin-deficient cells. *J. Cell Biol*. 170: 781-791.
67. Lee KK, Starr D, Cohen M, Liu J, Han M, Wilson KL, Gruenbaum Y (2002). Lamin-dependent localization of UNC-84, a protein required for nuclear migration in *Caenorhabditis elegans*. *Mol. Biol. Cell*. 13: 892-901.

68. Lenz-Bohme B, Wismar J, Fuchs S, Reifegerste R, Buchner E, Betz H, Schmitt B (1997). Insertional mutation of the *Drosophila* nuclear lamin Dm0 gene results in defective nuclear envelopes, clustering of nuclear pore complexes, and accumulation of annulate lamellae. *J. Cell Biol.* 137: 1001-1016.
69. Lickert H, Bauer A, Kemler R, Stappert J. (2000). Casein kinase II phosphorylation of E-cadherin increases E-cadherin/beta-catenin interaction and strengthens cell-cell adhesion. *J. Biol. Chem.* 275:5090-5095.
70. Lin F, Blake DL, Callebaut I, Skerjanc IS, Holmer L, McBurney MW, Paulin-Levasseur M, Worman HJ (2000). MAN1, an inner nuclear membrane protein that shares the LEM domain with lamina-associated polypeptide 2 and emerin. *J. Biol. Chem.* 275: 4840-4847.
71. Macara IG (2001). Transport into and out of the nucleus. *Microbiol. Mol. Biol. Rev.* 65: 570-594.
72. Malone CJ, Fixsen WD, Horvitz HR, Han M (1999). UNC-84 localizes to the nuclear envelope and is required for nuclear migration and anchoring during *C. elegans* development. *Development.* 126: 3171-3181.
73. Malone CJ, Misner L, Le Bot N, Tsai MC, Campbell JM, Ahringer J, White JG (2003). The *C. elegans* hook protein, ZYG-12, mediates the essential attachment between the centrosome and nucleus. *Cell.* 115: 825-836.
74. Manilal S, Nguyen TM, Sewry CA, Morris GE (1996). The Emery-Dreifuss muscular dystrophy protein, emerin, is a nuclear membrane protein. *Hum. Mol. Genet.* 5: 801-808.
75. Maniotis AJ, Chen CS, Ingber DE (1997). Demonstration of mechanical connections between integrins, cytoskeletal filaments, and nucleoplasm that stabilize nuclear structure. *Proc. Natl. Acad. Sci. U S A.* 94: 849-854.
76. Mislow JM, Holaska JM, Kim MS, Lee KK, Segura-Totten M, Wilson KL, McNally EM (2002). Nesprin-1alpha self-associates and binds directly to emerin and lamin A in vitro. *FEBS Lett.* 525: 135-140.
77. Mislow JM, Kim M.S, Davis DB, McNally EM (2002). Myne-1, a spectrin repeat transmembrane protein of the myocyte inner nuclear membrane, interacts with lamin A/C. *J. Cell Sci.* 115: 61-70.
78. Moir RD, Yoon M, Khuon S, Goldman RD (2000). Nuclear lamins A and B1: different pathways of assembly during nuclear envelope formation in living cells. *J. Cell Biol.* 151: 1155-1168.

79. Mosley-Bishop KL, Li Q, Patterson L, Fischer JA (1999). Molecular analysis of the *klarsicht* gene and its role in nuclear migration within differentiating cells of the *Drosophila* eye. *Curr. Biol.* 9: 1211-1220.
80. Muchir A, Bonne G, van der Kooij AJ, van Meegen M, Baas F, Bolhuis PA, de Visser M, Schwartz K (2000). Identification of mutations in the gene encoding lamins A/C in autosomal dominant limb girdle muscular dystrophy with atrioventricular conduction disturbances (LGMD1B). *Hum. Mol. Genet.* 9: 1453-1459.
81. Nedivi E, Fieldust S, Theill LE, Hevron D (1996). A set of genes expressed in response to light in the adult cerebral cortex and regulated during development. *Proc. Natl. Acad. Sci. USA.* 93: 2048-2053.
82. Nikolova V, Leimena C, McMahon AC, Tan JC, Chandar S, Jogia D, Kesteven SH, Michalicek J, Otway R, Verheyen F, Rainer S, Stewart CL, Martin D, Feneley MP, Fatkin D (2004). Defects in nuclear structure and function promote dilated cardiomyopathy in lamin A/C-deficient mice. *J. Clin. Invest.* 113: 357-369.
83. Ohba T, Schirmer EC, Nishimoto T, Gerace L (2004). Energy- and temperature-dependent transport of integral proteins to the inner nuclear membrane via the nuclear pore. *J. Cell Biol.* 167: 1051-1062.
84. Okada Y, Suzuki T, Sunden Y, Orba Y, Kose S, Imamoto N, Takahashi H, Tanaka S, Hall WW, Nagashima K, Sawa H (2005). Dissociation of heterochromatin protein 1 from lamin B receptor induced by human polyomavirus agnoprotein: role in nuclear egress of viral particles. *EMBO Rep.* 6: 452-457.
85. Paddison PJ, Caudy AA, Bernstein E, Hannon GJ, Conklin DS. (2002). Short hairpin RNAs (shRNAs) induce sequence-specific silencing in mammalian cells. *Genes Dev.* 16: 948-958.
86. Padmakumar VC Ph.D thesis (2004). Characterisation of Enaptin and Sun1, two novel mammalian nuclear envelope proteins.
87. Padmakumar VC, Abraham S, Braune S, Noegel AA, Tunggal B, Karakesisoglou I, Korenbaum E (2004). Enaptin, a giant actin-binding protein, is an element of the nuclear membrane and the actin cytoskeleton. *Exp. Cell Res.* 295: 330-339.
88. Padmakumar VC, Libotte T, Lu W, Zaim H, Abraham S, Noegel AA, Gotzmann G, Foisner R, Karakesisoglou I (2005). The inner nuclear membrane protein Sun1 mediates the anchorage of Nesprin-2 to the nuclear envelope. *J. Cell Sci.* 118: 3419-30.

89. Patterson, K., Molofsky, A. B., Robinson, C., Acosta, S., Cater, C. and Fischer, J. A (2004). The functions of Klarsicht and nuclear lamin in developmentally regulated nuclear migrations of photoreceptor cells in the *Drosophila* eye. *Mol. Biol. Cell.* 15: 600-610.
90. Phair RD, Scaffidi P, Elbi C, Vecerova J, Dey A, Ozato K, Brown DT, Hager G, Bustin M, Misteli T (2004). Global nature of dynamic protein-chromatin interactions in vivo: three-dimensional genome scanning and dynamic interaction networks of chromatin proteins. *Mol. Cell Biol.* 24: 6393-6402.
91. Polioudaki H, Kourmouli N, Drosou V, Bakou A, Theodoropoulos PA, Singh PB, Giannakouros T, Georgatos (2001). Histones H3/H4 form a tight complex with the inner nuclear membrane protein LBR and heterochromatin protein 1. *EMBO Rep.* 2: 920-925.
92. Rabut G, Doye V, Ellenberg J (2004). Mapping the dynamic organization of the nuclear pore complex inside single living cells. *Nat. Cell Biol.* 6: 1114-1121.
93. Rober RA, Sauter H, Weber K, Osborn M (1990). Cells of the cellular immune and hemopoietic system of the mouse lack lamins A/C: distinction versus other somatic cells. *J. Cell Sci.* 95: 587-598.
94. Rosenberg-Hasson Y, Renert-Pasca M, Volk T (1996). A *Drosophila* dystrophin-related protein, MSP-300, is required for embryonic muscle morphogenesis. *Mech. Dev.* 60: 83-94.
95. Schirmer EC, Florens L, Guan T, Yates JR 3rd, and Gerace L (2003). Nuclear membrane proteins with potential disease links found by subtractive proteomics. *Science.* 301: 1380–1382.
96. Shimi T, Koujin T, Segura-Totten M, Wilson KL, Haraguchi T, Hiraoka Y J (2004). Dynamic interaction between BAF and emerin revealed by FRAP, FLIP, and FRET analyses in living HeLa cells. *Struct. Biol.* 147: 31-41.
97. Shumaker DK, Lee KK, Tanhehco YC, Craigie R, Wilson KL (2001). LAP2 binds to BAF.DNA complexes: requirement for the LEM domain and modulation by variable regions. *EMBO J.* 20: 1754-1764.
98. Somech R, Shaklai S, Amariglio N, Rechavi G, Simon AJ (2005). Nuclear envelopathies-raising the nuclear veil. *Pediatr. Res.* 57: 8-15.
99. Spann TP, Goldman AE, Wang C, Huang S, Goldman RD (2002). Alteration of nuclear lamin organization inhibits RNA polymerase II-dependent transcription. *J. Cell Biol.* 156: 603-608.

100. Speckman RA, Garg A, Du F, Bennett L, Veile R, Arioglu E, Taylor SI, Lovett M, Bowcock AM (2000). Mutational and haplotype analyses of families with familial partial lipodystrophy (Dunnigan variety) reveal recurrent missense mutations in the globular C-terminal domain of lamin A/C. *Am. J. Hum. Genet.* 66: 1192-1198.
101. Starr DA, Hermann GJ, Malone CJ, Fixsen W, Priess JR, Horvitz HR, Han M (2001). *unc-83* encodes a novel component of the nuclear envelope and is essential for proper nuclear migration. *Development.* 28: 5039-50.
102. Starr DA, Han M (2002). Role of ANC-1 in tethering nuclei to the actin cytoskeleton. *Science.* 298: 406-409.
103. Starr DA, Han M (2003). ANChors away: an actin based mechanism of nuclear positioning. *J. Cell Sci.* 116: 211-216.
104. Starr DA, Fischer JA (2005). KASH 'n Karry: the KASH domain family of cargo-specific cytoskeletal adaptor proteins. *Bioessays.* 27: 1136-1146.
105. Stuurman N, Heins S, Aebi U (1998). Nuclear lamins: their structure, assembly, and interactions. *J. Struct. Biol.* 122: 42-66.
106. Sullivan T, Escalante-Alcalde D, Bhatt H, Anver M, Bhat N, Nagashima K, Stewart CL, Burke B (1999). Loss of A-type lamin expression compromises nuclear envelope integrity leading to muscular dystrophy. *J. Cell Biol.* 147: 913-920.
107. Takeichi M (1991). Cadherin cell adhesion receptors as a morphogenetic regulator. *Science.* 251: 1451-1455.
108. Thiery JP (2002). Epithelial-mesenchymal transitions in tumour progression. *Nat. Rev. Cancer.* 2: 442-54.
109. Tzur YB, Wilson KL, Gruenbaum Y (2006). SUN-domain proteins: 'Velcro' that links the nucleoskeleton to the cytoskeleton. *Nat. Rev. Mol. Cell Biol.* 7: 782-788.
110. Vergnes L, Peterfy M, Bergo MO, Young SG, and Reue K (2004). Lamin B1 is required for mouse development and nuclear integrity. *Proc. Natl. Acad. Sci. USA.* 101: 10428–10433.
111. Vleminckx K, Vakaet L Jr, Mareel M, Fiers W, van Roy F (1991). Genetic manipulation of E-cadherin expression by epithelial tumor cells reveals an invasion suppressor role. *Cell.* 66: 107-119.
112. Wang Q, Du X, Cai Z, Greene MI (2006). Characterization of the structures involved in localization of the SUN proteins to the nuclear envelope and the centrosome. *DNA Cell Biol.* 25: 554-562.

-
113. Wang X, Bregegere F, Soroka Y, Kayat A, Redziniak G, Milner Y (2004). Enhancement of Fas-mediated apoptosis in ageing human keratinocytes. *Mech. Ageing Dev.* 125: 237-249.
114. Warren DT, Zhang Q, Weissberg PL, Shanahan CM (2005). Nesprins: intracellular scaffolds that maintain cell architecture and coordinate cell function? *Expert Rev. Mol. Med.* 7: 1-15.
115. Wei Wu, Feng Lin and Howard J. Worman (2002). Intracellular trafficking of MAN1, an integral protein of the nuclear envelope inner membrane. *J. Cell Sci.* 115: 1361-1371.
116. Welte MA, Gross SP, Postner M, Block SM, Wieschaus EF (1998). Developmental regulation of vesicle transport in *Drosophila* embryos: forces and kinetics. *Cell.* 92: 547-557.
117. Wheelock MJ, Johnson KR (2003). Cadherins as modulators of cellular phenotype. *Annu. Rev. Cell Dev. Biol.* 19:207-235.
118. Wilhelmsen K, Ketema M, Truong H, Sonnenberg A (2006). KASH-domain proteins in nuclear migration, anchorage and other processes. *J. Cell Sci.* 119: 5021-5029.
119. Wilson KL, Newport J (1988). A trypsin-sensitive receptor on membrane vesicles is required for nuclear envelope formation in vitro. *J. Cell Biol.* 107: 57-68.
120. Wilson KL (2000). The nuclear envelope, muscular dystrophy and gene expression. *Trends. Cell Biol.* 10: 125-129.
121. Wolff N, Gilquin B, Courchay K, Callebaut I, Worman HJ, Zinn-Justin S (2001). Structural analysis of emerin, an inner nuclear membrane protein mutated in X-linked Emery-Dreifuss muscular dystrophy. *FEBS Lett.* 501: 171-176.
122. Worman HJ, Courvalin JC (2000). The inner nuclear membrane. *J. Membr. Biol.* 177: 1-11.
123. Yang L, Guan T, Gerace L (1997). Integral membrane proteins of the nuclear envelope are dispersed throughout the endoplasmic reticulum during mitosis. *J. Cell Biol.* 137: 1199-1210.
124. Ye Q, Worman HJ (1996). Interaction between an integral protein of the nuclear envelope inner membrane and human chromodomain proteins homologous to *Drosophila* HP1. *J. Biol. Chem.* 271: 14653-14656.
125. Ye Q, Callebaut I, Pezhman A, Courvalin JC, Worman HJ (1997). Domain-specific interactions of human HP1-type chromodomain proteins and inner nuclear membrane protein LBR. *J. Biol. Chem.* 272: 14983-14989.

-
126. Yu J, Starr DA, Wu X, Parkhurst SM, Zhuang Y, Xu T, Xu R, Han M (2006). The KASH domain protein MSP-300 plays an essential role in nuclear anchoring during *Drosophila* oogenesis. *Dev. Biol.* 289: 336-345.
127. Zhang Q, Skepper JN, Yang F, Davies JD, Hegyi L, Roberts RG, Weissberg PL, Ellis JA, Shanahan CM (2001). Nesprins: a novel family of spectrin-repeat-containing proteins that localize to the nuclear membrane in multiple tissues. *J. Cell Sci.* 114: 4485-4498.
128. Zhang Q, Ragnauth C, Greener MJ, Shanahan CM, Roberts RG (2002). The nesprins are giant actin-binding proteins, orthologous to *Drosophila melanogaster* muscle protein MSP-300. *Genomics.* 80: 473-481.
129. Zhang Q, Ragnauth CD, Skepper JN, Worth NF, Warren DT, Roberts RG, Weissberg PL, Ellis JA, Shanahan CM (2005). Nesprin-2 is a multi-isomeric protein that binds lamin and emerin at the nuclear envelope and forms a subcellular network in skeletal muscle. *J. Cell Sci.* 118: 673-687.
130. Zhang X, Xu R, Zhu B, Yang X, Ding X, Duan S, Xu T, Zhuang Y, Han M (2007). Syne-1 and Syne-2 play crucial roles in myonuclear anchorage and motor neuron innervation. *Development.* 134: 901-908.
131. Zhen YY, Libotte T, Munck M, Noegel AA, Korenbaum E (2002). NUANCE, a giant protein connecting the nucleus and actin cytoskeleton. *J. Cell Sci.* 115: 3207-3222.
132. Zheng R, Ghirlardo R, Lee MS, Mizuuchi K, Krause M, Craigie R (2000). Barrier-to-autointegration factor (BAF) bridges DNA in a discrete, higher-order nucleoprotein complex. *Proc. Natl. Acad. Sci. U S A.* 97: 8997-9002.

7. Appendix

7.1 Abbreviations

BSA	Bovine serum albumin
cDNA	complementary DNA
DAPI	
DMEM	Dulbecco`s modified Eagle medium
DMSO	dimethylsulfoxide
DNA	desoxyribonucleic acid
dNTP	2'-desoxyribonucleotid-5'- triphosphate
EDTA	ethylenediaminetetraacetic acid
ER	endoplasmic reticulum
FCS	fetal calf serum
G418	geneticin
GAPDH	glyceraldehydephosphate dehydrogenase
GFP	green fluorescent protein
GST	glutathione S-transferase
IgG	immunglobulin
INM	inner nuclear membrane
IPTG	isopropyl- β -D- thiogalactopyranoside
kb	kilobases
kDa	kilodalton
mRNA	messenger RNA
NE	nuclear envelope
NPCs	nuclear pore complexes
OD	optical density
ONM	outer nuclear membrane

PAGE	polyacrylamid gel electrophoresis
PBS	phosphate buffered saline
PCR	polymerase chain reaction
RNA	ribonucleic acid
SDS	sodium dodecyl sulfate
Taq	Thermophilus aquaticus
TBS	tris buffered saline
T _m	melting temperature

7.2 Amino acid code

A	Ala	Alanine	M	Met	Methionine
C	Cys	Cysteine	N	Asn	Asparagine
D	Asp	Aspartic acid	P	Pro	Proline
E	Glu	Glutamic acid	Q	Gln	Glutamine
F	Phe	Phenylalanine	R	Arg	Arginine
G	Gly	Glycine	S	Ser	Serine
H	His	Histidine	T	Thr	Threonine
I	Ile	Isoleucine	V	Val	Valine
K	Lys	Lysine	W	Trp	Tryptophane
L	Leu	Leucine	Y	Tyr	Tyrosine

Acknowledgement

*First, I would like to express my heartiest gratitude to **Prof. Dr. Noegel** for giving me an opportunity to work under her supervision. Her positive attitude, constant encouragement and sustained interest in my project proved essential for my successful PhD work.*

*I convey my sincere heartfelt gratitude to **Dr. Akis Karakesisoglou**, our group leader, for providing valuable guidance, excellent advice with my work. His constant encouragement and immense optimism are highly acknowledged. It was a privilege to work with him.*

I would also like to thank Dr. Francisco as he helped me learn confocal microscopy and being friendly. Thanks to Christoph and Julia, who were always so friendly and ever ready to offer help and constructive ideas. A special thank to Budi for rendering help with the computer problem.

Special thanks to Martina Munch who helped me a lot in the beginning with the laboratory techniques. I would forward my thanks to her for being so nice. Thanks to Maria, Rosi and Berthold for being really friendly and cooperative.

I also owe my thanks to all my dear colleges in lab 10. Thanks to Ria, Yvonne, Verena and Sascha for their valuable friendship and making my stay in the lab extremely wonderful. Thanks also to my ex lab members Hafida, Sabu and Kumar for their encouragement and help. I would also like to thank Jessica, Hua, Jianbo, Georgia, Charles, Subhanjan, Christian, Eva, Tanja, Carola, Surayya, Rui, Monika, Kristina, Claudia and all others for being so kind, friendly and helpful.

I would like to thank Prof. Dr. Jan Ellenberg and Dr. Lucia Sironi in Heidelberg for warmhearted accommodation and help. I owe my thanks to Dr. Joseph Gotzmann for providing Sun1 antibodies and constructs.

I would like to thank all the people who directly or indirectly helped me in the completion of my PhD project.

*Finally, I owe my acknowledgement to the **Graduate School in Genetics and Functional Genomics, University of Köln** for offering me the fellowship for my PhD studies.*

Erklärung

Ich versichere, dass ich die von mir vorgelegte Dissertation selbständig angefertigt, die benutzten Quellen und Hilfsmittel vollständig angegeben und die Stellen der Arbeit- einschließlich Tabellen und Abbildungen-, die anderen Werke im Wortlaut oder dem Sinn nach entnommen sind, in jedem Einzelfall als Entlehnung kenntlich gemacht habe; dass diese Dissertation noch keiner anderen Fakultät oder Universität zur Prüfung vorgelegen hat; dass sie- abgesehen von unten angegebenen beantragten Teilpublikationen- noch nicht veröffentlicht ist, sowie, dass ich eine Veröffentlichung vor Abschluss des Promotionsverfahrens nicht vornehmen werde. Die Bestimmungen dieser Promotionsordnung sind mir bekannt. Die von mir vorgelegte Dissertation ist von Frau Prof. Dr. Angelika A. Noegel betreut worden.

Köln den

Wenshu Lu

Teilpublicationen:

1. Padmakumar VC, Libotte T, **Lu W**, Zaim H, Abraham S, Noegel AA, Gotzmann J, Foisner R, Karakesisoglou I (2005). The inner nuclear membrane protein Sun1 mediates the anchorage of Nesprin-2 to the nuclear envelope. *J Cell Sci.* 118: 3419-3430.
2. Libotte T, Zaim H, Abraham S, Padmakumar VC, Schneider M, **Lu W**, Munck M, Hutchison C, Wehnert M, Fahrenkrog B, Sauder U, Aebi U, Noegel AA, Karakesisoglou I (2005). Lamin A/C-dependent localization of Nesprin-2, a giant scaffold at the nuclear envelope. *Mol. Biol. Cell.* 16: 3411-3424.

Curriculum Vitae

Name: Wenshu Lu
Address: Escher Str. 125,
50739, Köln, Deutschland
E-mail: wenshu.lu@uni-koeln.de
Date of Birth: 22.02.1977
Place of Birth: Changchun, P. R. China
Nationality: P. R. China

School studies

1992-1995: Jilin Province Shiyan High School,
Chang Chun, P.R. China

University studies

1995-1999: Bachelor of Science (Biology),
Northeast Normal University, Chang Chun, P.R. China

2000-2003: Master of Science (Cell Biology),
Northeast Normal University, Chang Chun, P.R. China

Doctoral studies

04.2004- 05.2007: Faculty of Mathematics and Natural Science
University of Cologne
Supervisor: Prof. Dr. Angelika A. Noegel
Group leader: Dr. Iakowos Karakesisoglou
Institute for Biochemistry I, Medical Faculty
University of Cologne, Cologne, Germany

Lebenslauf

Name: Wenshu Lu
Adresse: Escher Str, 125,
50739, Köln, Deutschland.
E-mail: wenshu.lu@uni-koeln.de
Geburtsdatum: 22.02.1977
Geburtsort: Changchun, V. R. China
Nationalität: V. R. China

Schulausbildung

1992-1995: Jilin Province Shiyan High School,
Chang Chun, P.R. China

Universität Studium

1995-1999: Bachelor of Science (Biology),
Northeast Normal University, Chang Chun, V.R. China

2000-2003: Master of Science (Cell Biology),
Northeast Normal University, Chang Chun, V.R. China

Promotions Studium

04.2004- 05.2007: Mathematisch-Naturwissenschaftliche Fakultät
Universität zu Köln
Betreuerin: Prof. Dr. Angelika A. Noegel
Gruppenleiter: Dr. Iakowos Karakesisoglou
Institut Für Biochemie I, Medizinische Fakultät
Universität zu Köln, Köln, Deutschland